50272-101

REPORT DOCUMENTATION PAGE	1. REPORT NO. NSF/ENG-85025	2.	3. Recipient's Accession No. PB86 135340/AS
4. Title and Subtitle: Effect of Inelastic Behavior on the Analysis and Design of Earthquake Resistant Structures			5. Report Date: June 1985 6.
7. Author(s): J. Lin and S. A. Mahin			8. Performing Organization Rept. No. UCB/EERC-85/08
9. Performing Organization Name and Address: Earthquake Engineering Research Center University of California, Berkeley 1301 South 46th Street Richmond, Calif. 94804			10. Project/Task/Work Unit No. 11. Contract(C) or Grant(G) No. (C) (G) CEE81-07217
12. Sponsoring Organization Name and Address: National Science Foundation 1800 G. Street, N.W. Washington, D.C. 20550			13. Type of Report & Period Covered 14.

15. Supplementary Notes

16. Abstract (Limit: 200 words)

The first part deals with the interaction between ground motion and structural response parameters. Major emphasis is placed on assessing ways to define the damaging potential of a ground motion. Various indices are suggested for measuring the damaging potential of a ground motion. Validity tests of these indices, including the effects of the severity of inelastic deformation and different structural damage measurements, are conducted for two sets of ground motions. Guidelines for scaling ground motions are developed.

The second part involves developing an efficient analysis procedure for use in the preliminary stage of design. Response of typical shear-beam type structures in their initial linear elastic mode shape coordinate systems is presented. Current practices of implementing the response spectrum method for analysis of inelastic multiple-degree-of-freedom systems are assessed. A rational procedure, using a proposed modal hysteresis model, for implementing the response spectrum method is suggested, and its reliability evaluated.

In the third part, a preliminary investigation of the seismic behavior of non-structural subsystems supported on inelastic structures is performed. An amplification factor is defined to quantify the effects of inelastic deformations of the supporting structure on subsystem response. Design guidelines are formulated for predicting the amplification factor based on statistical evaluation of the results generated for ten earthquake ground motions.

17. Document Analysis a. Descriptors

b. Identifiers/Open-Ended Terms

c. COSATI Field/Group

18. Availability Statement: Release Unlimited	19. Security Class (This Report)	21. No. of Pages 164
	20. Security Class (This Page)	22. Price A08

(See ANSI-Z39.18) See Instructions on Reverse OPTIONAL FORM 272 (4-77) (Formerly NTIS-35) Department of Commerce

PB86-135340

REPORT NO.
UCB EERC-85 08
JUNE 1985

EARTHQUAKE ENGINEERING RESEARCH CENTER

EFFECT OF INELASTIC BEHAVIOR ON THE ANALYSIS AND DESIGN OF EARTHQUAKE RESISTANT STRUCTURES

by

J. LIN
S. A. MAHIN

Report to the National Science Foundation

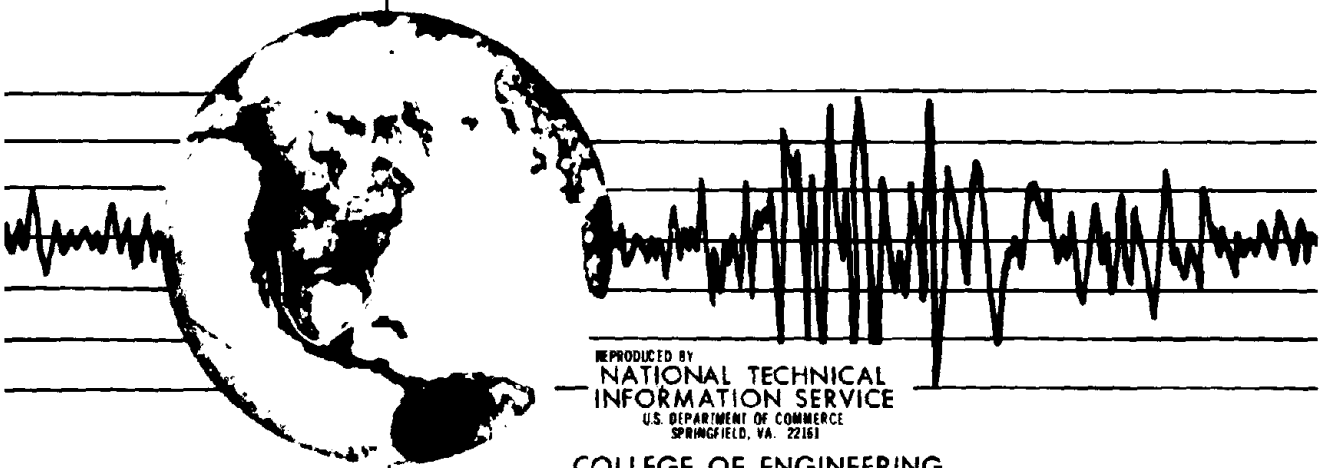

COLLEGE OF ENGINEERING

UNIVERSITY OF CALIFORNIA · Berkeley, California

For sale by the National Technical Information Service, U S Department of Commerce, Springfield, Virginia 22161

See back of report for up to date listing of EERC reports

EFFECT OF INELASTIC BEHAVIOR ON THE ANALYSIS AND DESIGN OF EARTHQUAKE RESISTANT STRUCTURES

by

J. Lin and S.A. Mahin

A report on research sponsored by the

National Science Foundation

Report No. UCB/EERC-85/08

Earthquake Engineering Research Center

College of Engineering

Univeristy of California

Berkeley, California

June, 1985

ABSTRACT

This report presents an evaluation of the effect of inelastic deformation on the preliminary analysis and design of earthquake resistant structures. Three related, but seperate topics are addressed.

The first part of the study deals with the interaction between ground motion and structural response parameters. The purpose is to provide a more consistent basis for selecting the design earthquake for systems that response inelastically. Major emphasis is placed on assessing ways to define the damaging potential of a ground motion. A review of the various suggested indices for measuring the damaging potential of a ground motion is presented. Validity tests of these indices, including the effects of the severity of inelastic deformation and different structural damage measurements, are conducted for two sets of ground motions. Guidelines for scaling ground motions are developed.

The second part of the study involves developing an efficient analysis procedure for use in the preliminary stage of design. Response of typical shear-beam type structures in their initial linear elastic mode shape coordinate systems is presented. Current practices of implementing the response spectrum method for analysis of inelastic multiple-degree-of-freedom systems are assessed. A rational procedure, using a proposed modal hysteresis model, for implementing the response spectrum method is suggested. The reliability of the recommended procedure is evaluated.

In the last part of the study, a preliminary investigation of the seismic behavior of non-structural subsystems supported on inelastic structures is performed. The effects of the severity of inelastic deformations, of different hysteretic characteristics of the structure and of the amount of viscous damping of the subsystem are investigated. Current design

recommendations for subsystems accounting for yielding of the supporting structure are assessed. An amplification factor is defined to quantify the effects of inelastic deformations of the supporting structure on subsystem response. Design guidelines are formulated for predicting the amplification factor based on statistical evaluation of the results generated for ten earthquake ground motions.

The report concludes with summaries of the results obtained. In addition, areas needing further research are identified.

ACKNOWLEDGEMENT

The research presented in this report was sponsored by the National Science Foundation. This support is gratefully acknowledged. Opinions, findings, and conclusions or recommendations expressed in this report are, however, those of the author and do not necessarily reflect the views of the National Science Foundation.

The effort of Richard Steele in preparing the figures is greatly appreciated.

Table of Contents

List of Symbols

A_g	Maximum ground acceleration
ABS	Abso'ute sum
AI	Arias intensity
ATC	Applied Technology Council
C,[C]	Damping matrix of a building
$[C_n]$	Modal damping matrix
D_g	Maximum ground displacement
D.O.F.	Degree of freedom
$\delta_{y,j}$	Jth story yield displacement
ξ	Viscous damping coefficient
EPP	Elasto-perfectly plastic
FAS	Fourier amplitude of ground acceleration
F_j	Jth story shear due to unit ith modal displacement
$F_{i,j}$	Required jth story shear in the ith mode
$F_{y,j}$	Required jth story shear strength by elastic design
$F_{y,j}^{inel}$	Required jth story shear strength by inelastic design
FRS	Floor response spectrum method
g	Gravitational acceleration
Γ_i^*	$\{\phi_i\}^T[M]\{r\}$
$\{\Gamma_n\}$	$[\phi]^T[M]\{r\}$
HE	Hysteretic energy
I	Ground motion intensity

K_j	Jth story stiffness
K_i^*	Modal stiffness of the ith mode
MDOF	Multiple-degree-of-freedom
M,[M]	Mass matrix of a building
$[M_n]$	Modal mass matrix
NRC	Nuclear Regulatory Commission
PSA	Pseudo-spectral Acceleration
PSV	Pseudo-spectral velocity
$[\phi]^T\{R(\{Y\})\}$	Modal force vector
$[\phi]$	Mode shape vector matrix
$\{\phi_i\}$	Ith mode shape vector
ϕ_{ij}	Jth entry of the ith mode shape vector
$\{\phi_i\}^T\{R_y\}$	Modal yield strength of the ith mode
{r}	A vector relating structural degree of freedom to ground movement
RMS	Root-mean square acceleration
R(t),{R(u)},{R({Y})}	Resistance force developed by a building
R_{el}	Yield strength required for structural ductility of 1
R_y	Yield strength of a SDOF system
$\{R_y\}$	{R(u)} when all stories are yielding in the same direction
μ_i	Reduction factor for S_{di}
σ_i	Reduction factor for computed modal yield strength
SI	Spectral intensity
SRSS	Square root of sum of the squares

S_{d_i}	Maximum modal displacement determined from an elastic response spectrum
SDM	Stiffness degrading
SDOF	Single-degree-of-freedom
T	Fundamental period of a building
t	Time
τ	Dummy integration variable
T_D	Duration of an earthquake
T_b	Period of point b in Figure 4.4
T_c	Period of point c in Figure 4.4
T_d	Period of point d in Figure 4.4
T_{sub}	Subsystem period
UBC	Uniform building code
{u}	Displacement response of a building
u_y	Yield displacement of a SDOF system
$\{\dot{u}\}$	Velocity response of a building
$\{\ddot{u}\}$	Acceleration response of a building
$\ddot{u}_g$	Ground acceleration
$\ddot{u}_{g_{max}}$	Maximum ground acceleration
μ_H	Normalized hysteretic energy
μ_i^*	Modal ductility in the ith mode
$\mu_{i,j}$	Jth story ductility in the ith mode
$\mu_{all,j}$	Jth story ductility
V_g	Maximum ground velocity

v_j^i	Jth story displacement in the ith mode
$(v_j^i)_{max}$	maximum jth story displacement in the ith mode
ω	Natural frequency of a structure
$\{Y\}$	Generalized displacement in the modal coordinate system
Y_{yi}	Modal yield displacement of the ith mode
$(Y_i)_{max}, Y_{imax}$	Maximum ith mode displacement

List of Tables

List of Figures

CHAPTER 1 INTRODUCTION

1.1 Introductory Remarks

Earthquakes are a severe natural hazard in many parts of the world. Construction of earthquake-resistant structures is of vital concern in these areas. Because of economic considerations, structures are usually designed to respond inelastically when subjected to severe earthquake ground motions. Such structures must be designed, detailed and constructed to develop the required inelastic deformations. When this is properly done, the structure will sustain, without collapse, the earthquake loading with only local damages. This is in compliance with the objectives of most current seismic design recommendations for buildings [Ref. 78], which are the prevention of significant structural damages during a moderate earthquake and the avoidance of structural collapse during major earthquake ground shaking. Some of the problems related to a rational implementation of this philosophy in preliminary stage of design are discussed herein.

In designing buildings to resist strong earthquake ground motions, many codes [Refs. 7, 93] are available which provide an efficient and effective means for obtaining preliminary design lateral forces. In such codes, earthquake effects are usually represented by a set of equivalent static lateral forces. For example, in the Uniform Building Code (UBC) [Ref. 93] these forces are distributed based on an approximation of the fundamental mode shape of a regular, uniform building. To account for possible higher mode response, an approximate correction force is applied to the top floor. The magnitudes of the applied forces are scaled according to the past seismic performance of the type of structure considered, the importance of the structure, its seismic characteristics and the intensity of the expected excitation. This code approach will provide lateral forces leading to reasonably satisfactory designs for conventional buildings with no

significant irregularities in configuration, stiffness or strength [Refs. 7, 78].

For irregular structures, the current UBC code requires that the distribution of lateral forces be determined considering the dynamic characteristics of the structure. Some design guidelines suitable for the preliminary design of such structures have been suggested. For example, Smilowitz *et al* [Ref. 88] have recommended lateral force distributions accounting for higher mode contributions, setback effects and soil-structure interaction. These distributions, however, are for idealized structures derived on the basis of elastic response. The extent to which they hold for other types of structures or for structures expected to respond inelastically is not certain. Moreover, building codes do not usually attempt to quantify the degree of damage expected for a given level of design force. Thus, such codes give little explicit guidance to the designers of special structures where the tolerable level of damage may be reduced.

It is, thus, often necessary to perform dynamic analyses of irregular and other special structures to assess their adequacy during severe seismic events. Considerable research has been directed at developing computer software capable of predicting the elastic as well as inelastic response of structures [Refs. 4, 11, 34, 36, 59, 60, 77]. However, to use such analysis programs, it is necessary to know the mechanical and dynamic characteristics of the building and nature of the design earthquake. If this information is accurately known, such programs are generally capable of adequately simulating seismic response. However, at the preliminary stage of design, precise information about the dynamic characteristics of the building is generally unavailable. Since the building properties depend on the magnitude and distribution of design forces and influence the dynamic characteristic of the structure, such analyses must be performed on an iterative basis. To facilitate this process in the preliminary stages of design, it would be desirable to develop approximate methods for characterizing the design earthquake in terms of its damage potential and for selecting the magnitude and distribution of preliminary design forces accounting for the acceptable damage level and characteristics of the ground motion. While considerable work on these topics has been done for elastic systems, considerable uncertainties remain regarding their applicability to inelastic systems. These topics will be

investigated in this study. Additionally, related problems associated with establishing design forces for nonstructural elements in structures that yield during severe earthquake shaking will also be addressed.

(a) Problems Associated with the Selection of Design Earthquake

Considerable uncertainty is associated with the selection of the design earthquake or earthquakes [Ref. 15]. The selection of design earthquake(s) involves many disciplines and requires the cooperation among many professionals such as geologists, seismologists, architects, structural engineers, geotechnical engineers and the owner. Although continual progress is being made, there is still no consensus about what ground motion characteristics or parameters are significant in exciting a building, and how they can best be quantified for design purposes, especially for structures that respond inelastically. The various aspects of a ground motion affecting structural response include intensity, frequency content, duration, the number, size and sequence of acceleration pulses. In addition, it is not certain what structural response parameters should control the design, particularly in the inelastic range. For example, displacement, drift, ductility, acceleration and other factors have been suggested. Moreover, it is not certain how these ground motion and structural response parameters are related.

The first objective of this study then, is to investigate the interaction between the ground motion and structural response parameters. This will lead to a better understanding of the relationship and will provide a more consistent basis for selecting the design earthquake for systems that respond inelastically.

(b) Simplified Methods of Analysis for Inelastic Multiple-Degree-of-Freedom Structures

At present, inelastic dynamic analyses can only be conducted through step-by-step integration. While computer programs employing step-by-step integration are versatile and reliable, they generally are unsuitable for preliminary design. In this stage of design, the designer needs guidance on how to select the overall stiffness and strength of the structure in order to limit its inelastic deformations to acceptable levels. Alternatively, the designer may wish to quickly

assess the sensitivity of the overall response of a proposed structure to uncertainties in its mechanical and dynamic characteristics or to different excitations. Step-by-step integration is time-consuming and requires detailed knowledge of the mechanical characteristics of the structure. Both of these factors are contrary to the conditions existing during preliminary design.

Several simplified analytical techniques have been suggested for use in the preliminary stage of design. These include the equivalent linear structure method [Refs. 47, 85], the equivalent nonlinear single-degree-of-freedom (SDOF) system method [Refs. 76, 86, 87] and the response spectrum method [Refs. 3, 6, 10, 13, 16, 17, 38, 54, 56, 91, 98, 99, 100]. Although the equivalent linearization concept is palpable and the procedure for its implementation well-established, the method fails to recognized that the types of excitation that induce maximum response in elastic and inelastic systems may differ [Refs. 13, 14]. Consequently, the accuracy of the method relies on the design earthquake having characteristics similar to those used in developing the procedure.

Procedures for implementing the equivalent nonlinear structure methods are also well-developed [Refs. 76, 86, 87]. In such cases, a complex structure is reduced to an equivalent nonlinear single-degree-of-freedom system. This speeds up the computation, and, depending on the method used to develop the equivalent SDOF structure, may require less explicit information on the structure. Thus, it may be suitable for preliminary design. However, uncertainties arise in the accuracy of the one degree-of-freedom idealization and refinements in computation may be counter to preliminary design.

Response spectra can be generated for simple SDOF inelastic systems. Suggestions exist for developing these by modifying elastic response spectra or by computing them directly by step-by-step integration. Such spectra can be useful in designing structures that respond as SDOF systems. However, whether the method can be used for analysis of inelastic multiple-degree-of-freedom systems (MDOF) is unclear. Although several procedures have been proposed for implementing the response spectrum method [Refs. 3, 6, 10, 13, 16, 17, 38, 54, 56, 91, 98, 99, 100], they vary considerably in their approach and often lack satisfactory theoretical

justifications.

Thus, the second objective of this investigation is to explore a rational procedure for implementing the response spectrum method for the preliminary analysis of inelastic structures and to evaluate the reliability of such a procedure.

(c) Design of Equipment Attached to the Structure

Observations following recent major earthquakes have indicated that a considerable portion of the total cost of damage is often associated with nonstructural components [Ref. 9.]. In addition to economic losses incurred by the damages to the nonstructural elements and equipments (will be called nonstructural subsystems or just subsystems hereafter), such subsystem failures may also create life safety hazards due to falling ceilings, facades, etc., and disrupt the operation of essential facilities such as hospitals or important communication centers. To ensure public safety and to minimize property damages, it is important to have a proper understanding of the seismic behavior of nonstructural subsystems in addition to having a sound knowledge of the behavior of the supporting structure.

There is a wide range of nonstructural subsystems that may be encountered in practice. In terms of how loads are induced, subsystems can be divided into two categories: deformation sensitive subsystems and acceleration sensitive subsystems. Loads in the first category of subsystems arise mainly as a result of the deformations imposed by the supporting structure, e.g., in-plane forces in infilled walls. The second category includes subsystems that are sensitive to accelerations developed at their attachment points. This report focuses only the latter category of subsystems.

While increasing attention is being focused on the design of subsystems, most studies assume that the supporting structure will remain elastic during a severe earthquake excitation. This may be true for critical structures, such as primary structures in a nuclear power plant [Ref. 30]. Most other structures, however, are expected to experience inelastic deformation when subjected to rare and unusually intense earthquake excitations. Rational design methods

for equipment and other nonstructural elements in this case are not certain.

The last objective of this investigation is to conduct a preliminary investigation of the seismic behavior of subsystems supported on inelastic structures, to assess current design methods in terms of this behavior, and to develop improved design recommendations.

1.2 Objectives

The main objectives of this study are to investigate some of the problems associated with the preliminary design of structures that respond inelastically to major earthquake ground shaking and to develop methods to resolve these problems. The specific tasks undertaken in this study are:

(a) To investigate the relation between ground motion and structural response parameters.

(b) To explore a rational procedure for implementing the response spectrum method for inelastic structures and to evaluate the reliability of such a procedure.

(c) To conduct a preliminary investigation on seismic behavior of subsystems supported on inelastic structures, to assess current design methods in terms of this behavior, and to develop improved design recommendations.

1.3 Organization

In Chapter 2, methods for characterizing design earthquakes for intense ground shaking capable of significant structural damage are briefly reviewed. Major emphasis is placed on assessing the effectiveness of various indices for characterizing the damaging potential of a ground motion record.

In Chapter 3, the inelastic response of some selected inelastic structures is computed and transformed into the initial linear elastic mode shape coordinate system. These equivalent modal responses are evaluated and a procedure for applying the inelastic response spectrum method is described. The reliability of this procedure is evaluated.

Preliminary analyses performed to identify behavioral characteristics of subsystems sup-

ported on structures that yield during severe earthquake ground motions are presented in Chapter 4. In addition, design guidelines for predicting subsystem response accounting for the yielding are formulated.

In Chapter 5, conclusions reached in this report are summarized. Recommendations for further research are also offered.

CHAPTER 2 ON SCALING OF EARTHQUAKE GROUND MOTIONS

2.1 Introductory Remarks

For structures designed to deform inelastically when subjected to severe earthquake ground motions, overall seismic safety will depend on the interaction between its energy dissipating capacity and the severity of ground shaking. This interaction is complex and difficult to predict. This can be illustrated by considering the response of a single-degree-of-freedom (SDOF) system subjected to the S15W component of the Pacoima Dam record (originally identified as the S16E component) shown in Figure 2.1.a. Examination of this ground motion reveals that the record contains, in addition to the sharp acceleration peak of 1.25g at about the 8th second, two acceleration pulses having a magnitude of about 0.6 g and duration of about 0.6 second between the 2nd and 4th second. The inelastic response of two systems developing the same maximum inelastic deformation when subjected to this record are shown in Figures 2.1.b and 2.1.c. For a structure with an initial period of 0.3 seconds, the maximum response is primarily due to the sharp acceleration peak of 1.25 g and is little affected by the 0.6 g acceleration pulses. On the other hand, if the structure has a period of 0.7 seconds, the largest plastic excursion is associated with the smaller acceleration pulses between the 2nd and 4th second. Thus, different features of a ground motion can influence structural response and it may, therefore, be difficult to establish a single parameter to characterize the damaging potential of a ground motion.

Traditionally, the intensity of a ground motion, for structural analysis purposes, has been defined in terms of the peak ground acceleration. There is increasing evidence that peak ground acceleration, when used as an index of ground motion intensity, may lead to inconsistent results. On one hand, structures designed to current code recommendations have suffered damage that is more than would be expected considering the moderate level of peak ground acceleration recorded [Ref. 13]. On the other hand, damages observed in other buildings have been relatively moderate in spite of high recorded peak ground acceleration [Refs. 51,

81, 89]. Because of this, it is generally felt that peak ground accelerations, especially those associated with isolated, short-duration, high frequency acceleration spikes, are not effective in exciting most structures. Consequently, the concept of "effective" acceleration has been suggested [Refs. 21, 31, 103]. However, it remains difficult to quantify the "effective' acceleration of a particular ground motion record.

Other ground motion intensity indices have also been suggested. Those frequently used in seismic design and seismic risk mapping were identified in Ref. 8. The effects of various ground motion characteristics on seismic behavior were was also qualitatively discussed. A few attempts have also been made to evaluate quantitatively the relative effectiveness of some of these intensity indices. For example, Nau [Ref. 64] found that spectral intensity values calculated for three period ranges provide a good indication of damage potential for buildings in each range. Similarly, a modified spectral intensity based on weighted spectral acceleration was found to be effective in measuring the structural damage potential of a ground motion [Ref. 52]. Cornell *et al* [Ref. 27] indicated that Fourier amplitudes of the ground acceleration record at 0.25 seconds, 1.0 seconds and 3.33 seconds provided a better set of intensity indices for short, intermediate and long period buildings than peak ground acceleration, velocity or displacement. Chang [Ref. 25] found that normalizing parameters directly related to ground motion records (e.g. peak ground acceleration, etc) are not as good as parameters based on elastic or inelastic spectrum. Nishikawa *et al* [Ref. 72] concluded that for structural periods greater than 0.3 seconds, it is preferable to use maximum velocity or spectral intensity; for structural periods less than 0.2 seconds, they suggested that the maximum acceleration or root mean square of the strong phase of the ground acceleration be used.

In most of these studies, structural damage was measured by the maximum displacement reached only once in the course of the ground shaking. When inelastic deformation is likely, other response quantities may provide additional insight into the behavior of the system [Refs. 53, 57]. For example, the maximum inelastic excursion during one cycle, the total cumulative inelastic deformations, or other factors may be important parameters for structures with limited

energy dissipation capacity. Thus, inherent in characterizing ground motion intensity is how structural damage is quantified. Given this fact and the inconsistencies in the previously mentioned findings, it appears that a comprehensive study using a variety of parameters and damage indices should be undertaken.

2.2 Scope of Study

A preliminary investigation on the effectiveness of various schemes for characterizing the intensity of a ground motion for structures that respond inelastically is reported herein. Intrinsic in this objective is the desire to scale ground motion records for the purposes of practical seismic response analysis and design. In such cases, it is frequently necessary to use an ensemble of records to ensure that a design does not depend on the features of one particular record. However, the records used should all have an intensity capable of producing similar overall levels of damage. Thus, guidelines for scaling ground motions in such cases are needed with a clear statement on limitations. Of course, it is expected that a comprehensive solution can not be reached herein, but that the relative effectiveness of various proposed intensity indices can be evaluated.

In this study, two sets of ground motions are used. One set contains five horizontal components of ground and free field motion recorded at the Imperial County Service Building during the 1979 Imperial Valley earthquake. These records represent motions with the same source and magnitude on similar site soil conditions. The other set of ground motions includes various moderate earthquake records obtained at different distances to the source on sites with "firm" soil conditions. Both sets are listed in Table 2.1. In view of the preliminary nature of this study, buildings are represented as single-degree-of-freedom systems. They are assumed to have 5% viscous damping and elasto-perfectly plastic hysteretic characteristics. The structural periods considered range from 0.1 sec to 2.0 sec at 0.1 sec intervals.

2.3 Characterization of Ground Motion Intensity

Many intensity indices and schemes have been suggested for characterizing ground

motion intensity. In order to achieve a compromise in design between the need for accuracy and simplicity, especially in the preliminary stages, only those parameters that can be easily deduced from geotechnical, seismological and structural information are considered in this study.

Intensity indices considered herein are grouped into two basic categories. In one category, indices are obtained from the basic features of the ground motion itself; in the other, indices are derived from information on the structural response these ground motions would produce

2.3.1 Parameters Based on Ground Motion Features

Various measured and derived parameters based on ground motion records have been used to characterize intensity. The measured parameters include the instrumental peak ground acceleration, velocity and displacement. Of these, the instrumental peak ground acceleration has been most commonly used because it is conceptually simple and easily obtainable. Various derived parameters have also been used. These include Arias intensity [Refs. 2, 5, 46], root-mean-square acceleration [Refs. 37, 41, 51, 55, 102] and Fourier amplitudes of the ground acceleration record at certain period values [Ref. 27].

Arias intensity (AI) represents, for a given earthquake and zero damping, the amount of total energy per unit weight absorbed by a series of elastic single-degree-of-freedoms with fundamental frequencies uniformly distributed between zero and infinity [Refs. 44, 46]. It is calculated as:

$$AI=\frac{\pi}{2g}\int_{T_{0.05}}^{T_{0.95}} \ddot{u}_g^2 dt$$

where $T_{0.05}$ and $T_{0.95}$ are the times at which the above integral reaches 5% and 95%, respectively, of the ultimate value. The equation can also be written as

$$AI=0.90\frac{\pi}{2g}\int_{0}^{\infty} \ddot{u}_g^2 dt$$

There are questions about how the total duration should be defined with this parameter; in this study, duration is defined as the entire length of time for which the ground motion record is

considered.

Root-mean-square acceleration (RMS) is defined as:

$$RMS=\sqrt{\frac{1}{T_{0.95}-T_{0.05}}\int_{t_{0.05}}^{T_{0.95}}\ddot{u}_g^2dt}=\sqrt{\frac{0.9}{T_{0.95}-T_{0.05}}\int_0^{\infty}\ddot{u}_g^2dt}$$

As the definition implies, root-mean-square acceleration represents a level of modified average acceleration for the record. By comparing it with the definition of Arias Intensity, it can be seen that RMS is also related to the square root of the amount of total energy per unit weight per unit time absorbed by a series of single-degree-of-freedom systems uniformly distributed between the frequency interval of zero and positive infinity. It has also been suggested that RMS could be related to the acceleration level having a particular probability of exceedance in a recorded accelerogram [Ref. 62] or in a stationary Gaussian ground motion [Ref. 97].

To improve intensity characterization for structures in different period ranges, Cornell *et al* have proposed using Fourier amplitudes (FAS) obtained for the ground acceleration record at 0.25 sec, 1.0 sec and 3.33 sec. These would be used as ground motion intensity indices for structures in the short, intermediate and long period ranges, respectively. Fourier amplitude of ground acceleration at a particular frequency, ω, can be computed by [Ref. 45]

$$FAS=\{[\int_0^T\ddot{u}_g(\tau)\cos\omega\tau d\tau]^2+[\int_0^T\ddot{u}_g(\tau)\sin\omega\tau d\tau]^2\}^{1/2}$$

where τ is a dummy integration variable. To improve stability, smoothing Fourier amplitudes over the neighboring period ranges was suggested by Cornell *et al*.

2.3.2 Parameters Based on Elastic Structural Response

Since the above parameters do not account for the effects of ground shaking on the structure, a variety of parameters have been proposed based on computed elastic response. Period independent parameters such as spectral intensity (standard and modified) have been used as well as period dependent indices such as spectral quantities evaluated at certain specific natural periods or period ranges. Spectral intensity (SI) has been proposed by Housner as a measure of ground motion intensity [Refs. 40, 42, 43]. It is defined as the area enclosed by the elastic

pseudo-spectral velocity spectrum of the corresponding ground motion between the periods of 0.1 sec and 2.5 sec

$$SI(\xi,T)=\int_{0.1}^{2.5} PSV(\xi,T)dT$$

In this fashion, spectral intensity attempts to relate the strength of ground shaking with the peak elastic response of a range of single-degree-of-freedom systems with periods commonly found in civil engineering practice. This index can be defined for any amount of viscous damping. Housner [Ref. 40] noted that relative intensities of several earthquake records varied depending on the value of damping assumed. This is apparently because the response of lightly damped structures is more sensitive to duration than that of more heavily damped systems. In this report, spectral intensities are computed based on 5% and 20% damping.

In their studies of ground motion normalization procedures, Nau [Ref. 64] and Kennedy [Ref. 52] found that spectral intensities calculated over local period ranges provide improved reliability for structures with fundamental periods in these ranges. Nau suggested three period ranges (low, intermediate and high) for computing spectral intensity.

This dependence of the apparent intensity on structural period was recognized earlier by Newmark *et al* in their recommendations for constructing response spectra based on peak ground acceleration, peak ground velocity and peak ground displacement [Refs. 58, 65, 66, 67, 68, 69]. Kennedy refined this approach by computing a modified SI based on a range determined by the initial fundamental period of the structure and an assumed design ductility of the structure, using a variety of weighting functions. Although this modified spectral intensity has produced extremely reliable results, it is not suitable for general quantification of ground motions and will not be considered here.

2.3.3 Response Magnitude Effect

For all of the preceding intensity indices, earthquake intensity is independent of the damage produced. Thus, for all of the indices considered except Arias intensity, if the original ground motion is scaled by a factor of N, the intensity index is also scaled by N. For Arias

intensity, if the original ground motion is scaled by a factor of N, the intensity index will be scaled by N^2. Whether either of these variations is reasonable can be illustrated by considering a SDOF structure (with, for example, a 0.2 second period and 5% viscous damping) subjected to two different ground motions: the S15W Pacoima Dam record and the EW 1940 El Centro record. The values of any of the previous intensity indices will be denoted as I_{el} and I_{pa}, respectively. The yield strength of the structure is selected such that it is just on the verge of yielding when subjected to the unscaled EW 1940 El Centro record. Let $N_{el}^{(1)}$ denote the factor by which the EW 1940 El Centro record must be scaled to produce a displacement ductility of 1 (i.e. $N_{el}^{(1)}$ is unity). Similarly, let $N_{pa}^{(1)}$ denote the factor by which the S16W Pacoima Dam record must be scaled to have the same peak displacement ductility as the EW 1940 El Centro record. If the ground motion intensity considered is independent of response magnitude, we would have

$$I_{el} \times N_{el}^{(1)} = I_{pa} \times N_{pa}^{(1)} \quad \text{for } \mu = 1$$

for intensity indices that vary linearly with the ground motion, and

$$I_{el} \times (N_{el}^{(1)})^2 = I_{pa} \times (N_{pa}^{(1)})^2 \quad \text{for } \mu = 1$$

for intensity indices that vary quadratically with the ground motion. Rearranging the equations, we get

$$\frac{N_{pa}^{(1)}}{N_{el}^{(1)}} = \frac{I_{el}}{I_{pa}}$$

or

$$\frac{(N_{pa}^{(1)})^2}{(N_{el}^{(1)})^2} = \frac{I_{el}}{I_{pa}}$$

for the linearly and quadratically varying intensity indices, respectively. Since $\frac{I_{el}}{I_{pa}}$ is assumed constant regardless of the displacement ductility, the ratio, $\frac{N_{pa}^{(1)}}{N_{el}^{(1)}}$, should be constant for linearly varying intensity indices. Similarly, for quadratically varying intensity indices, the ratio, $\frac{(N_{pa}^{(1)})^2}{(N_{el}^{(1)})^2}$, should be constant. The actual ratios derived for the case cited above are computed

for different displacement ductilities and plotted in Figure 2.2. As can be seen, the ratios are not constant, implying that both categories of intensity indices are susceptible to a response magnitude effect. Similar observations have been made by Vanmarcke [Ref. 96] and Bertero *et al* [Ref. 14]. They cautioned that scaling should be limited to avoided distortion of ground motion effects on nonlinear response. Thus, it is important to recognize that there is limited range over which ground motion intensities might be used in scaling ground motions.

2.4 Characterization of Structural Response

In addition to the previous considerations, the intensity of a ground motion is related to how damage is measured. To quantify the damage to a structure, maximum displacement ductility (defined as the maximum displacement of the structure divided by the displacement corresponding to overall yielding) is frequently employed as mentioned previously. Other measures taking into account the cyclic nature of the seismic structural response may be more meaningful in assessing the structural damage. In structures with limited energy dissipation capacities, measures of cyclic displacement ductility, accumulative inelastic displacement, hysteretic energy dissipation, and other inelastic response quantities can be defined. The effectiveness of such measures of structural damage is discussed in Ref. 57. When the design of the structure is controlled by the serviceability of structural and nonstructural components or by instability, story drift is also an important parameter. Unfortunately, it is difficult to include all of these factors in a preliminary study and only the maximum displacement ductility and the hysteretic energy dissipation are considered herein. For convenience, the hysteretic energy is normalized as μ_H:

$$\mu_H = \frac{HE}{R_y u_y} + 1$$

where HE is the hysteretic energy dissipation and R_y and u_y are the yield strength and displacement, respectively, of the structure.

2.5 Schemes of Ground Motion Intensity Characterization Considered

Usually a ground motion is characterized by a single intensity index regardless of the structural period, amount of damping in the structure and the expected structural damage level. As mentioned before, ground motion characterization taking into account the initial structural period have also been suggested [Refs. 27, 52, 64]. Typically, three period ranges (short, intermediate and long) are used to categorize the structure.

In this study, the peak ground acceleration, the peak ground velocity, the peak ground displacement, Arias intensity, RMS, Housner spectral intensity at 5% and 20% damping, pseudo-spectral velocity at 5% damping at 0.25 seconds ($PSV_{0.25}$), 1.00 second ($PSV_{1.00}$), and 3.33 sec ($PSV_{3.33}$), and Fourier amplitude of ground acceleration at 0.25 sec ($FAS_{0.25}$), 1.00 second ($FAS_{1.00}$) and 3.33 seconds ($FAS_{3.33}$) are included individually to evaluate their effectiveness. Numerical values for these parameters are listed in Tables 2.2 and 2.3 for the first and second set of ground motions, respectively. In addition, period dependent intensity characterization schemes are included. When the peak ground acceleration, peak ground velocity and peak ground displacement are used to define the intensity of the ground motion in the short, intermediate and long period ranges, respectively, this is denoted as min (A,V,D). Similarly, when $PSV_{0.25}$, $PSV_{1.00}$ and $PSV_{3.33}$ are used to define the intensity of the ground motion in the three period ranges respectively, this is denoted as min(PSV). Finally, when $FAS_{0.25}$, $FAS_{1.00}$ and $FAS_{3.33}$ are used, this is denoted as min(FAS). The three period ranges for each of the three schemes may be different. The precise values of these period ranges are discussed later.

2.6 Method of Evaluation

To evaluate the effectiveness of the various ground motion intensity indices considered, constant ductility spectra were constructed for one reference ground motion from each of the two sets of records mentioned. As will become apparent later, the choice of the reference is arbitrary. Trace 10 from the Imperial County Service Building and the north-south component of the 1940 El Centro earthquake record are selected as the reference ground motions.

Although displacement ductility and normalized hysteretic energy were used as damage indices in both cases, results for the normalized hysteretic energy were presented only for the first set of ground motions. Ductility levels of 8, 4, 2 and 1 are considered for the first set of ground motions; while ductility levels of 4 and 1 are presented for the second set. A ductility level of 1 corresponds to elastic response.

The yield strength required to develop the target ductility value in a system with a given initial period can be found for the reference ground motion. When this system is subjected to other ground motions, different ductility values will usually result. However, these ground motions can be scaled up or down so that the system will develop the target ductility values. Thus, for each ground motion and structural period value, one can obtain the factor by which a ground motion must be scaled to produce the target ductility. These factors will be called the "actual" scaling factors hereafter. They will generally vary with period and ductility level as well as from one ground motion to another.

The actual scaling factors generally differ from that inferred from the parameters used to characterize ground motion intensity. These factors will be denoted as the "predicted" scaling factors. For example, if peak ground acceleration is selected as the intensity index, the predicted scaling factor is computed as the ratio of the peak ground acceleration of the reference ground motion over the peak ground acceleration of the ground motion under consideration. Other predicted scaling factors are computed in a similar fashion except Arias intensity. For Arias intensity, the predicted scaling factor is computed as the square root of the ratio of the Arias intensity of the reference ground motion over that of the ground motion under consideration.

In contrast with the actual scaling factors, the predicted scaling factors do not vary with period. The difference between the predicted scaling factors and the actual scaling factors can be used to measure the effectiveness of a particular intensity index. Consequently, the ratio of the predicted scaling factor to the actual scaling factor is calculated for each ground motion, intensity index, ductility level and period value. A ratio of unity indicates that the particular

intensity index predicts correctly the factor by which one ground motion has to be scaled in order for the system to achieve the target ductility value. In general, these ratios differ from unity and typically, vary with period and ductility level. These ratios will be denoted "effectiveness" ratios. To assess the overall effectiveness of a particular intensity index, the sum of the squares of the deviation of the effectiveness ratio from unity is computed. This sum is accumulated over all ductility levels and all ground motions for the index considered. In order to provide comparable results, mean square error per ground motion per ductility level is calculated for each period value by dividing the sum by the product of the number of ground motions considered (e.g. four for the first set of ground motions and nine for the second set of ground motions) and the number of ductility levels (three for the first set of ground motions and two for the second set of ground motions). In this way, curves of mean square error versus period can be constructed for each of the intensity indices.

Similar curves for the period dependent intensity characterization schemes, such as min(A,V,D), can then be constructed by taking the minimum mean square error value of the three basic intensity indices at each period value. The period values where one of the three intensity indices is selected over the other two can also be determined in the process. However, due to the preliminary nature of this study, no attempt is made here to find the optimal period values.

2.7 Results and Evaluation

2.7.1 Actual Scaling Factors

In Figures 2.3 and 2.4, the actual scaling factor curves of the first set of ground motions for constant displacement ductility and constant normalized hysteretic energy ductility of 4, 2 and 1 are presented. The curve for a displacement ductility of 8 is also shown for Trace 11 to illustrate the response magnitude effect mentioned previously.

Generally speaking, the actual scaling factors for a particular ground motion differ slightly for different ductility levels (Figures 2.3 and 2.4) up to a ductility of 4. They might vary con-

siderably more for a larger ductility, indicating the effect of response magnitude indicated previously. The difference among ductility levels of 4, 2 and 1 seems to be random and there does not appear to be any correlation between ductility level and the actual scaling factor. While actual scaling factors remain nearly constant and close to unity for Trace 11, they frequently deviate from unity by a considerable amount and vary substantially over the period ranges considered. The latter observation suggests that a definition which takes into account this dependence on structural period should be better than one which ignores it. In addition, the actual scaling factors differ considerably among the records, indicating that, even for ground motions recorded at the same site during the same earthquake, the apparent intensity of a ground motion can vary considerably from one record to another as well as for different structural periods. Finally, there does not seem to be much difference in the actual scaling factor between the displacement ductility and the normalized hysteretic energy ductility cases. This is expected since all ground motions in this set have similar durations of ground shaking.

The actual scaling factor curves obtained for the second set of ground motions for constant displacement ductility levels of 4 and 1 are presented in Figure 2.5. For the east-west component of the 1940 El Centro record, the actual scaling factors are nearly constant and relatively close to unity. However, this is not so for records obtained during different earthquakes. For example, the actual scaling factor curves for the north-south component of the Helena record differ greatly from unity and vary quite significantly with period. Once again, there does not seem to be significant correlation between the actual scaling factor and the ductility level, and the actual scaling factors differ considerably among the records.

2.7.2 Mean Square Displacement Ductility Error Curves; First Set of Ground Motions.

To assess the effectiveness of the various intensity indices considered to characterize the above response trends, mean square error curves for all intensity indices are computed. These are presented in Figure 2.6 for the first set of ground motions and the case of constant displacement ductility. Typically, the mean square error curves vary significantly with the initial structural period. In particular, for each intensity index, there are certain period values where the

mean square error curve reaches a minimum. For example, the mean square error curves for peak ground acceleration, pseudo-spectral velocity (at 0.25 seconds) and Fourier amplitude of the ground acceleration (at 0.25 seconds) seem to reach a minimum at the short period range; whereas, the mean square error curves for peak ground velocity, pseudo-spectral velocity (at 1.0 second) and Fourier amplitude of the ground acceleration (at 1.0 second) seem to reach a minimum in the intermediate period range. For peak ground displacement, pseudo-spectral velocity (at 3.33 seconds), and Fourier amplitude of the ground acceleration (at 3.33 seconds), the mean square error curves seem to decrease as period increases. For spectral intensity, the mean square error curve at intermediate and long period ranges seems to be slightly lower than in the short period range. For Arias intensity and root mean square acceleration, the opposite is true.

To further simplify comparison of the effectiveness of the various intensity indices, the averages of the mean square errors over the period range considered in the study (from 0.1 seconds to 2.0 seconds) are computed and listed in Table 2.4 in ascending order. By averaging over period, these indices neglect the fact that one intensity index might be better than others at certain period values. Fortunately, for the more effective intensity indices, the mean square error curves are fairly constant, so that one simple index can be used to compare the overall effectiveness of these intensity indices. From Table 2.4, it appears that spectral intensity at 5% viscous damping is the most effective intensity index with min(PSV) and $PSI_{1.00}$ follow closely behind. Spectral intensity calculated for 20% viscous damping is slightly less effective than for 5% viscous damping. The worst intensity indices are provided by $FAS_{0.25}$, $PSI_{0.25}$, $FAS_{3.33}$ and $PSI_{3.33}$, in that order. The traditionally used intensity index, the peak ground acceleration, seems to be less effective than the spectral intensity, Arias intensity and root mean square acceleration for this set of ground motions. The period dependent intensity scheme of min(A,V,D) is only a slight improvement over the use of peak ground acceleration alone. However, for this set of ground motions, peak ground acceleration seems to be better than peak ground velocity which in turn seems to be better than peak ground displacement.

2.7.3 Mean Square Hysteretic Energy Ductility Error Curves; First Set of Ground Motions.

Because all ground motions in this case have similar durations of strong shaking, it can be expected that the results based on normalized hysteretic energy will be similar to those for displacement ductility. This can be observed from the mean square error curves shown in Figure 2.7. The observations made previously for constant displacement ductility about the tendency of the mean square error curves to reach minima at certain period values are equally applicable here. Similarly, the averages of mean square errors over the period values considered are calculated for the case of constant normalized hysteretic energy and are listed in Table 2.5 in ascending order. The order is the same as for the case of constant displacement ductility. However, because the ground motions used here have similar durations of strong shaking, it should not be concluded that the intensity of a ground motion is independent of how damage of the building is measured.

2.7.4 Mean Square Displacement Ductility Error Curves; Second Set of Ground Motions.

The mean square error curves are presented in Figure 2.8 for the second set of ground motions. Again, the curves tend to decrease toward certain period values, and the trends are similar to those observed previously for the first set of ground motions. Therefore, it appears that these tendencies are related to how good certain intensity indices are in measuring the damaging potential of a ground motion in certain period values. Again, averages of the mean square error curves over the period ranges considered are calculated to facilitate comparisons. These values are tabulated in Table 2.6 in ascending order. Comparing the values of the average mean square displacement ductility error in Table 2.6 to those in Table 2.4, it seems that the values in Table 2.6 are usually considerably greater than those in Table 2.4 for the corresponding intensity indices (except for $PSV_{0.25}$ and $FAS_{0.25}$). This is expected since Table 2.6 corresponds to the second set of ground motions which includes a diversified grouping of ground motions. For $PSV_{0.25}$, even though the average mean square error is higher for the first set of ground motions than for the second set of ground motions, the mean square errors in the short period range, where $PSV_{0.25}$ is more effective than at other period ranges, are actually

lower for the first set of ground motions than those for the second set (compare Figures 2.6 and 2.8). However, for $FAS_{0.25}$, both the average mean square error and mean square errors in the short period range, where $FAS_{0.25}$ is also more effective than at other two period ranges, are higher for the first set ground motions than those for the second set. This is due to the inherent unstable nature of FAS which may vary considerably for slight change in period value. As mentioned previously, to improve stability, Cornell *et al* suggested smoothing FAS over the neighboring period ranges.

In addition, the order of ranking of the intensity indices has changed also. For the second set of ground motions, min(A,V,D) represents the best way to define ground motion intensity. This conclusion differs from that reached by Nau [Ref. 24]. For a similar set of ground motions, Nau concluded that sums of pseudo-spectral velocity values over short, intermediate and long period ranges represent a better definition of ground motion intensity than min(A,V,D). The difference may be due to two factors. First of all, instead of the averages of the pseudo-spectral velocity values over short, intermediate and long period ranges, $PSV_{0.25}$, $PSV_{1.00}$ and $PSV_{3.33}$ are used in this study. These values would tend to fluctuate more than the average over the neighboring period range. Secondly, the method of evaluation differs from that used by Nau. In Nau's study, ground motions were first scaled to have the same intensity index. The scaled ground motions were then used to construct constant displacement ductility spectra. The differences among the spectra were then measured by the coefficient of variation of the required yield strengths. In the study here, the ground motions are scaled to achieve the same ductility. This requires different scaling factors for different period values. The differences between the actual scaling factors and those predicted by the intensity indices are measured for evaluating the effectiveness of the intensity indices.

The conclusion reached for the second set of ground motion records also differs from that for the first set. While the reasons for this are not perfectly clear, the difference suggests that a single simple index may be unable to characterize the damaging potential of strong earthquake ground motions.

From Table 2.6, it appears that if a period independent intensity index were to be selected, Arias intensity (or root mean square acceleration) and peak ground velocity are equally the most effective intensity indices. Peak ground acceleration is slightly worse than peak ground velocity. Spectral intensity, at 5% viscous damping, which is the most effective intensity index for the first set of ground motions, becomes slightly less effective than peak ground acceleration. This may be due to the inability of SI to differentiate among different spectral shapes. For the first set of records, spectra are similar and SI worked well. However, the spectral shapes for the records in the second set vary considerably. In addition, spectral intensity at 20% viscous damping performed better than at 5%, reversing the observation of the first record set. However, the differences between the results for spectral intensities at 5% and 20% viscous damping are small in both cases. Other changes in the order of ranking can be directly observed by comparing between Tables 2.4 and 2.6.

2.8 Summary and Conclusions

A preliminary investigation on the effectiveness of various schemes for characterizing the intensity of a ground motion for structures that response inelastically has been reported. Inherent in this study is the desire to scale ground motions for the purpose of practical seismic response analysis and design. Results are obtained for single-degree-of-freedom systems with elasto-perfectly plastic hysteretic characteristics and 5% viscous damping, considering two sets of ground motions and two measures of structural damage.

It seems that there is a limited range over which ground motion intensity parameters might be used for scaling. This should always be noted in applying the results of this study. From observations of Figures 2.3, 2.4 and 2.5, there does not appear to be any correlation between ductility level and the "actual" scaling factor. These factors may deviate considerably from unity and vary with structural period. In addition, they differ substantially among the records, indicating the apparent intensity of a ground motion can vary quite significantly even for ground motions recorded at the same site during the same earthquake. A definition of ground motion intensity which takes the period dependence into account will generally be

better than a definition which ignores it.

For the first set of ground motions consisting of ground motions from the same earthquake site, spectral intensity at 5% viscous damping has been found to be the most effective index for characterizing the damaging potential of a ground motion. It appears that spectral intensity calculated for different viscous damping values may be equally effective. However, for the second set of ground motions, min(A,V,D) is the most effective ground motion intensity index. If only one intensity index is wanted for this set of ground motion records, Arias intensity and peak ground velocity are equally effective. The difference in the best intensity indices between the two sets of ground motions suggests that a single simple index may be unable to characterize the damaging potential of strong earthquake ground motions.

Because the results are based on a limited number of structural damage indices and ground motion records, additional research using other structural damage indices and more ground motion records to include near-fault ground motion records which tend to contain acceleration pulses, is recommended. In addition, because the results are based on ground motion records of similar durations (first record set), the effectiveness of using hysteretic energy as a damaging index has not been fully explored. Extension of these studies to consider other structural viscous damping and hysteretic characteristics is also desired.

CHAPTER 3 INELASTIC RESPONSE SPECTRUM METHOD

3.1 Introductory Remarks

In the design of buildings to resist strong earthquakes, it has been recognized that the energy associated with inelastic deformations can be utilized to reduce the design forces. To facilitate such design, analytical methods have been developed based on step-by-step integration of the equations of motion derived from some convenient coordinate system. Frequently, step-by-step integration is time consuming even for simple structures. To expedite computation, it has been suggested [Refs. 12, 32, 33, 39, 61, 70, 74, 80, 84, 90] that the equations of motion be transformed to the initial linear elastic mode shape coordinate system before performing the step-by-step integration. The idea is to take advantage of the fact that for linear elastic structures under seismic excitation, only the response from the first few modes is usually significant.

A similar technique for reducing the number of degrees of freedom to be considered in static analyses of nonlinear structures has been suggested using linear buckling shapes as a new basis [Refs. 1, 63, 74]. While transformation to the initial linear elastic mode shape (hereafter called simply initial mode shape) coordinate system for inelastic structures leads to coupled equations, it has been shown [Refs. 12, 32, 33, 39, 61, 70, 73, 80, 84, 90] that computational efforts can be reduced by considering a smaller number of equations or by using larger integration time steps in the modes considered, or both. Variations exist among the implementations of the modal transformation concept. Some [Refs. 33, 39, 61, 70, 80] have suggested updating the mode shapes, using the current tangent stiffness matrix, at sufficient intervals to reduce the amount of coupling. Others [Refs. 32, 90] recommend that the difference between the actual nonlinear force and the ideal linear resistance force evaluated for the current displacement be treated as an additional force input into the system.

In spite of these apparent increases in computational efficiencies, these step-by-step integration methods are still unsuitable in the preliminary stage of design where many analyses

are needed to evaluate the sensitivity of response to various system and ground motion parameters. Frequently, only the estimates of maximum response quantities are needed, rather than detailed time history data. For elastic and inelastic single-degree-of-freedom systems, response spectra are commonly used as a design aid, since various maximum response quantities of interest can be easily obtained. For linear elastic MDOF systems, peak modal response quantities can also be estimated from response spectra. Maximum structural response quantities in the original coordinate system can then be estimated by appropriately combining the corresponding maximum modal response quantities. This method is commonly referred to as the response spectrum method and can be generalized to any orthogonal set of Raleigh-Ritz vectors. However, the response spectrum method based on modal transformation is most frequently used.

The implementation of the response spectrum method for the analysis of inelastic multiple-degree-of-freedom systems is not straight-forward. While modal response of a linear elastic MDOF system can be computed independently, modal response becomes coupled once the structure becomes inelastic. It is uncertain how the modes interact with each other. For the simple case of one "mode" dominating the response, modal interaction may be ignored. Furthermore, if all the members of the structure yield simultaneously, then the response of this multiple-degree-of-freedom systems can be approximated by the response of an elasto-perfectly plastic single-degree-of-freedom system. Unfortunately, this is not always the case.

Several procedures [Refs. 3, 6, 10, 13, 16, 17, 38, 54, 56, 91, 98, 99, 100] have been used in implementing the response spectrum method for inelastic systems. The reliability of these procedures have been investigated. It was found [Refs. 98 and 99] that the approximate design rules for single-degree-of-freedom systems can, for all practical purposes, be extended to two and three -degree-of-freedom shear-beam type structures with either uniform or "elastically balanced" stiffness distributions. For these same systems with more than three degrees-of-freedom, the design rules proposed for single-degree-of-freedom systems [Refs. 65, 66, 67, 68, 69] are not sufficient and may lead to an unconservative estimate of maximum deformation and

required resistance [Refs. 98, 99]. Furthermore, it was found that the errors tend to increase as the number of degrees-of-freedom increases. Other studies have been conducted for multiple-degree-of-freedom moment-resisting frames. It was found [Refs. 3, 19, 38, 54] that the average ductility factor of all the members is reasonably close to the intended level; however, local ductility demands may be excessive leading to an unacceptable design. To gain insight about the way in which conservatisms and unconservatisms are introduced, Baggett and Martin [Ref. 10] conducted a parametric study of two-degree-of-freedom systems. Based on the results obtained for a single artificial ground motion, they found the inelastic response spectrum method was, in general, conservative. It appears from these studies that the response spectrum method can be used for the preliminary analysis of inelastic MDOF systems; but, further refinement in the implementation of the method is needed.

3.2 Equation of Motion

For structures subjected to earthquake loadings, the equation of motion in some convenient coordinate system can be written as

$$[M]\{\ddot{u}\}+[C]\{\dot{u}\}+\{R(\{u\})\}=-[M]\{r\}\ddot{u}_g \tag{3.1}$$

where $[M]$, $[C]$ are the mass matrix and damping matrix, of the structure respectively. The resistance of the structure is denoted by $\{R(\{u\})\}$. The displacement response of the structure is denoted by $\{u\}$, with a dot representing differentiation with respect to time. The earthquake base excitations are represented by $-[M]\{r\}\ddot{u}_g$, where $\{r\}$ is a vector relating the structural degrees of freedom to the ground movement while $\ddot{u}_g$ denotes the ground acceleration.

To gain insights on modal coupling and the extent of modal interaction when a MDOF structure yields, it is illustrative to examine the response of a structure in its initial modal coordinate system. This may be carried out by computing the structural response in the original coordinate system and then transforming the response to the initial modal coordinate system. It should be emphasized that this change of basis can be done for both linear elastic as well as inelastic structures. After the transformation, we obtain

$$[M_n]\{\ddot{Y}\}+[C_n]\{\dot{Y}\}+[\phi]^T\{R(\{Y\},\dot{Y})\}=-\{\Gamma_n\}\ddot{u}_g \tag{3.2}$$

where

$$[M_n]=[\phi]^T[M][\phi]$$
$$[C_n]=[\phi]^T[C][\phi]$$
$$\{\Gamma_n\}=[\phi]^T[M]\{r\}$$

and $[\phi]$ is a matrix whose columns consist of the mode shape vectors derived from the elastic stiffness matrix of the structure. The vector $\{Y\}$ is related to $\{u\}$ by $\{u\}=[\phi]\{Y\}$, and represents the generalized displacements in the initial modal coordinates. The transformed mass matrix, $[M_n]$, is diagonal. If damping is mass or stiffness proportional, or both, the transformed damping matrix, $[C_n]$, is also diagonal. When the structure becomes inelastic, the set of equations will be coupled, however, because $[\phi]^T\{R(\{Y\},\dot{Y})\}$ (the product may be called the modal force vector) depends on all the generalized displacements. For small amounts of nonlinearity, analyses can be greatly simplified by neglecting the coupling. However, when significant amount of nonlinearity is expected, the transformed set of equations will be highly coupled.

The transformed equations can be written in component form as follow

$$M_i\ddot{Y}_i+C_i\dot{Y}_i+\{\phi_i\}^T\{R(\{Y\},\dot{Y})\}=-\Gamma_i\ddot{u}_g \tag{3.3}$$

where M_i and C_i are the "i"th diagonal terms of the transformed mass and damping matrix, respectively. It is desirable to replace the equations by

$$M_i\ddot{Y}_i+C_i\dot{Y}_i+R_i(Y_i,\dot{Y}_i)=-\Gamma_i\ddot{u}_g \quad i=1,\ldots,n \tag{3.4}$$

where $R_i(Y_i,\dot{Y}_i)$ depends only on Y_i in a nonlinear manner. In such a case, it is possible to evaluate modal response independently and to implement the response spectrum method for the analysis of inelastic MDOF systems.

3.3 Scope Of Study

The purpose of the study in this chapter is to explore and evaluate a rational procedure for implementing the response spectrum method for preliminary analysis of inelastic multiple-degree-of-freedom systems. For this purpose, inelastic structural response is examined in the

initial modal coordinate system. Particular attention is focused on the independence of the modal responses and the relative change in response contributions of the modes (i.e. whether or not higher mode contributions increase as a result of yielding and, if so, how much).

The analytical and design implications of the observed modal behavior are discussed. Tentative definitions of modal yield strength, yield displacement and modal ductility are offered. Expressions relating the defined modal ductility to story ductility are derived. The reliability of the defined modal hysteresis model for predicting response is assessed. A procedure for implementing the response spectrum method for analysis of inelastic MDOF systems and its reliability are discussed.

3.4 Inelastic Structural Response in the Modal Coordinate System

The purpose of this section is to study the inelastic structural response of some typical uniform buildings in their modal coordinate systems. While Raleigh-Ritz coordinate systems could also be used, initial modal coordinates are used exclusively herein due to their prevalence in design. The observations made here will form the basis for formulating a procedure for implementing the response spectrum method for the analysis of inelastic multiple-degree-of-freedom systems.

For simplicity in analysis, only shear-beam type buildings are considered. All the buildings have uniformly distributed mass, linearly distributed story stiffness and elasto-perfectly plastic story force-displacement relationships. Mass and stiffness proportional damping has been assumed for the buildings with 5% damping in the first and last mode. The earthquake excitation used is the east-west component of the 1934 El Centro earthquake ground motion.

3.4.1 Building Number One

To investigate the modal hysteretic characteristics, a five-story shear building is analyzed in its original coordinate system by the computer program, DRAIN-2D [Ref. 77]. The story strengths are derived from the Uniform Building Code requirements, including a concentrated force at the roof to account for higher mode effects. To account for safety factors encountered

in design, these working stress level story shears are tripled. The physical and modal properties for the structure are summarized in Tables 3.1 and 3.2. The mode shape vectors are calculated and normalized so that their vector lengths are unity (see Table 3.2). The structure is analyzed for the 1934 El Centro (EW) earthquake ground motion [Figure 3.1]. To ensure sufficient inelastic deformation, the ground motion is scaled up by a factor of two. The resulting time histories of the lateral story displacement vector and the resistance force vector ($\{R(u)\}$ in Eq. 3.1) are then transformed into the initial modal coordinate system so that the effects of inelastic deformation of the structure on the modal response and the modal hysteretic characteristics can be examined.

The relationships between story shear and story drift are plotted in Figure 3.2. From these figures, it appears that moderate amount of inelastic deformation occurs in every story. The peak story drift ductilities are listed in Table 3.2. It seems that story ductilities are generally uniform, ranging from 1.2 to 1.8. This may not be always the case, as other investigations [Refs. 22, 23, 24, 79] have reported that ductilities may be concentrated in some stories. The observed uniform ductility distribution can be attributed to the dominance of the first mode in the structural response and the similarity between the resistance force vector when all stories are yielding in the same direction, $\{R_1\}$ and the external force required to displace the building in the first mode (see Figure 3.3).

The relationships between $\{\phi_i\}^T\{R(\{Y\})\}$ and Y_i for the five modes are shown in Figure 3.4. It appears that only the first mode exhibits significant hysteretic loops. These resemble the elasto-perfectly plastic characteristics of the members of the structure. However, the transitions to yielding and to unloading are not as sharp. The gradual transitions are due to progressive story yielding.

Since the first mode exhibits significant hysteretic loops, its modal response merits further examination. The computed instantaneous first mode "stiffness" when the structure yields along with the yielding stories are listed in Table 3.4. It appears that when the structure is partially yielding (not all the stories are yielding), the values of the first mode's tangent "stiffness"

can be erratic, ranging from negative to greater than the initial elastic modal stiffness. The structure is in partially yielding when it is in transitions from elastic to complete yielding or when ground shaking is not strong enough to cause a complete yielding of the structure (all the stories are yielding).

Some of the negative stiffness values occur when the earthquake load and the modal displacement, $\{Y\}$, continue to increase. This is because some stories are observed to unload and become elastic while the increasing earthquake loads further concentrate inelastic deformation in those stories that continue to yield. This changes the shape of the resistance force vector, $\{R\}$. Thus, the "modal force", which is the product of the transpose of the first mode shape vector and the resistance force vector, may decrease, while modal displacement increases. Consequently, the effective tangent modal stiffness becomes negative. On the other hand, the first mode tangent "stiffness" has been observed to increase above the initial elastic modal stiffness on occasions. This occurs when the overall magnitude of the resistance force vector increases while one or more, but not all, of the stories are yielding. Because the yielding is localized to few stories, the displacement vector is highly distorted making higher mode contribution more significant and lower mode contribution less significant. This leads to a proportionally less first mode displacement and therefore higher first mode stiffness.

For the building considered here, the amount of time during which these erratic hysteretic characteristics occur is short so that generally speaking, the hysteretic curve for first mode is fairly stable and resembles the elasto-perfectly plastic characteristics of the members of the structure. Furthermore, it can be estimated from Figure 3.4 that the first mode ductility is about 1.5 which corresponds to the average of all the story ductilities.

Superficially, it appears that the product, $\{\phi_1\}'\{R_1\}$ is the maximum force that can be developed in the first mode, where $\{R_1\}$ is the vector of story yield strengths. This may be the case if $\{R_1\}$ is parallel to $\{\phi_1\}$. However, this is not always the case and there may be some resistance force vector, $\{R(\{Y\})\}$, which, by being closer in direction to the first mode shape vector than, $\{R_1\}$, produce a higher effective modal force than the product, $\{\phi_1\}'\{R_1\}$. For the

present building, the shapes of the first mode shape vector and the resistance force vector, $\{R_1\}$, are generally similar (see Figure 3.5). Thus, the product, $\{\phi_1\}^T\{R_1\}$, may actually represent the maximum force in the first mode of the building.

To examine the degree to which the interference from other modes resulting from yielding of the structure affects the displacement response in the first mode, trials were made to find an elasto-perfectly plastic single-degree-of-freedom system which, when subjected to the EW 1934 El Centro ground motion, would result in the same maximum displacement as that of the maximum first mode displacement, $Y_{1,max}$, of the present building. The single-degree-of-freedom system has the same period and damping as the first mode of the building. While it may be possible to find an equivalent inelastic single-degree-of-freedom system that results in the same maximum modal displacement in spite of significant modal interference, the required yield strengths will usually be different if significant modal interference exists. In the present case, the required yield strength of the single-degree-of-freedom system is found to be 9.90 Newtons compared to 9.98 Newtons, the maximum of the product, $\{\phi_1\}^T\{R\}$. So, it appears that the interference from other modes is insignificant. This is also evident by comparing the displacement time histories of the equivalent single-degree-of-freedom system and of the first mode of the building, as shown in Figure 3.6. It seems that the two time histories are almost identical except towards the end. This may be due to the slight difference in the maximum displacements which are not exactly matched. In addition, the period and damping values used for the equivalent single-degree-of-freedom system are not the exact values corresponding to the first mode of the building under study as a result of truncation. These factors and modal interference may largely account for the difference towards the very end of the displacement time histories.

To the extent that the well-behaved first mode hysteretic characteristics are due to the similarity between the story yield strength distribution and the story shear forces induced in the first mode, there is a need for further investigation for other buildings and ground motions. In the next section, a building will be studied which has been designed so that the first two modes

both contribute significantly to the story shear.

3.4.2 Building Number Two

This building has the same uniform mass distribution as building number one. The story stiffness is again linearly distributed and story hysteretic characteristics are assumed to be elasto-perfectly plastic. However, the new building has an initial fundamental period of 1.60 seconds compared to 0.53 seconds for the last building. From an examination of the elastic pseudo-acceleration spectrum [Figure 3.7], it is estimated that the response of the first two modes is expected to contribute to the response. The story shear strengths are again derived from the Uniform Building Code which provides a concentrated force at the roof to account for higher mode effects. However, to obtain a desired level of yielding, no factor of safety is used to increase story strengths of this building. Moreover, the structure is analyzed for three times the 1934 El Centro (EW) earthquake ground motion. The physical and modal properties for this building are summarized in Tables 3.5 and 3.6. The mode shape vectors normalized so that their vector lengths are unity are identical to those for building number one. The resulting analysis time histories of the lateral story displacement vector and the story resistance force vector are again transformed to the initial modal coordinate system.

The relationships between the story shear and story drift are shown in Figure 3.8. From these plots, it appears that a moderate amount of inelastic deformation occurs in all stories. The peak story drift ductilities are listed in Table 3.3 and range from 1.5 to 5.0, with an average of 2.8 and a coefficient of variation of 0.51. It appears that the story strengths, distributed according to UBC recommendations, now result in story ductilities far from uniform.

The relationships between $\{\phi_i\}^T\{R(t)\}$ and Y_i for the five modes are shown in Figure 3.9. In terms of modal displacement, only the first three modes are significant. However, to evaluate story deformation requirements, it is useful to examine the story drifts corresponding to the maximum modal displacements because the shapes of higher modes are more irregular than those for the lower modes. This will give some insight into the contribution of each mode to the story ductility requirements. These are shown in Figure 3.10. It seems that only the

first three or four modes are significant in deforming the building.

By examining the modal hysteretic characteristics in Figure 3.9, it appears that the hysteresis loops of the first two modes are similar to an ideal bilinear model. For the third mode, "yielding" seems to occur at very small modal forces. It may be difficult to model this mode independently as being bilinear. Because the response for the fourth and fifth modes is less significant, it may not be necessary to model them at all.

3.4.3 Building Number Three

It was observed that building number two did not have very uniform story ductilities when subjected to the 1934 El Centro (EW) earthquake ground motion. This is apparently a consequence of the contribution of the higher modes to the response. In this section, an attempt is made to modify the story strengths to achieve a more uniform story ductility distribution.

For this building, all properties are the same as for building number two except the story strengths are modified as follow:

$$F_{j,y}^{new} = \frac{\mu_{all}}{\mu_{all,1}} F_{j,y}^{old} \tag{3.5}$$

where $F_{j,y}$ is the required jth story strength and $\mu_{all,j}$ is the jth story ductility. In this way, stories with ductilities higher than the first story ductility will have their strengths increased, while stories with ductility smaller than the first story ductility will have their strengths decreased. The choice of first story as reference here is arbitrary; in practice, one might use the desired ductility level to change all values of $F_{j,y}$. The resulting physical properties for the building are summarized in Table 3.7. The modal properties are the same as those in Section 3.4.2. The structure is again subjected to three times the 1934 El Centro earthquake ground motion in the east-west direction. The resulting time histories of displacement vector and resistance force vector are again transformed to the modal coordinate system.

The resulting story ductilities are listed in Table 3.6. They range from 1.7 to 2.7, with an average of 2.4 and a coefficient of variation of 0.19. Compared to the building in the last

section, the story ductilities are more uniformly distributed, indicating the modification of story strengths by Eq. 3.5 is satisfactory.

Once again, the first three or four modes contribute significantly to the story deformation requirements as can be seen from the plot in Figure 3.11 of story drifts corresponding to each of the maximum modal displacements. The modal hystereses for the first three modes are shown in Figure 3.12. They are very similar to those of building number two.

3.4.4 Building Number Four

Rather than using the time consuming iterative procedure suggested in the previous section to reduce the variation in story ductility demands resulting from higher mode effects, it would be desirable to obtain a better starting story shear strength distribution by using response spectrum and modal analysis procedures. It is thus interesting to compare the response of a building designed according to the simplified UBC shear distribution and that of a building designed using an elastic response spectrum. Maximum story shears are estimated by combining the peak story shears due to each mode, obtained from the elastic response spectrum, by the square-root-of-the-sum-of-the-square modal combination (SRSS) method. These elastic story shears are then reduced to achieve a comparable level of inelastic deformations and assigned as design story shear strengths. For this building, the reduction factor used for each mode is constant and selected such that the first story yield strength (base shear) is the same as that of building number two. The reduction factor is found to be 3.42. The physical properties for the building are summarized in Table 3.8. The normalized mode shape vectors and other modal properties are the same as those in Section 3.4.2. The structure is again subjected to three times the 1934 El Centro earthquake ground motion in the east-west direction. The resulting time histories of the displacement vector and the resistance force vector are transformed to the initial modal coordinate system.

The resulting story drift ductilities are listed in Table 3.3. They range from 1.9 to 3.2 with an average of 2.4 and a coefficient of variation of 0.17. Compared to building number two, which is designed according to the UBC distribution, the present story ductilities are

smaller (even with the same base shear) and more uniformly distributed. It should be noted that in practice, the reduction factors needed to reduce the story strengths obtained from elastic response spectrum method for uniform story ductility and desired level of deformation are not known, so that a direct application of such method may be difficult. This example merely shows the need for incorporating the effects of higher modes when they contribute significantly to the story ductility requirements.

Once again, only the first three modes exhibit significant modal hystereses, these hystereses are shown in Figure 3.13. They are very similar in character to those observed previously.

3.5 Analytical and Design Implications

To implement an response spectrum method for analysis of inelastic MDOF systems, it is necessary to have some hysteretic model to characterize the modal behavior of the structure. While it is recognized that the modal behavior can be highly coupled, the observed relationship between the transformed displacement and force vectors in the initial modal coordination system suggests that simple hysteretic models may be used to independently describe the behavior in each of the more significant modes. The purpose of this section is to develop a simple modal hysteresis model, examine some of the problems with the model and evaluate the current practices of implementing the response spectrum method in terms of this model and the observed modal behavior.

3.5.1 Modal Hysteresis Model

Based on the observed form of the transformed modal responses, the modal hysteresis model is assumed to be elasto-perfectly plastic. Definitions of modal yield strength and yield displacement are developed. Subsequently, the relationship between modal ductilities and story ductilities will be demonstrated.

The modal yield strength of a given structure is defined as $\{\phi_i\}^T[K]\{\phi_i\}Y_i$, where $\{\phi_i\}Y_i$ is the maximum distortion of the structure in the direction of that mode shape vector just

before any yielding in the structure occurs. The modal yield displacement is denoted as Y_n. The definition of modal yield point is illustrated in Figure 3.14. Assuming no interference from other modes, this modal yield point corresponds to the point on a plot of modal force versus modal displacement where deviation from the initial linear elastic path starts. For simplicity, the modal yield strength will be denoted by $\{\phi_i\}^T\{R_i\}$ for the ith mode. Note this differs from the total story yield shear capacity, $\{R_i\}$, defined in Section 3.4.1. While the defined modal yield point corresponds to a distinct point on the modal force-displacement plot, depending on the story yield strength distribution, the modal force may increase until all stories yield, increase to a certain point then starts to decrease until all stories yield, or may decrease until all stories yield beyond the modal yield point (see Figure 3.15). The modal force will remain constant once all stories have yielded if all members of the structure have elasto-perfectly plastic force-deformation relationship.

Up to now, in defining the modal yield point, it has been assumed that each mode acts independently and that maximum modal responses not only occur at different times, but also that at the time when the response due to any one mode is sufficient to induce yielding in at least one of the stories, the combined response due to all other modes is insignificant. These assumptions are not valid since yielding of the structure depends on the total contributions of all the modes at any instant of time. It is entirely possible for the modal hysteresis loops to deviate prematurely from the ideal curve (like paths a and b in Figure 3.16) as a result of the combined response of all modes. It is also possible that the hysteresis loops would deviate from the ideal curve (like paths c and d in Figure 3.16) due to destructive modal interference delaying structural yielding. Thus, it would greatly improve the modal hysteresis model if the combined response due to all the other modes could be taken into account in determining modal yield strength. Typically, the previous definition of modal yield strength will be satisfactory for those modes that dominate the response, because when the modal response reaches its maximum, the combined response due to all the other modes is likely to be insignificant. For these modes, the defined modal yield displacement will generally be exceeded if the structure under-

goes some moderate amount of inelastic deformation while the defined modal yield strength are developed unless other significant modes (if there are any) also attain their maxima at about the same time. This can be seen by examining the data in Section 3.4.

However, for the less significant modes, the assumption of modal independence is usually not satisfied because the combined response due to the other modes, particularly the dominating modes (even when these modes are not at their maxima), will be greater than or equal to the response of the weak modes. For these weak modes, the modal displacement might also exceed the defined modal yield displacement. Typically, the distribution of the induced story shear force will vary significantly with time if more than one mode is responsive to the ground motion. In this case, it is reasonable to expect that the structure might yield partially for any story yield strength distribution selected. If yielding is concentrated in only certain floors, the displaced shape of the structure can become highly distorted. Consequently, larger modal displacements in the higher modes and slightly smaller modal displacements in the lower modes than would have resulted from a more uniform pattern of yielding can be anticipated. On the other hand, if a structure, whose members all have an elasto-perfectly plastic force-deformation relationship, is yielding completely, each mode would act as if it is yielding independently and there will be no interaction between the modes. While the modal displacements in the higher modes might in these cases exceed the defined modal yield displacements, the corresponding modal forces rarely reach the defined modal yield strengths.

Another point about the modal hysteresis model should to be noted. For the lower modes, modal hysteretic characteristics will generally be bilinear for the type of structure considered here. In general, it is difficult to predict the exact post-yielding stiffness characteristics and the elasto-perfectly plastic model is instead used to idealize the modal hysteretic characteristics. It is thought that the use of elasto-perfectly plastic modal model is a reasonable approximation in this case. On the other hand, the interference of modes due to the concentrated partial yielding of the structure can lead to large modal displacements in the higher modes, which in many cases, exceed their modal yield displacements. Since the modal force is

not expected to exceed the modal yield strength in the higher modes, the use of elasto-perfectly plastic model together with the defined modal yield strength could lead to unconservative response predictions in the higher modes.

3.5.2 Relationship Between the Modal Ductility and Story Ductilities

In this section, an exact expression relating the defined modal ductility to story ductilities will be developed. Modal ductility will be defined simply as the maximum modal displacement divided by the defined modal yield displacement. Since the jth story displacement in the ith mode (v_j^i) and the ith modal displacement (Y_i) are related by $v_j^i=\phi_{j,i}Y_i$ where $\phi_{j,i}$ is the jth entry of the ith mode shape vector, the maximum jth story displacement in the ith mode is given by

$$(v_j^i)_{max}=\phi_{j,i}(Y_i)_{max} \tag{3.6}$$

Because modal displacements are related to story displacement through coordinate transformation and can be viewed as describing response in a different coordinate system, the relations given above and later are valid whether the structure remains linear elastic or not.

Subtracting from Eq. 3.6 an equation corresponding to the (j-1)th story, we get

$$(v_j^i-v_{j-1}^i)_{max}=(\phi_{j,i}-\phi_{j-1,i})(Y_i)_{max} \tag{3.7}$$

Dividing Eq. 3.7 by the jth story yield displacement ($\delta_{y,j}$), we get

$$\mu_{j,i}=\frac{(v_j^i-v_{j-1}^i)_{max}}{\delta_{y,j}}=\frac{(\phi_{j,i}-\phi_{j-1,i})}{\delta_{y,j}}(Y_i)_{max} \tag{3.7b}$$

or

$$\mu_{j,i}=\frac{(\phi_{j,i}-\phi_{j-1,i})(Y_{yi})}{\delta_{y,j}}\mu_i^* \tag{3.8}$$

where $\mu_{j,i}$ is the jth story ductility in the ith mode and μ_i^* is the modal ductility of the ith mode. The product $(\phi_{j,i}-\phi_{j-1,i})Y_{yi}$ is the story drift when the structure is distorted in the direction of the ith mode shape vector by the amount Y_{yi}. Eq. 3.8 can also be written as

$$\mu_{j,i}=\frac{K_j(\phi_{j,i}-\phi_{j-1,i})(Y_{yi})}{K_j\delta_{y,j}}\mu_i^*$$

or

$$\mu_{j,j}=\frac{K_j(\phi_{j,j}-\phi_{j-1,j})(Y_n)}{F_{j,j}}\mu_j^* \tag{3.9}$$

The product $K_j(\phi_{j,j}-\phi_{j-1,j})Y_n$ is the induced jth story shear force when the structure displacement is given by $\{\phi\}Y_n$ corresponding to the initial yielding of the structure. In Eq. 3.9, $F_{j,j}$ represents the yield strength of the the jth story. Thus, we have arrived at an expression relating story ductilities to modal ductilities.

If we consider all modal contributions using the SRSS combination method then

$$\mu_{j,\text{SRSS}}=\sqrt{\frac{K_j}{F_{j,j}}\sum_{n=1}^{n}(\phi_{j,n}-\phi_{j-1,n})^2(Y_n)^2(\mu_n^*)^2} \tag{3.10}$$

where $\mu_{j,\text{SRSS}}$ is the jth story ductility. It should be noted that the relation between story ductilities and modal ductilities depends on the story yield strengths. In addition, the above relationship between the modal ductility and story ductilities is true regardless of how the modal yield displacement is defined. Only the numerical values of $\mu_{j,\text{SRSS}}$ will change for different definitions of the modal yield displacement.

3.5.3 Reliability of the Modal Hysteresis Model

To evaluate the reliability of the modal hysteresis model, modal yield strengths for buildings number two through four are computed as defined earlier and maximum modal displacements are calculated independently from the computed modal yield strengths. These "computed" maximum modal displacements are then divided by the modal yield displacements and are labeled "computed" ductility in Table 3.9. "Actual" maximum modal displacements are obtained by modal transformation of the displacement calculated by DRAIN-2D. These "actual" maximum modal displacements are again divided by the modal yield displacements and are labeled "actual" modal ductility in Table 3.9. In general, the computed modal ductilities are less than the actual modal ductilities. For higher modes, this is expected as discussed previously. However, for lower modes, the results are unexpected. Apparently, the assumed elasto-perfectly plastic modal hysteretic model does not realistically describe the modal response and deviations from the ideal curve due to modal interference mentioned previously (Figure 3.16) significantly influence the modal response.

By applying Eq. 3.9, the story ductilities corresponding to each mode can also be computed. If the modal contributions are combined by the SRSS method, then Eq. 3.10 can be used to compute the story ductilities. These are listed in Table 3.10. In addition to the actual story ductilities obtained from DRAIN2D, story ductilities, computed by combining the story drifts due to the actual maximum modal displacements by the SRSS method, are also listed. These are labeled SRSS story ductility in Table 3.10. By comparing the actual, SRSS and predicted story ductilities, it appears that the errors involved by the SRSS method and using the proposed modal yield strength to predict structural response are of about the same order of magnitude.

3.5.4 Evaluation of Current Practices of Implementing the Response Spectrum Method

It is useful to review the way the response spectrum method is used in the design of MDOF systems at present. For elastic design, the required jth story shear in the ith mode, $F'_{j,i}$, is

$$F'_{j,i}=(F_j)(S_{d_i})(\Gamma_i^*)$$

where F_j is the jth story shear force due to unit ith modal displacement, S_{d_i} is the maximum modal displacement determined from elastic design spectrum and Γ_i^* is $\{\phi_i\}^T[M]\{r\}$ over $\{\phi_i\}^T[M]\{\phi_i\}$. The required jth story shear strength, $F_{y,j}$, is (by SRSS modal combination method)

$$F_{y,j}=\sqrt{\sum_i (F'_{j,i})^2}=\sqrt{\sum_i (F_j)^2(S_{d_i})^2(\Gamma_i^*)^2} \qquad (3.11)$$

One advantage of this method is the ease by which S_{d_i} can be obtained from elastic design spectra. This makes the evaluation of Eq. 3.11 very easy, and enables quick assessment of alternate designs.

Typically, under current practices [Refs. 3, 6, 10, 13, 16, 17, 38, 54, 56, 91, 98, 99, 100], to implement the response spectrum method for analysis of inelastic multiple-degree-of-freedom systems, it is assumed that the responses among the "modes" are independent. The adequacy of the assumption has been discussed previously. Furthermore, it is usually assumed

that the hysteretic characteristics (i.e. the relation between $\{\phi_i\}^T\{R(Y)\}$ and Y_i) in all the modes are identical to some "global" hysteretic characteristics of the structure (one possible definition of the global ductility relating to local member ductilities can be found in Refs. 3, 22, 23, 24, 38, 79) if the hysteretic characteristics of the structure and member differ. From the observations made in Section 3.4, such assumptions regarding a modal hysteresis model are not unreasonable.

Furthermore, the ductility demands in the modes that are included in the analysis are frequently assumed to be uniform and the same as some measure of the "global" ductility. For the simple case of one mode dominating the response, such an assumption appears reasonable. However, an examination of Eq. 3.10 suggests that modal ductilities and member ductilities are not the same and, in general, these terms should not be interchanged.

When the structure undergoes inelastic deformation, it is expected that the story strengths required for elastic response can be reduced. However, unlike the case of an ideal inelastic SDOF system, it is unclear how the reduction in story strengths is related to the story or modal ductilities. This relationship can be examined as follows by using the results obtained in Section 3.4. It will be assumed that the story yield strengths required to achieve uniform story ductilities are known and are denoted as $F_{(i)}^{m\mu}$, then Eq. 3.11 for inelastic structures becomes

$$\begin{Bmatrix} (F_{(1)}^{m\mu})^2 \\ (F_{(2)}^{m\mu})^2 \\ \cdot \\ (F_{(n)}^{m\mu})^2 \end{Bmatrix} = \begin{bmatrix} (F_1^1)^2 & (F_1^2)^2 & \cdots & (F_1^n)^2 \\ (F_2^1)^2 & (F_2^2)^2 & \cdots & (F_2^n)^2 \\ \cdot & \cdot & \cdots & \cdot \\ (F_n^1)^2 & (F_n^2)^2 & \cdots & (F_n^n)^2 \end{bmatrix} \begin{Bmatrix} (\frac{S_{d_1}}{\rho_1}\Gamma_1^*)^2 \\ (\frac{S_{d_2}}{\rho_2}\Gamma_2^*)^2 \\ \cdot \\ (\frac{S_{d_n}}{\rho_n}\Gamma_n^*)^2 \end{Bmatrix} \tag{3.12}$$

One can solve for the ρ_i's. These ρ_i's are the reduction factors due to the inelastic energy dissipation capacity of the structure. Therefore, any change from the elastic design can be interpreted as reductions in story shear contribution of the modes, expressed by the reduction factors, ρ_i's as shown in Eq. 3.12. Under current practices, the ρ_i's are assumed to be the ratio between the inelastic and elastic response spectra constructed for the SDOF systems. The

actual ρ_i's corresponding to buildings number two to four are obtained by solving Eq. 3.12 and listed in Table 3.11.

For these same buildings, modal yield strengths have been computed in the previous section. Minimum story yield strengths for elastic response can also be obtained from Eq. 3.11 corresponding to ρ_i equals to unity in Eq. 3.12. For these story yield strengths, another set of modal yield strengths can be computed. By comparing these modal yield strengths with the corresponding modal yield strengths computed in the previous section, another set of reduction factors, σ_i, can also be obtained representing the effect of inelastic deformation on modal yield strengths. These reduction factors are also listed in Table 3.11. In general, the values for the two sets of reduction factors are different, unless the ρ_i's in Eq. 3.12 are the same for all the modes. In such a case, the direction of the vector containing story yield strengths (the left hand side of Eq 3.12) does not change. Consequently, the modal yield strength is changed by the same factor as the ρ_i's. Note that even though the story yield strengths for building number four are selected such that ρ_i's are the same, actually computed ρ_i's listed in Table 3.11 deviate slightly from uniformity due to truncation error in the actual story yield strengths used. Similarly, the actually computed σ_i's for building number four deviate slightly from uniformity for the same reason.

In considering the difference between the reduction factors, ρ_i and σ_i, it is worth pointing out that the modal yield strength, as defined, of a structure whose story shear strengths are obtained from Eq. 3.11 corresponding to elastic design, is not $(S_d)_i(\Gamma_i^*)K_i^*$ where K_i^* is the initial linearly elastic modal stiffness. The difference between $(S_d)_i(\Gamma_i^*)K_i^*$ and the defined modal yield strength of a structure designed elastically by Eq. 3.11 to three times the 1934 El Centro earthquake ground motion in the east-west direction is shown in Table 3.12. In summary, ρ_i is used to reduce the spectral displacement of an elastic response spectrum to account for inelastic deformation, while σ_i represents the reduction in the modal yield strength due to structural yielding.

It is difficult to predict structural response from the ρ_i's values. For example, by compar-

ing the ρ_i's used in buildings number three and four (see Table 3.11), one might infer that the story ductilities should be different. However, an examination of the story ductilities in these buildings (Table 3.3) shows close similarities. In contrast, this similarity in structure behavior is easily understood by making a comparison between the reductions in modal yield strengths, σ_r, (see Table 3.11).

It is interesting to consider the situation under which the current practice of specifying ρ_i's will result in desirable story ductilities. If the excitation and structure are such that only the lowest mode is excited to cause significant story shears with little combined contribution from all the other modes, the required story strengths in Eq. 3.12 will be dominated by the contribution from that mode only. In such a case, it is insignificant what reduction factors are used for higher modes, including assuming them to be same as ρ_1 like in the current practices.

Unfortunately, it is generally not possible to determine, *a priori*, the values for either set of reduction factors so that uniform story ductility distribution will result. Thus, in a typical design situation, one can not directly compute the story yield strengths from Eq. 3.12. Rather, it is best to assume the magnitude and distribution of story yield strengths and compute the modal yield strengths. Then, by using response spectra constructed for inelastic SDOF systems, modal ductilities and consequently, the story ductilities can be estimated to evaluate the adequacy of the assumed story yield strengths.

3.5.5 Suggested Procedure for Implementing the Response Spectrum Method

To use inelastic spectra constructed for SDOF systems in the design of MDOF systems, the following iterative procedure is suggested:

(1) Assume story yield strengths, $F_{i,y}$, (maybe using a code procedure or employing Eq. 3.12 and assuming some uniform value for ρ_i.)

(2) Calculate modal properties, $[\omega], [\phi], K_i^*, \xi_i^*, \Gamma_i^*, m_i^*$, etc.

(3) Calculate modal yield strength, $\{\phi_i\}^T\{R_y\}$

(4) From modal yield strengths and inelastic response spectrum, calculate modal ductilities, μ_i.

(5) From modal ductilities, calculate $\mu_{i,j}$ according to Eq. 3.9 using the assumed story yield strengths

(6) Using Eq. 3.10, find combined story ductilities, $\mu_{all,j}$

(7) Check whether $\mu_{all,j}$ is satisfactory or not. If not, modify story yield strengths using Eq 3.5 or a similar relation, then go back to step 3.

The accuracy of the suggested procedure depends greatly on two factors. The first factor is the ability to define equivalent inelastic SDOF systems for reliable prediction of the inelastic response spectrum. The other factor is the accuracy of the SRSS modal combination method for predicting the combined story ductilities. The assumptions made in defining the modal yield point (that maximum modal responses occur at different times and that when the response in any one mode is sufficient to cause yielding in at least one of the stories, the combined response due to other modes is insignificant) are not consistent with the concept underlying the SRSS modal combination method. However, it appears that in general the SRSS method might be conservative; this conclusion may be quite different under different conditions.

3.5.6 Example

To illustrate the procedure, a six story shear building is selected. Story yield strengths are derived from UBC requirements. The building has a linearly distributed story stiffness. Mass and stiffness proportional damping has been assumed for the building with 5% damping in the first and last modes. The properties of the building are listed in Table 3.13.

The response of the building under the east-west component of the 1940 El Centro earthquake ground motion is calculated by the computer program, DRAIN-2D, and listed in Table 3.14. Response calculated using the proposed procedure (steps 1 through 6) is also listed in Table 3.14. As can be seen, the story ductilities predicted are within satisfactory range of the

story ductilities computed by using DRAIN-2D except at the first story. Apparently, the proposed model hysteresis model is not adequate for the higher modes. Refined definition of the modal yield point may be needed in this case. One possibility is to assume some initial story shear forces, representing the presence of lower mode response, in determining the modal yield strengths of the higher modes. Questions about how much the initial story shear forces should be can only be answered in a more comprehensive study using more structures and ground motions. It will not be pursued further here.

3.6 Summary and Conclusions

Four shear-beam type structures have been analyzed. The response is then transformed to their initial linear elastic mode shape coordinate systems. The relationship between the transformed displacement and resistance force vectors is examined. It was found that inelastic response is dominated by the lower modes as in the elastic case for this type of structure. Although modes are expected to interfere with each other, the modal hystereses of the lower modes can be adequately modeled as being bilinear. Modal interference has little effect on these modes. Except the case where the structure has concentrated story ductilities, higher modes are largely insignificant to the structure response and can be ignored. Otherwise, their contributions may be important.

An elasto-perfectly plastic model is suggested for describing the modal hysteresis. Definitions of modal yield strength and modal ductility are presented. The relationship between the proposed modal ductility and story ductilities is derived. The error involved in predicting the story ductilities by using the proposed modal hysteresis model appears to be about of the same order of magnitude as inherent with the modal combination method (SRSS) used.

Current practices for implementing the response spectrum method for inelastic analysis are also evaluated. It was found that it is an over-simplification to assume that the modal ductilities are uniform and the same as the ductility of the structure. In addition, it is generally not possible to determine directly how the elastic modal response should be reduced to account for inelastic deformation.

A simple iterative procedure is suggested for implementing the response spectrum method for the analysis of inelastic MDOF systems. The accuracy of the procedure depends significantly on the veracity of the modal hysteresis model for predictions of the modal response and the applicability of the SRSS modal combination method. More research using structures other than the shear beam type and additional ground motions is recommended. Refined definition of the modal yield strength for higher modes is needed to account for concentrated story ductilities.

CHAPTER 4 DESIGN OF NONSTRUCTURAL SUBSYSTEMS

4.1 Introductory Remarks

The importance of proper seismic-resistant design of nonstructural subsystems in ensuring public safety and in minimizing property damages was mentioned in Chapter 1. In general, both deformation-sensitive and acceleration-sensitive subsystems need to be considered. For light acceleration-sensitive subsystems of the type considered herein, considerable research has been performed for the case of elastic structural response. However, many types of structures can be expected to experience significant inelastic deformations when subjected to severe earthquake ground motions. While nonstructural components might also be expected to behave inelastically, in many cases, safety and communications related subsystems must be designed to remain essentially elastic to insure functionality during, and following, an earthquake [Ref. 30]. Rational design of subsystems in these cases requires that the inelastic deformations of the supporting structure be considered.

In the most general approach to analysis and design, subsystems are included along with the supporting structure in the analytical model. This permits evaluation of their time history response to earthquake ground motions. This couple time history approach is not always feasible because of the scarcity of information regarding the engineering properties of the subsystems. In addition, large differences in the stiffnesses and masses of the structure and nonstructural components may lead to numerical difficulties. Furthermore, the coupled time history approach is not very economical, considering the number of subsystems usually encountered in a structure, and that several analyses are usually required to account for the uncertainties in the ground motions and properties of the structure and its subsystems. This is especially true if inelastic response is anticipated. It is, therefore, desirable to have simple, approximate methods for predicting maximum dynamic response of subsystems.

One simplifying technique is to use a response spectrum method applied to the coupled structure and subsystem. However, when a light subsystem has a frequency equal to, or near

one of the natural frequencies of the structure, conventional modal combination methods may be inadequate due to significant subsystems-structure interaction [Refs. 29, 49]. Kelly and Sackman [Refs. 29, 49, 50] have developed a simplified method for predicting subsystem response (taking into account the subsystem-structure interaction) from the ground response spectrum and the uncoupled properties of the subsystem and the structure. However, those methods assume that the structure is elastic and, therefore, are not applicable when the structure becomes inelastic.

Fortunately, in many cases of interest, subsystem-structure interaction can be neglected and computation of subsystem response can be simplified significantly. For example, some methods have been proposed for predicting the response of the subsystem by directly amplifying the ground response spectrum [Ref. 20]. However, the accuracy of these approximate methods has not been fully evaluated. A more common approach is to obtain a floor response spectrum (FRS) through time history analysis (the so-called floor response spectrum method). A time history analysis of the supporting structure is performed in this case to obtain the total acceleration time history at the attachment location. A response spectrum generated for this acceleration time history is then used in the analysis and design of nonstructural subsystems attached at this location.

The floor response spectrum method is theoretically correct if the subsystem mass is zero. For light subsystems, the subsystem response thus obtained has been shown to be generally conservative, although the conservatism can be very large for heavy subsystems [Refs. 28, 49]. To account for these and other uncertainties, guidelines [Ref. 95] have been developed for modification of FRS for design purposes in the elastic range. The FRS approach is amenable to structures that respond inelastically. While there have been a few case studies [Refs. 26, 48, 50, 101] on the seismic response of light subsystems supported on inelastic structures, no definite conclusions have yet been reached. In view of the likely inelastic behavior of structures during severe earthquake, it is, therefore, useful to systematically study the seismic response of light, nonstructural subsystems supported on structures which might be expected to

yield. From studies [Refs. 65, 66, 68, 69] of dynamic response of inelastic single-degree-of-freedom systems, it has been shown that the design lateral force for a structure expected to undergo inelastic deformations can be reduced by as much as one over the target ductility of the structure depending upon the period of the structure. It is desirable to establish similar design guidelines for subsystems.

4.2 Scope of Study

The objective of this chapter is to conduct a preliminary investigation on the seismic behavior of subsystems supported on structures that experience inelastic deformations, to assess current design methods in terms of this behavior, and to develop improved design guidelines. Due to the preliminary nature of this study, both the subsystem and the structure are modeled as single-degree-of-freedom systems. The resulting two-degree-of-freedom system is shown in Figure 4.1a. The subsystem will be assumed to remain elastic, while the supporting structure is allowed to yield. It will be generally assumed that the mass of the subsystem is much less than the mass of the structure so the floor response method (FRS) is applicable. Results are presented to evaluate, for different periods of subsystems and structure, the effects that different amounts of structural inelastic deformations, different structural hysteretic characteristics, and different amounts of subsystem viscous damping have on the subsystem response. The effects of different earthquake ground motions are also evaluated statistically for a few specific cases to formulate preliminary design guidelines. The applicability of the floor response spectrum method is assessed by considering several coupled two degrees of freedom structure/subsystem models.

4.3 Analysis Approach

Because the subsystems studied in this report focused on those cases where subsystem-structure interaction can be neglected and because only the supporting structure experiences inelastic deformation, floor response spectrum method is considered the simplest and the most efficient method of analysis. In practice, the floor spectrum method based on an elastic analysis

of the supporting structure is widely used for analysis and design of acceleration sensitive subsystems. Thus, the results obtained in this study might be directly used to modify those floor spectra.

As this is a preliminary study, supporting structures are approximated as equivalent single-degree-of-freedom systems. For some structures and ground motions where the acceleration response of the structure is dominated by the first mode, this approximation is reasonably satisfactory. For other structures and ground motions, higher modes may also influence significantly the structural acceleration response and a more refined representation of the supporting structure would be required.

The location of the subsystem in the structure is important in determining the intensity of excitation that the subsystem will experience. For this study, the subsystem is assumed to be located at where the equivalent mass is. Because the supporting structure is modeled as having only one horizontal degree of freedom, rocking of the subsystems as a result of the out-of-plane deformations of the floor and rotation of the subsystem as a result of torsional effects are ignored.

Periods of the supporting structure are assumed to be 0.2 sec, 0.3 sec, 0.5 sec and 1.0 sec. These period values provide structures ranging from one to possibly ten stories high. Damping of the structure is taken as 5%; while that of the subsystem is alternatively taken as 1% or 5%. Generally speaking, damping in many acceleration sensitive subsystems is smaller than that for the supporting structure. However, for cabinets with loose drawers or for machinery and other equipment with loose internal connections or attachments to supports, considerable amounts of energy may be dissipated during seismic excitations which can be conveniently modeled as viscous damping in the subsystems. For these reasons, damping of the subsystem is taken as 1% and 5% to represent a possible range that might be encountered. For buildings designed to conventional building codes, ductility of 4 or more can be expected when the earthquake ground motion is severe; whereas important structures in a nuclear power plant or other industrial facilities which must remain operative after an earthquake, a ductility of 2 or less has been

suggested [Ref. 65]. For this study, ductilities of 1 (elastic) , 2, 4 and 8 are assumed for the supporting structures. Hysteretic models considered are of the elasto-perfectly plastic (EPP, see Figure 4.1b) or stiffness degrading type with no post-yield strain hardening (SDM, also see Figure 4.1c). The EPP model is frequently used to model structures that exhibit stable and full hysteretic loops. The SDM model is used commonly to represent reinforced concrete structures that do not exhibit substantial degradation due to shear and/or bond deterioration.

A total of ten earthquake ground motions from five earthquake is used in this study. These earthquake ground motions are the same as the second set of ground motions considered in Chapter 2 and are re-listed in Table 4.1. One ground motion, the north-south component of the 1940 El Centro record, is used to illustrate the sensitivity of subsystem response to various parameters. The other ground motions are used in the statistical study for various structural periods and subsystems damping values.

In this report, the response of subsystems is described by floor response spectra expressed in terms of pseudo-spectral acceleration (PSA). Since the subsystems are elastic, this completely describes the peak subsystem response values. The first step in obtaining the FRS is to determine the yield strength required of the supporting structure to achieve the specified ductility when subjected to the ground motion under consideration. Once the structure's yield strength has been determined corresponding to the specified ductility ($\pm 1\%$), the total acceleration response time history of the structure is calculated and used as input for determination of the floor response spectrum. The FRS was determined for subsystem periods ranging between 0.03 sec and 2.0 sec. Two computer programs are used to compute the floor response spectrum. First, the computer program NONSPEC [Ref. 57] is used to determined the required yield strength to result in the specified ductility within the desired accuracy. Once the yield strength required is known, total acceleration time history is generated using the same computer program. Then a second computer program SPECEQ/UQ [Ref. 71] is used to compute elastic floor response spectrum.

4.4 Analysis of Results

As indicated, a large variety of cases has been evaluated. A few representative cases will be presented to illustrate behavioral patterns and design implications. Typical floor response spectra are shown in Figures 4.2 and 4.3 for the El Centro record. It can be seen that the FRS usually peaks near the natural period of the structure. This is because the dominant harmonic components of the floor acceleration time history have periods similar to the natural period of the structure in addition to the high frequency components that are usually associated with earthquake ground motions. Generally speaking, the effect of inelastic deformations of the structure is to lower the spectra. The reductions are most evident in the short period range where the subsystem PSA approaches the maximum total floor acceleration. By assuming that the damping force is negligible compared with other forces, the magnitude of the total floor acceleration can be approximated by dividing the maximum resisting force, R_1, of the structure by its mass (M). These values are indicated in Figures 4.2 and 4.3.

In addition, the peaks of the FRS have shifted slightly toward higher periods. It has been suggested [Ref. 47] that the shifts in the dominant natural period of an inelastic structure is about 13 and 32 percents for ductilities of 2 and 4, respectively. In general, the shifts in the periods corresponding to the peaks of the FRS observed for the cases studied are less than these numbers for EPP structures, and slightly higher for SDM structures. In any case, the shift in the peak floor response spectrum period is much less than square root of the ductility of the structure as suggested in Ref. 85 and in some subsystem design recommendations [Refs. 26, 48].

The effects of different hysteretic models can be seen in Figure 4.3a for a representative case with a structural period of 0.2 second, ductility of 4 and subsystem damping of 5%. It can be observed that the FRS for the SDM structure tends to be lower than the EPP one for subsystem periods near the initial structural period. In addition, the period where the FRS peaks shifts more for the SDM structure.

The effect of subsystem damping is to reduce the response of subsystem (except in the very short period range) as can be seen from a representative plot in Figure 4.3b. However, the period where the FRS peaks is not significantly affected by the damping of the subsystem.

4.4.1 Amplification Factor

To help quantify the effect of inelastic deformations of the structure on subsystems response, an amplification factor is defined as the ratio of the floor response spectral value for an inelastic structure over the corresponding value for an elastic structure. Values of amplification factors greater than unity indicate more severe subsystem response for inelastic structures and values less than unity indicate less severe response. This amplification factor may also be useful for estimating the FRS of an inelastic structure directly from the FRS of an elastic structure. In this regard, the amplification factor defined here is conceptually similar to the reduction factors presented in Refs. 66, 67 and 69 which are used to obtain inelastic design spectra for a building directly from an elastic design spectrum.

A representative plot of the resulting amplification factors is shown in Figure 4.4a. Several general observations can be made from this and other such plots. Firstly, the amplification factor varies with subsystem period. One might conjecture that the subsystem response should reduce in proportional to the reduction in the maximum total floor acceleration caused by structural yielding. Based on this conjecture, the amplification factor should be equal to the ratio of maximum total floor acceleration in the inelastic structure to that in the corresponding elastic structure. Again assuming negligibly small damping force, this ratio can be shown to equal $\frac{R_1}{R_{11}}$, where R_1 denotes the maximum elastic force that would be developed by the structure if it remained elastic (ductility = 1). For design purposes, one could estimate this ratio from the structural design recommendations of Newmark and Hall [Refs. 66, 67, 69]. However, the actual amplification factors are, with the exception of the short period range, higher than this value. Thus, the entire reduction in design force that one can apply to the structure on account of yielding is not available for the supported subsystem. This is illustrated

in Figure 4.5a for different structural periods and ductility values. In this figure, the actual amplification factor computed for the case of structure and subsystem having the same natural period is plotted. This is compared with the ratio of the maximum total floor acceleration in inelastic structure to that in a corresponding elastic structure. In addition, the $\frac{R_s}{R_e}$ ratio inferred from the recommendations of Newmark and Hall are also shown. Except for short period structures, these estimates unconservatively underestimate the value of the amplification factor. Another common subsystem design recommendation [Refs. 26, 35] has been that the peak of the elastic FRS can be reduced by one over the structural ductility factor to account for inelastic deformations in the structure. This corresponds to the $\frac{R_s}{R_e}$ values recommended by Newmark and Hall in the long period range. As can be seen by inspecting Figure 4.5a, this approach would be even more unconservative, especially for the short period range. Thus, the difference between the reduction in design forces available to the structure and to the subsystem must be recognized in design.

Secondly, some systematic pattern of variation of the amplification factor with subsystem period can also be observed from Figure 4.4a and other similar plots. For subsystem periods less than the initial structural period, the amplification factor generally increases with period up to about half of the initial natural period of the structure. From there on, the amplification factor decreases with subsystem period to a relative minimum at about the initial natural period of the structure. Then, the amplification factor again increases with period to somewhere around 1.3 times the initial natural period of the supporting structure. Beyond that, the amplification factor fluctuates around a value near unity. However, amplification factors occasionally reach values as high as 1.4; i.e., for subsystems with periods in excess of the structure's initial period, the response can be worse if the structure yields. This overall pattern of the variation is schematically illustrated in Figure 4.6 and appears to be generally independent of the level of ductility or hysteretic characteristics assumed for the structure and the value of damping considered for subsystem. However, higher damping or ductility levels lead to a lower

amplification factor over most of the period range considered and the SDM structures result in amplification factors that fluctuate about a higher plateau in the long period range. Details pertaining to each period range are discussed separately below.

4.4.1.1 Short Period Range

The FRS and consequently the amplification factor in the low period range (up to about half the initial natural period of the supporting structure) are predominantly influenced by the maximum total floor acceleration. Thus, the amplification factor in this period range should approach $\frac{R_1}{R_\mu}$ as subsystem period approaches zero. Generally speaking, yield strength and ductility are inversely related. This result in lower amplification factors for higher ductility values in this period range.

4.4.1.2 Period Range Near the Initial Period of the Structure

At periods around the initial natural period of the structure, the FRS is also very sensitive to the inelastic deformation of the structure. As can be seen from Figure 4.4a, a relative minimum of the amplification factor occurs at around this period range. This can be qualitatively explained as follows. The frequency content of the floor acceleration time history is dominated by the short period harmonic components in the input record, especially those components with periods near the natural period of the structure [Ref. 92]. When the maximum total floor acceleration is limited by structural yielding, the resonance components are more likely to be affected than other harmonic components. Consequently, the reduction in amplification factor is relatively large and the amplification factor reaches a relative minimum around this period range.

4.4.1.3 Long Period Range

At the high period end of the FRS, the amplification factor fluctuates around unity or slightly higher. In addition, no appreciable difference is observed between FRS for different levels of ductility at this period range. For EPP structures, the amplification factor averages

about one in most cases, for SDM structures, the average amplification factor may be in some cases 10 or 20 percent higher than unity. In this period range, the FRS is influenced by the long-period harmonic components of the total floor acceleration. Since the inelastic deformation of the structure primarily affects the short and resonance components of the floor acceleration time history, the floor response spectrum and amplification factor are not greatly affected by inelastic deformation of the structure. However, there is a tendency, especially for SDM structures, to have longer effective natural periods as a result of yielding. This would naturally result in increased response in this range.

4.5 Statistical Evaluation

Because of the uncertainties regarding future earthquake ground motions, a statistical study involving ten earthquake ground motions (Table 4.1) was conducted to evaluate the previous observations. All the parameters considered in the previous sections are retained except that structural ductilities were limited to 1 and 4. To examine the possibility of extending the results to other structural ductilities, the particular case of a structural period of 0.5 sec was evaluated for a structural ductility of 2..

One typical result of the statistical study is shown in Figure 4.4b for the mean, mean plus and minus one standard deviation levels of the amplification factor. For the purpose of deriving subsequent design recommendations, amplification factors of the mean plus one standard deviation level were used corresponding to a probability level of 84.1% of nonexcedance of a normally distributed random variable. To facilitate comparison, the amplification factors are plotted in Figure 4.7 for various structural periods considering different viscous damping and hysteretic models. The variations of the amplification factor are similar to those observed for a structure with the same initial period and damping subjected to the 1940 El Centro record only.

4.5.1 Design Recommendations for Amplification Factors

On the basis of these results, it appears that the amplification factor plot can be divided into five regions as shown in Figure 4.6. The regions are defined by four points, A, B, C, D.

Point A is the point below which the amplification factor is point C is the point with its period close to the initial period of the structure where a relative minimum occurs. Point B is located between point A and point C where a relative maximum of amplification factor occurs. Point D is the point above which the amplification factor remains nearly constant.

The magnitude of point A can be estimated from the ratio, $R_1/R_{1.0}$, as discussed previously. To determine the magnitude of point C, the magnitudes of point C at structure ductility of 4 are plotted versus initial structural periods in Figure 4.8 for EPP and SDM supporting structures with 1% and 5% subsystem damping. It appears that the magnitude of point C varies inversely and nearly linearly with the initial period of the structure. Therefore, straight lines are fitted by the least square method. These lines are also shown in Figure 4.8 and it appears that the lines would have a slope of -0.4 independent of hysteretic characteristics of the structure and/or subsystem damping. However, for SDM structures, the lines are about 40 percent lower. The magnitude of point B is determined similarly. It was found that the magnitude of point B also varies inversely and nearly linearly with the initial structural (Figure 4.9). The least square fit lines have a slope of about -0.2.

To determine the magnitude of point D, the average of the amplification factor for the periods higher than the period of point D is computed for each case considered. Finally, the means and coefficients of variation of these average amplification factors are computed for all cases. Results are listed in Table 4.2. The magnitudes of point D do not vary significantly and average about 1.02 and 1.11 for EPP and SDM structures respectively.

The average results for all the ground motions considered confirm the observation made on the basis of Figure 4.5a that the reduction in the subsystem acceleration is not generally as large as that for the structure acceleration. The average amplification factors at points B and C are plotted in Figure 4.5b. Again, the reduction in structural acceleration shown in the figure is approximated by Newmark and Hall [Refs. 66, 67, 69] recommendations. As noted previously, one over the structural ductility [Refs. 26, 35] is an unconservative estimate of the amplification factor, especially in the short period range. It should be noted that the asymptotic

behavior of the least square fit lines is incorrect; thus the recommended values should be applied to structures with periods between 0.3 sec and 1.0 sec only.

Generally speaking, the minimum of amplification factors occurs when the structure and the subsystem have about the same natural period; thus the period of point C is taken as the natural period of the supporting structure. From Figure 4.7, it seems reasonable that the periods of points B, C and D may be related and that the relationships may be independent of the initial period, hysteretic characteristics and ductility of the structure and/or subsystem damping. To determine these relationships, ratios and logarithmic ratios of period of point C (T_c) to the period of point B (T_b) are computed and listed in Table 4.2 for a structural ductility of 4. The periods of point B and C are multiplied by one thousand to avoid taking logarithm of 1, which is equal to zero. By comparing the coefficients of variation associated with the linear and logarithmic ratios, it is seen that the logarithmic ratios provide a more consistent basis for relating the periods of points B and C. From Table 4.2, it can be said that, on the average, for a structural ductility of 4 regardless of the initial period, hysteretic characteristics of the structure and/or subsystem damping, the natural logarithm of one thousand times the period of point C is about 10 percent higher than the natural logarithm of one thousand times the period of point B.

To determine the relationship between the periods of point C and point D (T_d), similar logarithmic ratios are listed in Table 4.2 for a structural ductility of 4. The period of point D is defined as the beginning period where the amplification factor starts to exceed unity. Once again, the ratios do not vary significantly for the different initial periods, hysteretic characteristics of the structure and/or subsystem dampings. Moreover, on the average, the natural logarithm of one thousand times the period of point D is about 10 percent higher than the natural logarithm of one thousand times the period of point C.

To determine the period of point A or its relationship to other points such as point B or point C, it would be necessary to extend the amplification factors to subsystem periods much less than 0.03 sec (the lower bound of the amplification factor calculated in this study). This is

especially true for structure periods of 0.2 sec and 0.3 sec. For simplicity, the amplification factor is assumed to approach a constant value, $\frac{R_s}{R_{el}}$, at 0.01 sec as shown in Figure 4.6 by point A'. This assumption seems conservative for structural periods greater than 0.5 sec but it may not be so for shorter period structures.

Finally, in Table 4.3, results for structural period of 0.5 sec and ductility of 2 are shown. As can be observed from the table, statistical relationship similar to those for a structural ductility of 4 may be derived. Therefore, the extension of the design recommendations for a structural ductility of 4 to other structural ductilities may be possible.

With the results obtained in this section, the amplification factor curve can be constructed easily for a structural ductility of 4 and possibly for other structural ductilities as well. However, one consideration limits the amplification factor to be no less than R_s/R_{el}. This point will be illustrated for the case of a structure designed to have a ductility of 4. Although the structure is designed to resist the design earthquake ground motion, it may also be subjected to other less intense earthquake ground motions. If one of these less intense earthquake ground motions has similar frequency content and duration as that of the design earthquake ground motion (e.g. a scaled down design earthquake ground motion) and causes the structure to respond elastically with a maximum base shear equal to R_s, the total floor acceleration time history in this case is exactly the same as that of a structure designed to have ductility of 1 when subjected to the original design earthquake ground motion (design base shear = R_{el}) except it is also scaled down by a factor R_s/R_{el}. Consequently, the floor response spectrum is the same as that for a ductility of 1, except it is also scaled down by the same factor. This corresponds to a constant amplification factor of $\frac{R_s}{R_{el}}$ (the zero-period amplification factor) for all subsystem periods. However, amplification factors presented here for a ductility of 4 may sometimes be less than the zero-period amplification factor. Such amplification factors, which are based on inelastic response to the design earthquake ground motion, may therefore be unsafe in the event of some less intense earthquake ground motions.

4.5.2 Example

To illustrate the application of the design amplification factor, a FRS for subsystems supported on a structure with a period of 0.3 sec and a ductility of 4 will be estimated from the FRS for subsystems on an corresponding elastic structure ($T_s = 0.3$ sec, $\mu = 1$).

For this example, the ground motion is the north-south component of the Helena, Montana record. The elastic structure's FRS was obtained from floor response spectrum method; although, in practice, it may be more convenient to use approximate methods suggested in Refs. 18, 20, 29, 49, 75 or 82. In Figure 4.10, the FRS obtained from the recommended amplification factors and the actual FRS for structural ductility of 4 are plotted for both hysteretic models considered. As can be seen, the estimated FRS will generally provide conservative design forces except for subsystems in the short period range. This unconservatism was anticipated when the period of A' was selected.

4.6 Mass Tuning Effects

In developing the amplification factors, it was assumed that the floor response spectrum method was applicable. In order to investigate the applicability of the amplification factors to the cases where the weight of the subsystem makes up a significant portion of the total weight of the structure, amplification factors for the perfectly tuned cases (when the periods of the subsystem and the supporting structure are identical) are computed. It has been shown for elastic cases that the effect of non-zero mass of the subsystem is most significant for the perfectly tuned case [Ref. 28]; therefore, these cases are selected here for investigating mass tuning effects.

For this study, structure periods are kept the same as before at 0.2, 0.3, 0.5 and 1.0 second. Amplification factors, accounting for mass tuning effects by analyzing a two degree of freedom, subsystem-structure model, are computed for a structural ductility of 4. The results are evaluated in terms of mass ratios (defined as the mass of the subsystem over the mass of the supporting structure) of 0.0001, 0.001, 0.01, 0.1 and 1.0. The ground motion record used

is the north-south component of the Lower California earthquake.

The effects of non-zero subsystem mass on structural response can be seen in Figure 4.11. In these cases, the strength of the structure is selected as that required to achieve the target ductility when the subsystem mass is zero. Generally speaking, as the mass ratio increases, the structural ductility also increases, the rate of increase accelerates as mass ratio approaches one. On the other hand, the shear force developed in the subsystem decreases as the mass ratio increases. These observations are in agreement with those by Crandall and Mark [Ref. 28] for elastic structures subjected to white noise excitation.

The effects of non-zero subsystem mass on the amplification factors for a structural ductility of 4 can be seen in Figure 4.12. In general, the amplification factors seem to be independent of mass ratio. Using the definition of amplification factor to obtain the required shear force of the subsystem on an inelastic structure, one would multiply the amplification factor by the shear force of a subsystem on an elastic structure. Since the amplification factors change very little and shear force of the subsystem on an elastic structure decreases substantially as mass ratio increases for the range of mass ratio considered here, the use of the amplification factor and subsystem shear force based on uncoupled analyses would appear to be conservative. To use the amplification factors based on uncoupled analyses with subsystem shear force based on coupled analyses maybe more realistic, but will be more time consuming and might be unconservative on some occasions.

Based on the these considerations, it is clear that the amplification factors derived from uncoupled analyses can be used with response of a subsystem on an elastic structure based on either uncoupled or coupled analyses depending on whether conservatism or computational efficiency is desired.

4.7 Summary and Conclusions

Some preliminary analyses have been performed to identify the behavioral characteristics of light nonstructural subsystems supported on systems that yield during severe earthquake

ground motions. The effects of the severity of the inelastic deformations, of different hysteretic characteristics of the structure and of the amount of viscous damping of the subsystem have been considered. To simplify the of development possible design guidelines, the study has been carried out using the floor response spectrum approach, which is reasonably satisfactory when subsystem-structure interaction can be neglected.

In the first part of the study, the seismic response of subsystems subjected to the north-south component of the 1940 El Centro record was presented for a wide variety of parameters. In the second part, statistical analyses were made using ten earthquake ground motions for a limited number of parameters. Finally, the effect of non-zero subsystem mass are examined.

The significant observations made from this study are summarized below.

(1) Inelastic deformations of the structure tend to shift the floor response spectrum down and toward higher periods. For elasto-perfectly plastic structures, the shifting of floor response spectrum toward higher periods is insignificant; however, for stiffness-degrading structures, the shifting is slightly greater. Damping of the subsystem tends to decrease the response of the subsystem.

(2) The reduction in design force of the subsystem is usually less than that permissible for the structure; and when more reduction is theoretically possible, such reduction maybe unsafe for some ground motions less intense than the design ground motion. It appears that many current design recommendations [Refs. 26, 35] are unconservative in this regard.

(3) The variations of the ratio of the floor response spectrum on an inelastic structure over the floor response spectrum on an elastic structure, defined as amplification factor, can be characterized by three regions with two transition regions in between. In the low period range up to about half the natural period of structure, the amplification factor is controlled by the maximum total floor acceleration and is nearly constant. In the period range around the natural period of the structure, the amplification factor reaches a local minimum. In the high period range, the amplification factor settles into a fluctuating

plateau around unity or slightly higher. Values have been recommended for predicting the amplification factors. Using these values, a design floor response spectrum can be obtained from a conventional linear elastic floor response spectrum without having to perform inelastic analysis.

(4) The effects of non-zero subsystem mass are to increase the ductility demands of the supporting structure and to decrease the shear force of the subsystem. It appears that the amplification factors can be conservatively used even when mass of subsystem is significant.

CHAPTER 5 SUMMARY AND CONCLUSIONS

Because of economic considerations, buildings and other structures are usually designed to respond inelastically when subjected to severe earthquake ground motions. Three related, but separate problems in the preliminary analysis and design of earthquake-resistant structures related to this inelastic behavior have been considered in this report.

(a) Problems Associated with the Selection of Design Earthquake

The first part of the study involves investigating the interaction between ground motion and structural response parameters to provide a more consistent basis for selecting design earthquakes for systems that response inelastically. In Chapter 2, methods for characterizing design earthquakes for intense ground shaking capable of significant structural damages are briefly reviewed. Major emphasis is placed on assessing the effectiveness of various indices for quantifying the damaging potential of a ground motion record. Inherent in the objective is the desire to scale ground motions for the purpose of practical seismic response analysis and design.

Two sets of ground motion records are considered, one set containing records of similar nature and the other set containing various moderate earthquake records obtained at different distances to the source on sites with firm soil conditions. Buildings are represented as single-degree-of-freedom systems and damages are measured by displacement ductility and normalized hysteretic energy ductility.

From observations of the results, it seems that there is a limited range over which ground motion intensity indices might be used for scaling. This should always be noted in applying the results of this study. However, there does not appear to be any correlation between ductility level and the "actual scaling" factors. These factors may deviate considerably from unity and vary with structural period. Furthermore, they differ substantially among the records considered, indicating the apparent intensity of a ground motion can vary quite significantly, even for ground motion recorded at the same site during the same earthquake. A definition of

ground motion intensity which takes into account this period dependence will generally be better than one which ignores it.

For the first set of ground motion records, spectral intensity at 5% viscous damping has been found to be the most effective index. It appears that spectral intensity calculated for a different viscous damping value may be equally effective. For the set of ground motion records with a more diverse nature (record set two), the use of peak ground acceleration, velocity and displacement in the short, intermediate and long period ranges has been found to be most effective. For this latter set of ground motion records, if a single index of damaging potential is desired, Arias intensity and peak ground velocity are equally effective. The difference in the most effective intensity indices between the two sets of ground motions suggests that a single simple index may be unable to characterize the damaging potential of strong earthquake ground motions.

Because the results are based on ground motion records of similar durations (first record set), the effectiveness of using hysteretic energy as a damaging index has not been fully explored. Additional research using other structural damage indices, more ground motions to include near-fault records and different structural viscous damping and hysteretic characteristics is recommended.

(b) Simplified Methods of Analysis for Inelastic Multiple-Degree-Of-Freedom Structures

The second part of the study involves exploring a procedure for implementing the response spectrum method for the preliminary analysis of inelastically responding structures and to evaluate the reliability of such a procedure.

Several shear-beam type structures were analyzed in Chapter 3 using the computer program, DRAIN2D which employs the direct step-by-step integrating technique. The resulting time histories of displacement vector and resistance force vector are transformed to the initial linear elastic mode shape coordinate system to facilitate study of their relation.

From the results obtained, it can be concluded that inelastic response is dominated by

lower modes as in the elastic case and that a simple hysteretic model, such as an elasto-perfectly plastic model, might be used to describe the relationship between the transformed displacement and resistance force vectors in the lower modes for the structures considered.

An elasto-perfectly plastic model is suggested to described modal hysteresis for this type of structure. Definitions of modal yield strength and modal ductility are developed in Chapter 3. The relationship between the proposed modal ductility and story ductilities is derived. The error involved in predicting the story ductilities by using the proposed modal hysteresis model appears to be of about the same order of magnitude as the SRSS modal combination method.

Current practices of implementing the response spectrum method are also evaluated. It was found that it is an oversimplification to assume modal ductilities are uniform and the same as the overall ductility of the structure. In addition, it is generally not possible to determine directly how the elastic modal response should be reduced to account for the inelastic deformation.

A simple procedure for implementing the response spectrum method for the analysis of inelastic multiple-degree-of-freedom systems is suggested. The accuracy of the procedure depends significantly on the veracity of the modal hysteresis model for predictions of modal response and the accuracy of the SRSS modal combination method used. More research using structures other than those of the shear-beam type and additional ground motions is recommended. Refined definition of modal yield strength for higher modes is needed to account for concentrated story ductilities.

(c) Design of Nonstructural Components Attached to Yielding Structures

In the last part of study, preliminary analyses are performed to identify behavioral characteristics of nonstructural subsystems supported on structures that yield during severe earthquake ground motions. Both the subsystem and the structure are modeled as single-degree-of-freedom systems. The subsystem is assumed to remain elastic, while the supporting structure is allowed to yield. It is found that inelastic deformation of the structure tends to shift the floor

response spectrum down and toward higher periods and that damping of the subsystem tends to decrease the subsystem response. The reduction in design force of the subsystem is usually less than that permissible for the structure as a whole; and even if more reduction is theoretically possible, such reductions maybe unsafe in the event of another some ground motion with less intensity than the design ground motion. It appears that many current design recommendations are unconservative in this regard.

Design guidelines for predicting subsystem response accounting for yielding are formulated in the form of recommended amplification factors. Using these factors a design floor response spectrum can be obtained from a conventional linear elastic floor response spectrum without having to perform inelastic analysis. The amplification factors are characterized by three regions with two transition regions in between. In the low period range (up to about half the natural period of the structure), the amplification factor is controlled by the maximum inelastic floor (total) acceleration and is nearly constant. In the period range around the natural period of the structure, the amplification factor reaches a local minimum. In the higher period range, the amplification factor settles into a fluctuating plateau around unity or slightly higher.

The effects of having subsystem with non-zero mass are to increase the ductility demand of the supporting structure and to decrease the shear force of the subsystem. The amplification factors obtained in this study can be used even when mass of the subsystem is significant.

Further study using more ground motions and more realistic structure and subsystem characteristics are needed. In particular, consideration of the effect of yielding in multiple-degree-of-freedom supporting structures on subsystem response should be investigated.

REFERENCES

(1) Almroth, B. O., Brogan, F. A., and Stern, P., "Automatic Choice of Global Shape Functions in Structural Analysis," *AAIA Journal*, American Institute of Aeronautics and Astronautics, Vol. 16, No. 5, May 1978.

(2) Anagnostopoulos, S.A., "Nonlinear Dynamic Response and Ductility Requirements for Building Structures Subjected to Earthquakes," *Publication R72-54*, Massachusetts Institute of Technology, Cambridge, MA, Sept. 1972.

(3) Anagnostopoulos, S.A., Haviland, R.W., and Biggs, J.M., "Use of Inelastic Spectra in Aseismic Design," *Journal of the Structural Division*, ASCE, Vol. 104, NO. ST1, Jan. 1978.

(4) ANSYS, Engineering Analysis Systems User's Manual, *Swanson Analysis System, Inc.*, Pennsylvania, U.S.A.

(5) Arias, A., "A Measure of Earthquake Intensity," *Seismic Design for Nuclear Power Plants*, R.J. Hansen, ed., MIT Press, Cambridge, MA, 1970.

(6) ATC-2, "An Evaluation of a Response Spectrum Approach to Seismic Design of Buildings," *Applied Technology Council Publication*, 1974.

(7) ATC-3-06, "Tentative Provisions for the Development of Seismic Regulations for Buildings," *Prepared by Applied Technology Council*, National Bureau for Standards, 510, Washington, D.C., June 1978.

(8) ATC-10, "Investigation of the Correlation between Earthquake Ground Motion and Building Performance," *Applied Technology Council*, 1982.

(9) Ayres, J.M., and Sun, T.Y., "Non-Structural Damages," *San Fernando, California Earthquake of February 9, 1971*, National Oceanic and Atmospheric Administration, U.S. Department of Commerce, Washington, D.C., 1973.

(10) Baggett, J. F., and Martin, J. F., "Evaluation of the Inelastic Spectrum Design Method for Two Degree-of-Freedom Structures under Seismic Loading," *Engineering Structures*, Vol. 5, Oct. 1983.

(11) Bathe, K. J., "ADINA - A Finite Element Program for Automatic Dynamic Incremental Nonlinear Analysis," *Report 82448-1*, Acoustics and Vibration Laboratory, Department of Mechanical Engineering, Massechusetts Institute of Technology, 1975.

(12) Bathe, K-J, and Gracewski, S., "On Nonlinear Dynamic Analysis Using Substructuring and Mode Superposition," *Computers and Structures*, Vol. 13, 1981.

(13) Bertero, V.V., in collaboration with Herrera, R.A., Mahin, S.A., "Establishment of Design Earthquake - Evaluation of Present Methods," *International Symposium on Earthquake Structural Engineering*, St. Louis, 1976.

(14) Bertero, V.V., Mahin, S.A., and Herrera, R.A., "Aseismic Design Implications of Near-Fault San Fernando Earthquake Records," *Earthquake Engineering and Structural Dynamics*, Vol. 6, 1978, pp. 31-42.

(15) Bertero, V.V., and Mahin, S.A., "Need for a Comprehensive Approach in Establishing Design Earthquakes," *Proceedings of the Second International Conference on Microzonation for Safer Construction, Research and Application*, San Francisco, CA, Nov-Dec 1978.

(16) Bertero, V.V., and Kamil, H., "Nonlinear Seismic Design of Multistory Frames," *Canadian Journal of Civil Engineering*, Vol. 2, No. 4, December 1975.

(17) Bertero, V.V., and Zagajeski, S.W., "Computer Aided Seismic-Resistant Design of Reinforced Concrete Multistory Frames," *Proceedings of the 6th European Conference on Earthquake Engineering*, Vol. II, Dubrovnik, Yugoslavia, September 1978, pp. 289-296.

(18) Biggs, J.M., "Seismic Response Spectra for Equipment Design in Nuclear Power Plants," *Proceedings of the 1st International Conference on Structural Mechanics in Reactor Technology*, Paper K4/7, Berlin, September 1971.

(19) Biggs, J. M., "Evaluation of Aseismic Design Procedures for Reinforced Concrete Frames," *Proceedings of the 7th World Conference on Earthquake Engineering*, Istanbul, Turkey, 1980.

(20) Biggs, J.M., and Roesset, J.M., "Seismic Analysis of Equipment Mounted on a Massive

Structure," *Seismic Design for Nuclear Power Plants*, R.J. Hansen, ed., MIT Press, Cambridge, MA, 1970, PP. 319-343.

(21) Blume, J.A., "On Instrumental Versus Effective Acceleration and Design Coefficient," *Proceedings of the Second U.S. National Conference on Earthquake Engineering*, Stanford University, CA, August 1979, pp. 868-882.

(22) Capecchi, D., Rega, G., and Vestroni, F., "Non-linear Dynamic Analysis and Ductility Requirements of Multidegree-Of-Freedom Structures," *Proceedings of the 6th European Conference on Earthquake Engineering*, Vol. 2, Dubrovnik, Yugoslavia, 1978.

(23) Capecchi, D., Rega, G., and Vestroni, F., "A Study of the Effect of Stiffness Distribution on Nonlinear Seismic Response of Multidegree-of-Freedom Structures," *Engineering Structures*, Vol. 2, Oct. 1981.

(24) Capecchi, D., Rega, G., and Vestroni, F., "Ductility Request in Seismic Analysis of Nonlinear Multidegree-of-Freedom Structures," *Proceedings of the 7th World Conference On Earthquake Engineering*, Istanbul, Turkey, 1980.

(25) Chang, C.-C., "Normalization of Input Motions for Seismic Analysis," *Master's Thesis*, University of Texas at Austin, December 1983.

(26) Coats, D.W., "Recommended Revisions to Nuclear Regulatory Commission Seismic Design Criteria," *NUREG/CR*-1151, U.S. Nuclear Regulatory Commission, Washington, D.C., May 1980.

(27) Cornell, C.A., Banon, H., and Shakal, A.F., "Seismic Motion and Response Prediction Alternatives," *Earthquake Engineering and Structural Dynamics*, Vol. 7, 1979, pp. 295-315.

(28) Crandall, S.H., and Mark, W.D., "*Random Vibration in Mechanical Systems*," Academy Press Inc., New York, N.Y., 1963, pp. 85-101.

(29) Der Kiureghian, A., Sackman, J.L., and Nour-Omid, B., "Dynamic Response of Equipment in Structures," *Report No. UCB/EERC-81/05*, Earthquake Engineering Research Center, University of California, Berkeley, April 1981.

(30) "Design Response Spectra for Nuclear Power Plants," *Nuclear Regulatory Guide No. 1.60*, Rev. 1, U.S. Nuclear Regulatory Commission, Washington, D.C., 1973.

(31) Donovan, N.C., Bolt, B.A., and Whitman, R.V., "Development of Expectancy Maps and Risk Analysis," *Journal of the Structural Division*, ASCE, Vol. 104, No. ST8, August 1978, pp. 1179-1192.

(32) Geschwindner, L.F. Jr. "Nonlinear Dynamic Analysis by Modal Superposition," *Journal of the Structural Division*, ASCE, Vol. 107, No. ST12, Dec 1981.

(33) Gillies, A.G., and Shepherd, R., "Prediction of Post-Elastic Seismic Response of Structures by a Mode Superposition Technique," *Bulletin of the New Zealand National Society for Earthquake Engineering*, Vol. 16, No. 3, Sept. 1983

(34) Golafshani, A., and Powell, G.H., "DRAIN-2D2, A Program for Inelastic Response of Structures," *Ph.D. Thesis*, Dept. of Civil Engineering, University of California, Berkeley, April 1982.

(35) Goldberg, A., and Rukos, E.A., "Nonstructural Elements," *Design of Earthquake Resistant Structures*, E. Rosenbleuth, ed., John Wiley and Sons, Inc., New York, N.Y., 1981, PP. 267.

(36) Guendelman-Israel, R., and Powell, G. H., "DRAIN-TABS : A Computer Program for Inelastic Earthquake Response of Three Dimensional Buildings," *Report No. UCB/EERC 77/08*, Earthquake Engineering Research Center, University of California, Berkeley, 1977.

(37) Gurpinar, A., "An Alternative to Peak Ground Acceleration as a Design Parameter," *Proceedings of the 6th European Conference on Earthquake Engineering*, Dubrovnik, Yugoslavia, 1978, pp. 219-226.

(38) Haviland, R.W., Biggs, J.M., and Anagnostopoulos, S.A., "Inelastic Response Spectrum Design Procedures for Steel Frames," *Publication R76-40* Dept. of Civil Engineering, Massechusetts Inst. of Tech., Cambridge, Mass., Sept. 1976.

(39) Horii, K., and Kawahara, M., "A Numerical Analysis on the Dynamic Response of Struc-

tures," *Proceedings of the 19th Japan National Congress for Applied Mechanics*, 1969

(40) Housner, G.W., "Behavior of Structures During Earthquakes," *Journal of the Engineering Mechanics*, ASCE, Vol. 85, No. EM4, October 1959, pp. 109-129.

(41) Housner, G.W., "Intensity of Earthquake Ground Shaking Near the Causative Fault," *Proceedings of the Third World Conference on Earthquake Engineering*, Aukland and Wellington, New Zealand, 1965.

(42) Housner, G.W., "Measures of Severity of Earthquake Ground Shaking," *Proceedings of the U.S. National Conference on Earthquake Engineering*, EERI, Ann Arbor, Michigan, June 1975, pp. 25-33.

(43) Housner, G.W., "Spectrum Intensities of Strong Motion Earthquakes," *Proceedings of the Symposium of Earthquake and Blast Effects on Structures*," EERI, June 1975, pp. 20-36.

(44) Housner, G.W., and Jennings, P.C., "The Capacity of Extreme Earthquake Motions to Damage Structure," *Structural and Geotechnical Mechanics*, W.J. Hall ed., Prentice-Hall, 1977, pp. 102-116.

(45) Hudson, D.E., "Reading and Interpreting Strong Motion Accelerogram," *Engineering Monographs on Earthquake Criteria, Structural Design, and Strong Motion Records*, Vol. 1, EERI, Berkeley, CA, 1979.

(46) Husid, R., "Earthquake: Spectral Analysis and Characteristics of Acceleration as a Basis of Earthquake Resistant Design," Santiago, Chile, 1973.

(47) Iwan, W.D., and Gates, N.C., "The Effective Period and Damping of a Class of Hysteretic Structures," *Journal of the International Association of Earthquake Engineering*, Vol. 7, No. 3, May-June 1979, pp199-211.

(48) Kawakatsu, T., Kitada, K., Takemori, T., Kuwabara, Y., and Ogiwara, Y., "Floor Response Spectra Considering Elasto-Plastic Behavior of Nuclear Power Facilities," *Transactions of the 5th International Conference on Structural Mechanics in Reactor Technology*, Paper K9/4, Berlin, August 1979.

(49) Kelly, J.M. and Sackman, J.L., "Conservatism in Summation Rules for Closely Spaced Modes," *Report No. UCB/EERC-79/11*, Earthquake Engineering Research Center, University of California, Berkeley, May 1979.

(50) Kelly, T.E., "Floor Response of Yielding Structures," *Bulletin of the New Zealand National Society for Earthquake Engineering*, Vol. 11, No. 4, December 1978.

(51) Kennedy, R.P., *et al*, "Engineering Characterization of Ground Motion - Task I: Effects of Characteristics of Free-Field Motion on Structural Response," *Structural Mechanics Associates*, Feb. 1984.

(52) Kennedy, R.P., "Peak Acceleration as a Measure of Damage," *Fourth International Seminar on Extreme-Load Design of Nuclear Power Facilities*, Paris, France, August 1981.

(53) Krawinkler, H., and Zohrei, M., "Cumulative Damage in Shell Structures Subjected to Earthquake Ground Motions," *Computers and Structures*, Vol. 16, 1983, pp. 531-541.

(54) Lai, S.-S., and Biggs, J.M., "On Inelastic Response Spectra for Aseismic Building Design," *Proceedings of the 7th World Conference on Earthquake Engineering*, Istanbul, Turkey, 1980.

(55) Liu, S.C., "On Intensity Definition of Earthquakes," *Journal of the Structural Division*, ASCE, Vol. 95, No. ST5, May 1968, pp. 1037-1042.

(56) Mahin, S.A., Bertero, V.V., "An Evaluation of Inelastic Seismic Design Spectra," *Journal of the Structural Division*, ASCE, Vol. 107, No. ST9, September 1981, pp. 1777-1795.

(57) Mahin, S.A., and Lin, J., "Construction of Inelastic Response Spectra for Single-Degree-of-Freedom Systems: Computer Program and Application," *Report No. UCB/EERC-83/17*, Earthquake Engineering Research Center, University of California, Berkeley, June 1983.

(58) Mohraz, B., "A Study of Earthquake Response Spectra for Different Geological Conditions," *Bulletin of the Seismological Society of America*, Vol. 66, No. 3, June 1976, pp. 915-935.

(59) Mondkar, D.P., and Powell, G.H., "ANSR-I, General Purpose Computer for Analysis of

Non-linear Structural Response," *Report No. UCB/EERC-79/17*, Earthquake Engineering Research Center, University of California, Berkeley, 1975.

(60) Mondkar, D. P., and Powell, G. H., "ANSR-II, Analysis of Nonlinear Structural Response, Users Manual," *EERC Report 79-17*, Earthquake Engineering Research Center, University of California, Berkeley, 1979.

(61) Morris, N.F. "The Use of Mode Superposition in Nonlinear Dynamics," *Computers and Structures*, Vol. 7, 1977.

(62) Mortgat, C.P., "A Probabilistic Definition of Effective Acceleration," *Proceedings of the Second U.S. National Conference on Earthquake Engineering*, Stanford University, CA, August 1979, pp. 743-752.

(63) Nagy, D. A., "Modal Representation of Geometrically Nonlinear Behavior by the Finite Element Method," *Computers and Structure*, Vol. 10, 1979.

(64) Nau, J.M., and Hall, W.J., "An Evaluation of Scaling Methods for Earthquake Response Spectra," *Civil Engineering Studies*, Structural Research Series, No. 499, University of Illinois, Urbana, May 1982.

(65) Newmark, N.M., and Hall, W.J., "Development of Criteria for Seismic Review of Selected Nuclear Power Plants," *NUREG/CR-0098*, Nuclear Regulatory Commission, Washington D.C., 1978.

(66) Newmark, N.M., "Current Trends in the Seismic Analysis and Design of High-Rise Structures," *Earthquake Engineering*, R.L. Wiegel, ed., Prentice-Hall, Englewood Cliffs, N.J., 1970.

(67) Newmark, N.M., "Earthquake Resistant Design and ATC Provisions," *Third Canadian Conference on Earthquake Engineering*, Montreal, June 1979.

(68) Newmark, N.M., "Seismic Design Criteria for Structures and Facilities of the Trans-Alaska Pipelime System," *Proceedings of the U.S. National Conference on Earthquake Engineering*, EERI, Oakland, CA, 1975.

(69) Newmark, N.M., and Hall, W.J., "Procedures and Criteria for Earthquake Resistant Design," *Building Practice for Disaster Mitigation, Building Science Series 45*, National Bureau of Standards, Washington, D.C., Feb. 1973, pp 209-236.

(70) Nickell, R.E., "Nonlinear Dynamics by Mode Superposition," *Computer Methods in Applied Mechanics and Engineering*, Vol. 7, 1976.

(71) Nigam, N.C., and Jennings, P.C., "SPECEQ/UQ-Digital Calculation of Response Spectra from Strong-Motion Earthquake Records," Earthquake Engineering Research Laboratory, California Institute of Technology, June 1968.

(72) Nishikawa, T., Hayama, S., and Seki, T., "Normalization Parameters of Maximum Values of Earthquake Motion for Non-linear Response Analysis of Structures," *Proceedings of the Eighth World Conference on Earthquake Engineering*, San Francisco, CA, 1984, pp. 33-46.

(73) Noor, A.K., "Recent Advances in Reduction Methods for Nonlinear Problems," *Computers and Structures*, Vol. 13, 1981.

(74) Noor, A. K., Peters, J. M., and Anderson, C. M. "Two-Stage Rayleigh-Ritz Technique for Nonlinear Analysis of Structures," *Proceedings of the Second International Symposium on Innovative Numerical Analysis in Applied Engineering Sciences*, Montreal, Canada, 1980.

(75) Peter, K.A., Schmitz, D., and Wagner, U., "Determination of Floor Response Spectra on the Basis of the Response Spectrum Method," *Nuclear Engineering and Design, Vol. 44, 1977, pp. 255-262.*

(76) Pique, J.R., "On the Use of Simple Models in Nonlinear Dynamic Analysis," *Publication 76-43*, Department of Civil Engineering, Massachusetts Inst. of Technology, Cambridge, Mass., Sept. 1976.

(77) Powell, G. H., "DRAIN-2D Users Guide," *Report No. UCB/EERC-73/22*, Earthquake Engineering Research Center, University of California, Berkeley, 1973.

(78) "Recommended Lateral Force Requirements and Commentary," *Seismology Committee*, Structural Engineers Association of California, San Francisco, 1975.

(79) Rega, D., and Vestroni, F., "Statistical Analysis of the Inelastic Response of Shear Structures Subjected to Earthquake," Submitted for Review in Earthquake Engineering and Structure Dynamics.

(80) Remseth, N.F., "Nonlinear Static and Dynamic Analysis of Framed Structures," *Computers and Structures*, Vol. 10, 1979.

(81) Rizzo, P.C., "A Note on Detailed Evaluation of Strong Ground Motions for Input to Seismic Design," *State-of-Art in Earthquake Engineering*, 1981, pp. 33-46.

(82) Sackman, J.L., and Kelly, J.M., "Rational Design Methods for Light Equipment in Structures Subjected to Ground Motion," *Report No. UCB/EERC-78/19*, Earthquake Engineering Research Center, University of California, Berkeley, Sep. 1978.

(83) Sackman, J.L., and Kelly, J.M., "Equipment Response Spectra for Nuclear Power Plant Systems," *Nuclear Engineering and Design*, No. 57, 1980.

(84) Sheikh, T.M., Roesset, J.M., and Johnson, C.P., "Modal Analysis of Nonlinear Systems," *Proceedings of the 7th World Conference on Earthquake Engineering*, Istanbul, Turkey, 1980.

(85) Shibata, A., and Sozen, M., "Substitute-Structure Method for Seismic Design for R/C," *Journal of the Structural Division*, ASCE, Vol. 102, No. ST1, January 1976, pp1-18.

(86) Saiidi, M., and Sozen, M.A., "Simple and Complex Models for Nonlinear Seismic Response of Reinforced Concrete Structures," *Civil Engineering Studies*, Structural Response Series, No. 645, University of Illinois, Urbana, August 1979.

(87) Saiidi, M., and Sozen, M.A., "Simple Nonlinear Seismic Analysis of R/C Structures," *Journal of the Structural Division*, ASCE, Vol. 107, No. ST5, May 1981.

(88) Smilowitz, R., and Newmark, N.M., "Design Seismic Acceleration in Buildings," *Journal of the Structural Division*, ASCE, Vol, 105, No. ST12, Dec. 1979, pp2487-2496.

(89) Steinhardt, O.W., "Earthquake Effect at El Centro Power Plant," *Reconnaissance Report*, Imperial County, California Earthquake, Oct. 15, 1979, D.J. Leeds, ed., Feb. 1980.

(90) Stricklin, J.A., and Haisler, W.E., "Formulations and Solution Procedures for Nonlinear Structural Analysis," *Computers and Structures*, Vol. 7, 1977.

(91) Tansirikongkol, V., and Pecknold, D.A., "Approximate Modal Analysis of Bilinear MDF Systems Subjected to Earthquake Motions," Civil Engineering Studies, *SRS 449*, Department of Civil Engineering, University of Illinois at Urbana-Champaign, Urbana, Illinois, August 1978.

(92) Trifunac, M.D., "Response Envelope Spectrum and Interpretation of Strong Earthquake Ground Motion," *Bulletin of the Seismological Society of America*, Vol. 61, April 1971, pp343-356.

(93) Uniform Building Code, *International Conference of Building Officials*, Whittier, CA, 1982.

(94) U.S. Nuclear Regulatory Commission, *Code of Federal Regulations*, Title 10, Chapter 1, Part 100, Appendix A, "Seismic and Geologic Siting Criteria for Nuclear Power Plants."

(95) U.S. Nuclear Regulatory Commission, "Development of Floor Design Response Spectra for Seismic Design of Floor Supported Equipment or Components," Washington, D.C., *Regulatory Guide 1.122*, Rev. 1 (1978).

(96) Vanmarcke, E.H., "State-of-the-Art for Assessing Earthquake Hazards in the United States, Representation of Earthquake Ground Motion: Scaled Accelerograms and Equivalent Response Spectra," Corps of Engineers, Waterways Experiment Station, *Misc. Paper S-73-1, Report 14*, 83pp.

(97) Vanmarcke, E.H., and Lai, S.P., "Strong Motion Duration and RMS Amplitude of Earthquake Records," *Bulletin of the Seismological Society of America*, Vol. 70, No. 4, August 1980, pp. 1293-1307.

(98) Veletsos, A. S., "Maximum Performance of Certain Nonlinear Systems," *Proceedings of the Fourth World Conference on Earthquake Engineering*, Santiago, Chile, Vol. 2, 1969.

(99) Veletsos, A. S., and Vann, W. P., "Response of Ground-Excited Elastoplastic Systems," *Journal of the Structural Division*, ASCE, Vol. 97, No. ST4, April 1971.

(100)Villaverde, R., "Response Spectrum Method for the Analysis of Nonlinear Multistory Structures," *Proceedings of the Eighth World Conference Of Earthquake Engineering*, San Francisco, 1984.

(101)Vitti, G., Olivieri, M., and Travi, S. "Development Of Non-Linear Floor Response Spectra," *Nuclear Engineering and Design*, Amsterdam, Vol. 64, No. 1, March 1981, pp33-38.

(102)Werner, S.D., "Engineering Characteristics of Earthquake Ground Motions," *Nuclear Engineering and Design*, No. 36, 1976.

(103)Whitman, R.V., "Effective Peak Acceleration," *Proceedings of the Second International Conference on Microzonation*, Vol. III, San Francisco, CA, 1978, pp. 1247-1255.

Date	Earthquake	Redording Site	Component	Abbreviation
First Set of Ground Motions				
1979, Oct. 15	Imperial Valley	Imperial County Service Building, Basement	Trace10	TR10
1979, Oct. 15	Imperial Valley	Imperial County Service Building, Basement	Trace11	TR11
1979, Oct. 15	Imperial Valley	Imperial County Service Buiiding, Basement	Trace13	TR13
1979, Oct. 15	Imperial Valley	Imperial County Service Building Free Field	Free Field 1	FF1
1979, Oct. 15	Imperial Valley	Imperial County Service Building Free Field	Free Field 3	FF3
Second Set of Ground Motions				
1934, Dec. 30	Lower California	El Centro, Imperial Valley	S00W	Lowcans
1934, Dec. 30	Lower California	El Centro, Imperial Valley	S90W	Lowcaew
1935, Oct. 31	Helena, Montana	Carrol College	S00W	Helenans
1935, Oct. 31	Helena, Montana	Carrol College	S90W	Helenaew
1940, May 18	Imperial Valley	Ei Centro	S00W	Elcentrons
1940, May 18	Imperial Valley	El Centro	S90W	Elcentroew
1949, Apr. 13	Western Washington	Olympia Highway Test Lab	N04E	Olympians
1949, Apr. 13	Western Washington	Olympia Highway Test Lab	N68E	Olympiaew
1952, July 21	Kern County	Taft, Lincoln School Tunnel	N21E	Taft21
1952, July 21	Kern County	Taft, Lincoln School Tunnel	S69W	Taft69

TABLE 2.1 Ground Motion Records

	TR10	TR11	TR13	FF1	FF3
A_g (cm/sec^2)	330.6	280.4	325.0	231.4	209.0
V_g (cm/sec)	43.3	42.4	64.6	64.4	36.2
D_g (cm)	14.5	16.0	27.4	28.2	16.4
$FAS_{0.25}$ (cm/sec)	52.80	35.37	50.14	9.91	55.50
$FAS_{1.00}$ (cm/sec)	77.10	70.16	73.21	93.86	59.48
$FAS_{3.30}$ (cm/sec)	59.22	69.40	181.17	180.25	60.79
$PSV_{0.25}$ (ft/sec)	1.5359	1.2966	0.8053	0.5019	0.6730
$PSV_{1.00}$ (ft/sec)	2.6404	2.6098	1.9551	1.8179	2.1651
$PSV_{3.30}$ (ft/sec)	1.3657	1.4794	4.0503	3.9336	1.4485
$S.I._{5\%}$ (ft)	5.359	5.227	5.465	5.055	4.657
$S.I._{20\%}$ (ft)	3.152	3.176	3.625	3.302	2.784
A.I. (m^2/sec^3)	5.560	4.880	3.320	2.509	2.611
R.M.S. (m/sec^2)	0.888	0.815	0.643	0.544	0.562

TABLE 2.2 Computed Values of the Intensity Indices Considered. (First Ground Motion Set)

	Lowcans	Lowcaew	Helenans	Helenaew	Elcentrons
A_g (cm/sec^2)	156.8	179.1	143.5	142.5	341.7
V_g (cm/sec)	20.5	11.5	7.3	13.3	33.4
D_g (cm)	4.2	3.7	1.4	3.7	10.9
$FAS_{0.25}$ (g sec)	0.0511	0.1030	0.0105	0.0300	0.0330
$FAS_{1.00}$ (g sec)	0.0430	0.0811	0.0056	0.0414	0.0951
$FAS_{3.30}$ (g sec)	0.0037	0.0205	0.0037	0.0091	0.0445
$PSV_{0.25}$ (ft/sec)	0.4792	0.8124	0.2722	0.4166	1.1756
$PSV_{1.00}$ (ft/sec)	1.0633	0.7958	0.1563	0.9248	2.6355
$PSV_{3.30}$ (ft/sec)	0.7804	0.4596	0.1186	0.2813	1.5042
$S.I._{5\%}$ (ft)	1.783	1.513	0.542	1.472	4.404
$S.I._{20\%}$ (ft)	1.163	0.849	0.357	1.010	2.659
A.I. (in^2/sec^3)	1.805	2.076	0.260	0.412	5.528
R.M.S. (m/sec^2)	0.367	0.375	0.349	0.456	0.628

	Elcentroew	Olympians	Olympiaew	Taft21	Taft69
A_g (cm/sec^2)	210.1	161.6	274.6	152.7	175.9
V_g (cm/sec)	36.9	21.4	17.0	15.7	17.7
D_g (cm)	19.8	8.5	10.4	6.7	9.2
$FAS_{0.25}$ (g sec)	0.0414	0.0406	0.0617	0.0210	0.0289
$FAS_{1.00}$ (g sec)	0.0694	0.0559	0.0598	0.0251	0.0534
$FAS_{3.30}$ (g sec)	0.0764	0.0327	0.0862	0.0160	0.0340
$PSV_{0.25}$ (ft/sec)	0.5723	0.5507	0.7420	0.4135	0.4649
$PSV_{1.00}$ (ft/sec)	1.4185	1.1576	0.9461	0.9219	0.8124
$PSV_{3.30}$ (ft/sec)	2.1482	0.7955	1.4932	0.4161	0.6622
$S.I._{5\%}$ (ft)	3.769	2.598	2.457	1.914	2.114
$S.I._{20\%}$ (ft)	2.235	1.522	1.296	1.180	1.238
A.I. (m^2/sec^3)	3.590	2.363	3.668	1.634	1.845
R.M.S. (m/sec^2)	0.472	0.380	0.485	0.353	0.384

TABLE 2.3 Computed Values of the Intensity Indices Considered. (Second Ground Motion Set)

Rank	Method	Average Mean Square Error
1	$S.I._{5\%}$	0.0497
2	Min(PSV)	0.0565
3	$PSV_{1.00}$	0.0588
4	$S.I._{20\%}$	0.0662
5	Min(FAS)	0.0778
6	$FAS_{1.00}$	0.0778
7	Arias Intensity	0.0862
8	Min(A,V,D)	0.0904
9	A_g	0.111
10	R.M.S.	0.131
11	V_g	0.133
12	D_g	0.199
13	$PSV_{3.30}$	0.286
14	$FAS_{3.30}$	0.298
15	$PSV_{0.25}$	0.989
16	$FAS_{0.25}$	2.740

TABLE 2.4 Average Mean Square Error Based on Displacement Ductility. (First Ground Motion Set)

Rank	Method	Average Mean Square Error
1	$S.I._{5\%}$	0.0487
2	Min(PSV)	0.0587
3	$PSV_{1.00}$	0.0608
4	$S.I._{20\%}$	0.0651
5	Min(FAS)	0.0766
6	$FAS_{1.00}$	0.0766
7	Arias Intensity	0.0883
8	Min(A,V,D)	0.0889
9	A_g	0.112
10	R.M.S.	0.131
11	V_g	0.135
12	D_g	0.197
13	$PSV_{3.30}$	0.284
14	$FAS_{3.30}$	0.296
15	$PSV_{0.25}$	1.013
16	$FAS_{0.25}$	2.811

TABLE 2.5 Average Mean Square Error Based on Normalized Hysteretic energy Ductility. (First Ground Motion Set)

Rank	Method	Average Mean Square Error
1	Min(A,V,D)	0.115
2	Arias Intensity	0.151
3	V_g	0.152
4	R.M.S.	0.184
5	A_g	0.193
6	$S.I._{20\%}$	0.220
7	$S.I._{5\%}$	0.221
8	D_g	0.239
9	Min(PSV)	0.245
10	Min(FAS)	0.266
11	$PSV_{0.25}$	0.318
12	$FAS_{0.25}$	0.352
13	$PSV_{3.30}$	0.648
14	$FAS_{1.00}$	0.887
15	$PSV_{1.00}$	1.090
16	$FAS_{3.30}$	3.363

TABLE 2.6 Average Mean Square Error Based on Displacement Ductility. (Second Ground Motion Set)

Story Number	Story Mass (kg)	Story Stiffness (kg/sec/sec)	Story Yield Strength (Newton)
1	1.	2304.	20.1.0
2	1.	1920.	18.78
3	1.	1536.	16.13
4	1.	1151.	12.16
5	1	768.	6.86

TABLE 3.1 Physical Properties of Building Number One.

Mode	Period (Second)	Modal Mass (Kg)	Modal Stiffness (Kg/sec^2)	Modal Damping (%)
1	0.533	1.0	139.	5.0
2	0.212	1.0	879.	3.4
3	0.136	1.0	2130.	3.7
4	0.102	1.0	3770.	4.2
5	0.080	1.0	6137.	5.0

Mode Shape Vectors					
D.O.F	Mode 1	Mode 2	Mode 3	Mode 4	Mode 5
1	-.1207	-.2972	-.4199	.5261	.6664
2	-.2569	-.5177	-.4578	.1244	-.6641
3	-.4039	-.4970	.1299	-.6830	.3263
4	-.5512	-.0902	.6732	.4758	-.0915
5	-.6727	.6233	-.3742	-.1217	.0131

TABLE 3.2 Modal Properties of Building Number One.

Story	Building #1	Building #2	Building #3	Building #4
	Ductility	Ductility	Ductility	Ductility
1	1.6	2.4	2.6	2.9
2	1.2	1.8	2.7	2.3
3	1.7	1.5	1.7	2.2
4	1.4	3.5	2.7	2.7
5	1.8	5.0	2.1	1.9

TABLE 3.3 Computed Story Ductilities.

Time (sec)	Yielded Story	First Mode Tangent Stiffness (kg/sec^2)	Time (sec)	Yielded Story	First Mode Tangent Stiffness (kg/sec^2)
5.32	5	95	9.68	1,2,3,4	-8
5.33	4,5	15	9.69	1,3,4,5	-91
5.34	4,5	+ ∞	9.70	1,3,4,5	1900
5.35	4,5	216	9.71	3,4,5	158
5.36	5	138	9.72	3,4,5	133
			9.73	4	98
5.55	1,2,3,4,5	0			
5.56	1,2,3,4,5	0	9.88	5	125
5.57	1,2,3,4,5	0	9.89	5	115
5.58	1,3,4,5	-36	9.90	5	95
5.59	1,3,4,5	-108	9.91	4,5	115
5.60	1,3,4,5	-10[illegible]	9.92	3,4,5	129
5.61	1,3,4,5	-250	9.93	3,5	- ∞
5.62	3,4,5	117	9.94	5	142
5.63	3,4,5	215	9.95	5	182
8.29	5	119	10.47	1	50
8.30	5	146	10.48	1,2	-17
8.31	4,5	112	10.49	1,2	33
8.32	3,4,5	32	10.50	1	-100
8.33	1,3,4	-17	10.51	1	-100
8.34	1,3	100	10.52	1	25
8.35	1,3	283	10.53	1	120
8.36	1,3	215			
8.37	1	123	10.74	5	140
			10.75	5	105
8.59	1,2	87	10.76	4,5	128
8.60	1,2	15	10.77	4,5	95
8.61	1,2,3,4,5	0	10.78	5	140
8.62	1,2,3,4,5	0	10.79	5	-100
8.63	3,4,5	233			
8.64	3,4,5	163	12.90	5	104
8.65	3,4	136	12.91	5	133
			12.92	5	75

TABLE 3.4 Computed First Mode Instantaneous Stiffness and the Yielding Stories.

Mode	Period (Second)	Modal Mass (Kg)	Modal Stiffness (Kg/sec^2)	Modal Damping (%)
1	1.599	1.0	15.4	5.0
2	0.636	1.0	97.7	3.4
3	0.409	1.0	236.7	3.7
4	0.307	1.0	418.9	4.2
5	0.241	1.0	681.9	5.0

TABLE 3.5 Modal Properties of Building Number Two.

Story Number	Story Mass (kg)	Story Stiffness (kg/sec/sec)	Story Yield Strength (Newton)
1	1.	256.00	3.88
2	1.	213.33	3.644
3	1.	170.67	3.184
4	1.	128.00	2.496
5	1.	85.333	1.58

TABLE 3.6 Physical Properties of Building Number Two.

Story Number	Story Mass (kg)	Story Stiffness (kg/sec/sec)	Story Yield Strength (Newton)
1	1.	256.00	3.88
2	1.	213.33	3.01
3	1.	170.67	2.85
4	1.	128.00	2.70
5	1.	85.333	2.30

TABLE 3.7 Physical Properties of Building Number Three.

Story Number	Story Mass (kg)	Story Stiffness (kg/sec/sec)	Story Yield Strength (Newton)
1	1.	256.00	3.88
2	1.	213.33	3.14
3	1.	170.67	2.62
4	1.	128.00	2.51
5	1.	85.333	2.33

TABLE 3.8 Physical Properties of Building Number Four.

Mode	Building #2			Building #3			Building #4		
	Modal Yield Strength (Newtown)	Actual Modal Ductility	Predicted Modal Ductility	Modal Yield Stregth (Newtown)	Actual Modal Ductility	Predicted Modal Ductility	Modal Yield Strength (Newton)	Actual Modal Ductility	Predicted Modal Ductility
1	1.94	1.83	1.68	1.60	2.10	1.77	1.60	1.93	1.77
2	2.54	2.92	2.78	3.69	1.79	1.99	3.71	1.86	2.00
3	4.16	2.10	1.38	6.06	1.60	1.08	6.10	1.47	1.07
4	7.05	1.47	0.53	7.62	1.34	0.49	7.40	1.43	0.89
5	8.76	0.69	0.51	7.23	1.61	0.62	7.53	1.34	1.01

TABLE 3.9 Comparison Between the Computed and Predicted Modal Ductilities.

Mode	Building #2			Building #3			Building #4		
	Actual Story Ductility	SRSS Story Ductility	Predicted Story Ductility	Actual Story Ductility	SRSS Story Ductility	Predicted Story Ductility	Actual Story Ductility	SRSS Story Ductility	Predicted Story Ductility
1	2.4	2.7	2.3	2.6	2.7	2.3	2.9	2.6	2.4
2	1.8	2.3	2.0	2.7	2.9	2.2	2.3	2.6	2.3
3	1.5	2.4	1.9	1.7	2.9	2.0	2.2	2.9	2.3
4	3.5	3.0	2.4	2.7	2.7	2.1	2.7	2.7	2.3
5	5.0	4.0	3.4	2.1	2.7	2.4	1.9	2.6	2.4

TABLE 3.10 Comparison Among the Exact, SRSS and Predicted Story Ductilities.

Mode	Building #2		Building #3		Building #4	
	ρ_i	σ_i	ρ_i	σ_i	ρ_i	σ_i
1	2.64	2.83	3.48	3.43	3.42	3.43
2	9.15	5.00	3.87	3.44	3.42	3.42
3	4.62	5.02	2.76	3.45	3.45	3.42
4	2.73	3.59	2.07	3.32	3.39	3.42
5	2.61	3.00	4.23	3.63	3.45	3.48

TABLE 3.11 Comparison of Different Reduction Factors.

Mode	$(S_{d_i})(\Gamma_i^*)(K_i^*)$ (Newton)	Mode Yield Strength (Newton)
1	4.53	5.49
2	10.4	12.7
3	8.84	20.9
4	7.87	25.3
5	9.18	26.2

TABLE 3.12 Comparison Between $(S_{d_i})(\Gamma_i^*)(K_i^*)$ and Modal Yield Strength

Story Number	Story Mass (kg)	Story Stiffness (kg/sec/sec)	Story Yield Strength (Newton)
1	1.	2025.	7.32
2	1.	1800.	6.98
3	1.	1575.	6.32
4	1.	1350.	5.32
5	1.	1125.	3.99
6	1.	900.	2.33

TABLE 3.13 Physical Properties of Example Building.

Story	Exact Story Ductility	Predicted Story Ductility
1	3.60	2.69
2	2.89	2.67
3	2.36	2.65
4	2.44	2.65
5	2.43	2.70
6	2.71	2.80

TABLE 3.14 Comparison Between the Computed and Predicted Story Ductilities.

Date (1)	Earthquake (2)	Recording Site (3)	Component (4)
1934, Dec 30	Lower California	El Centro, Imperial Valley	S00W S90W
1935, Oct 31	Helena, Montana	Carrol College	S00W S90W
1940, May 18	Imperial Valley	El Centro	S00W S90W
1949, Apr 13	Western Wahsington	Olympia, Hwy. Test. Lab.	N04E N68E
1952, Jul 21	Kern County	Taft, Lincoln School Tunnel	N21E S69E

TABLE 4.1 Ground Motion Records.

Structural Period	Subsystem Damping	Elasto-Perfectly Plastic				Stiffness Degrading Model			
		$\frac{T_c}{T_b}$	$\frac{(ln1000 \cdot T_c)}{(ln1000 \cdot T_b)}$	$\frac{(ln1000 \cdot T_d)}{(ln1000 \cdot T_c)}$	average amplification factor *	$\frac{T_c}{T_b}$	$\frac{(ln1000 \cdot T_c)}{(ln1000 \cdot T_b)}$	$\frac{(ln1000 \cdot T_d)}{(ln1000 \cdot T_c)}$	average amplification factor *
(1)	(2)	(3)	(4)	(5)	(6)	(7)	(8)	(9)	(10)
0.2	1%	1.37	1.06	1.05	1.04	1.37	1.06	1.09	1.15
0.2	5%	1.37	1.06	1.08	1.04	1.37	1.06	1.12	1.13
0.3	1%	2.16	1.16	1.11	1.05	2.16	1.16	1.10	1.16
0.3	5%	2.16	1.16	1.20	1.02	2.16	1.16	1.12	1.11
0.5	1%	1.46	1.06	1.10	1.06	1.75	1.10	1.06	1.17
0.5	5%	1.46	1.06	1.13	1.02	2.13	1.14	1.10	1.12
1.0	1%	2.02	1.11	1.06	0.99	2.30	1.14	1.07	1.11
1.0	5%	2.12	1.12	1.08	0.95	2.61	1.16	1.09	1.08
mean		1.77	1.10	1.10	1.02	1.98	1.12	1.09	1.11
std. dev		0.35	0.04	0.04	0.03	0.42	0.04	0.02	0.04
COV		0.20	0.04	0.04	0.03	0.21	0.04	0.02	0.04

* Period > T_d

TABLE 4.2 Statistical Values For The Proposed Amplification Factors For Structural Ductility Of 4.

(1)	EPP 0.5 sec		SDM 0.5 sec	
	1% (2)	5% (3)	1% (4)	5% (5)
T_c / T_b	1.64	1.48	1.75	2.13
$\ln(1000 \cdot T_c)/\ln(1000 \cdot T_b)$	1.08	1.07	1.10	1.14
$\ln(1000 \cdot T_d)/\ln(1000 \cdot T_c)$	1.04	1.11	1.04	1.07
average amplification factor	1.04	1.04	1.11	1.07

TABLE 4.3 Statistical Values For The Proposed Amplification Factors For Structural Ductility Of 2 And Period Of 0.5 Second.

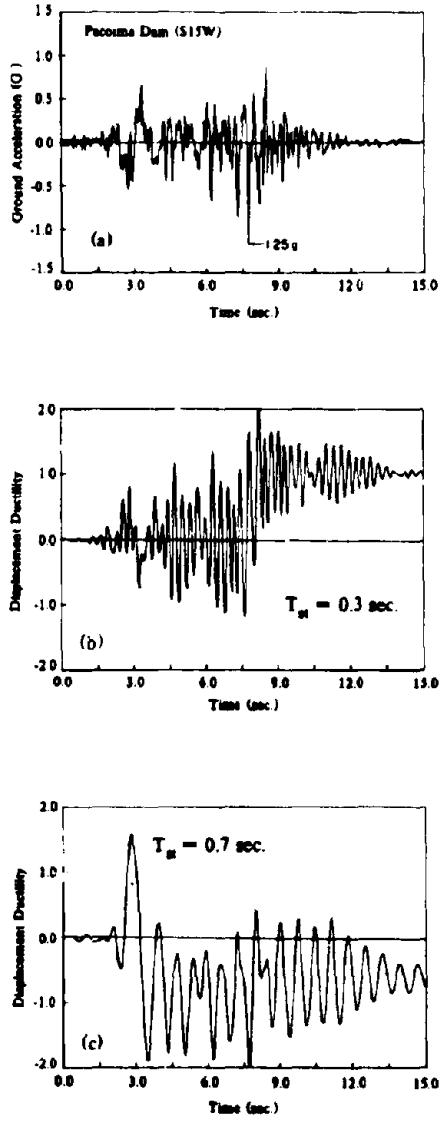

Fig. 2.1 Ground Motion for the S15W Component of the Pacoima Dam Record of February 9, 1971 and the Response Ductility Time Histories.

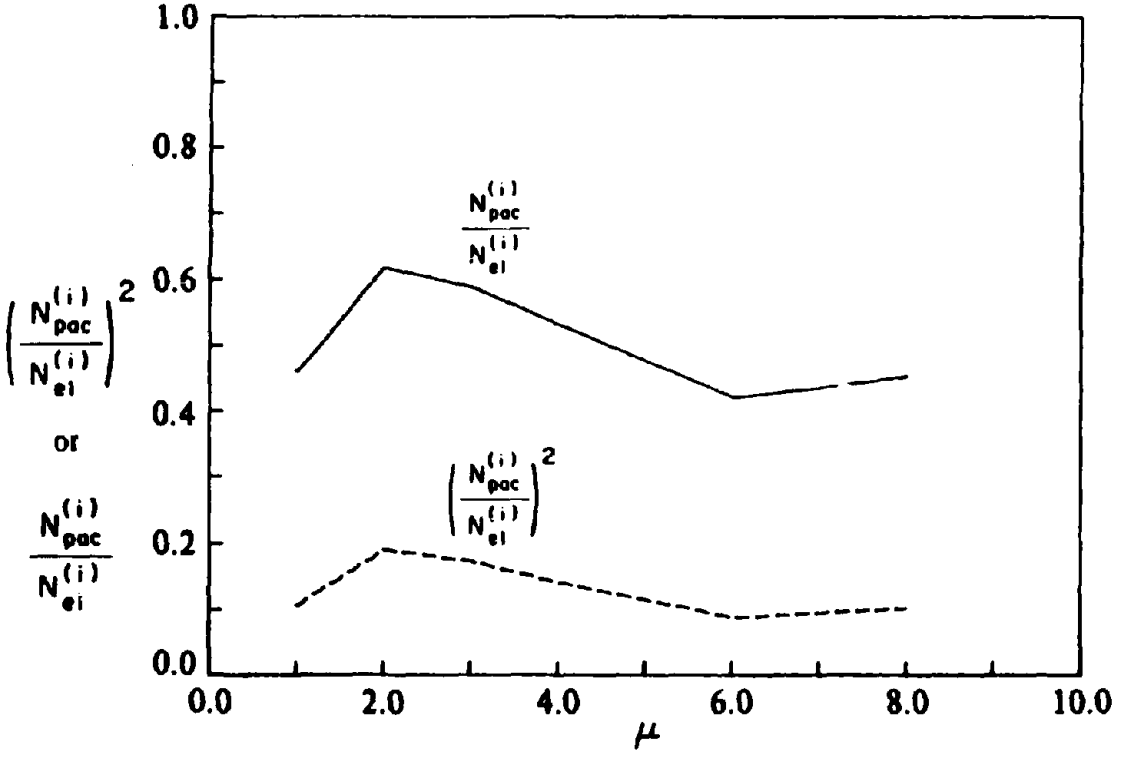

FIG. 2.2 Scaling Relationship Between the S15W Pacoima Dam Record and the EW 1940 El Centro Record.

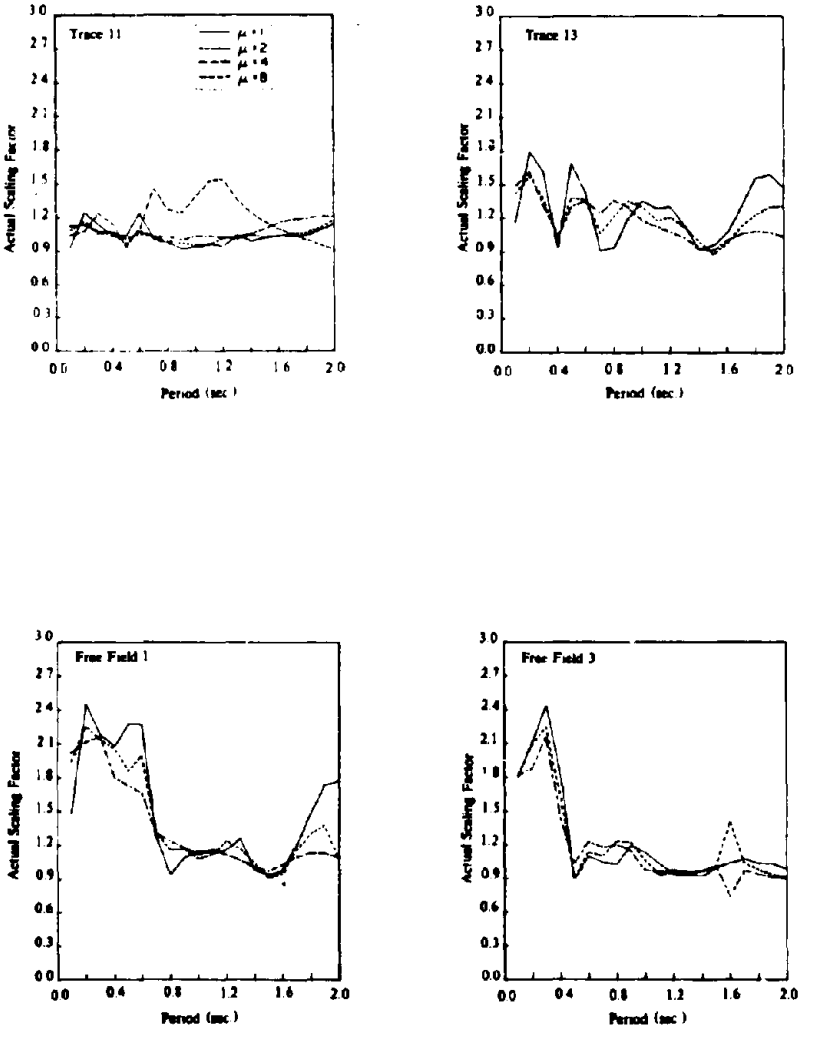

Fig. 2.3 Actual Scaling Factors Based on Displacement Ductility. (First Ground Motion Set)

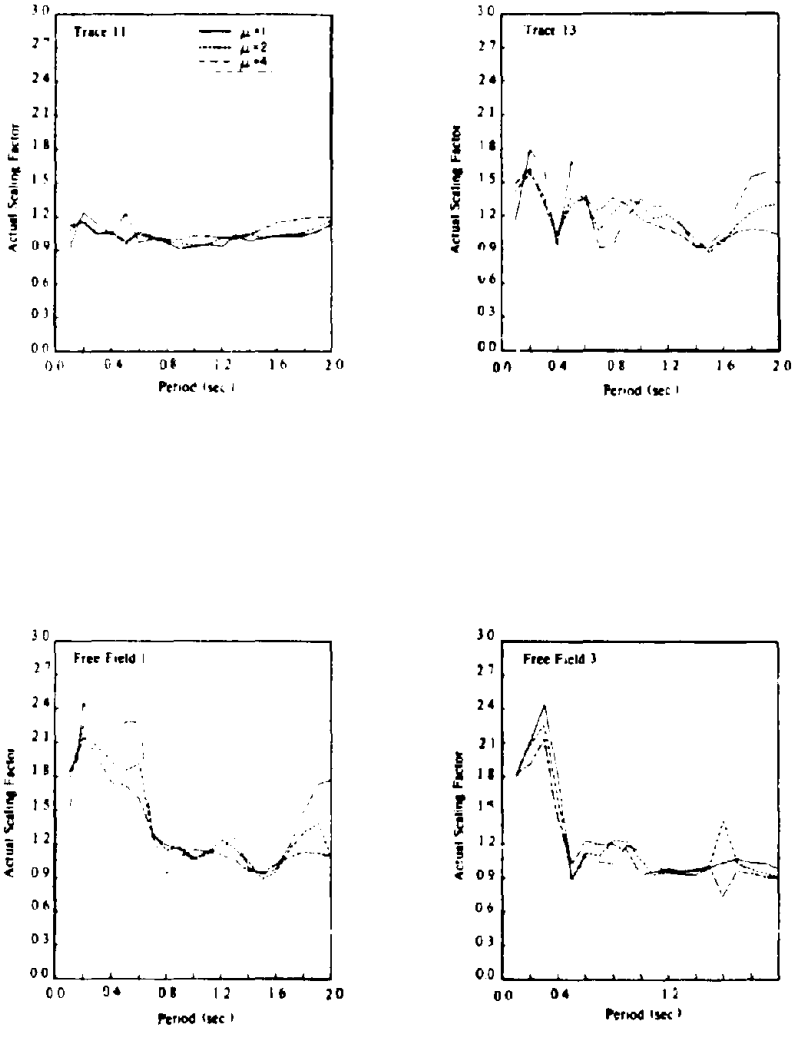

Fig. 2.4 Actual Scaling Factors Based on Normalized Hysteretic Energy Ductility. (First Ground Motion Set)

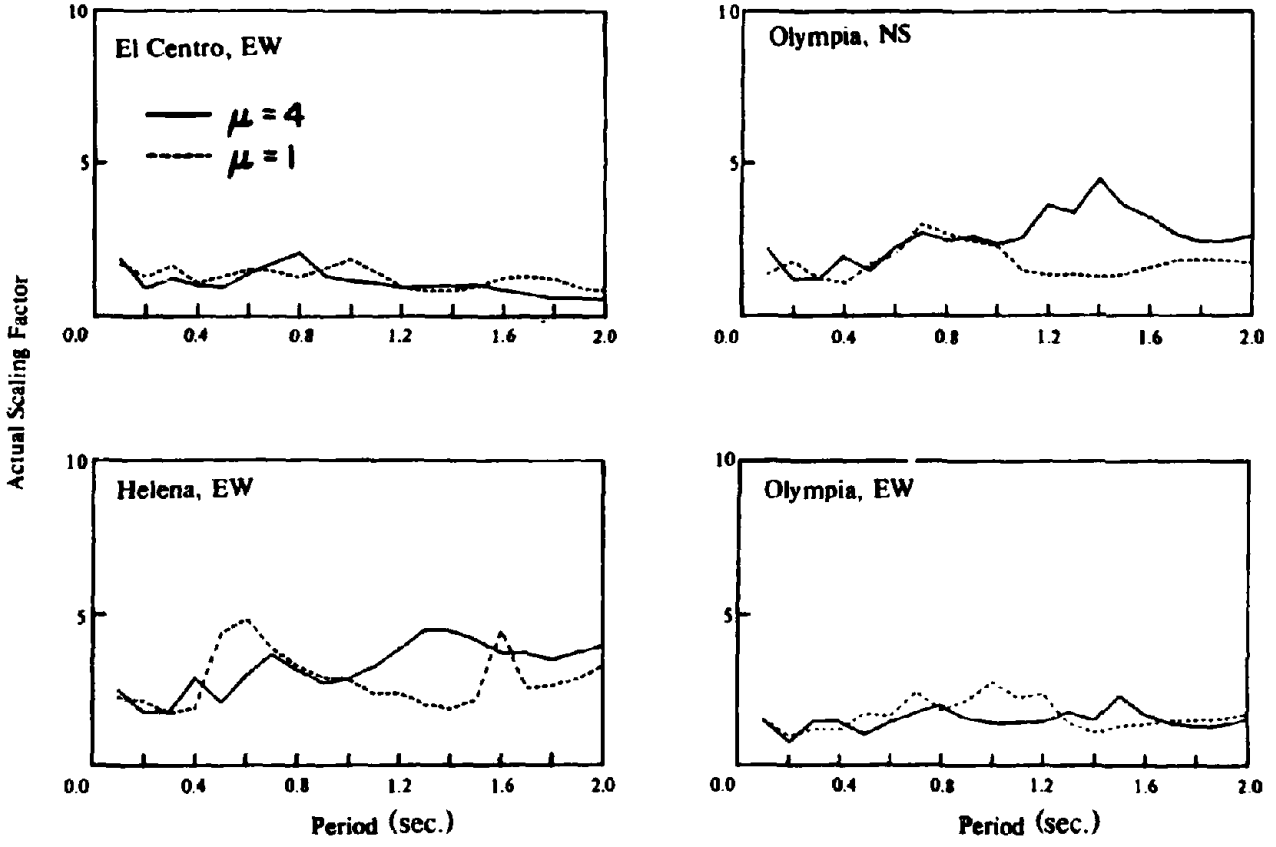

Fig. 2.5 Actual Scaling Factors Based on Displacement Ductility. (Second Ground Motion Set)

Continued

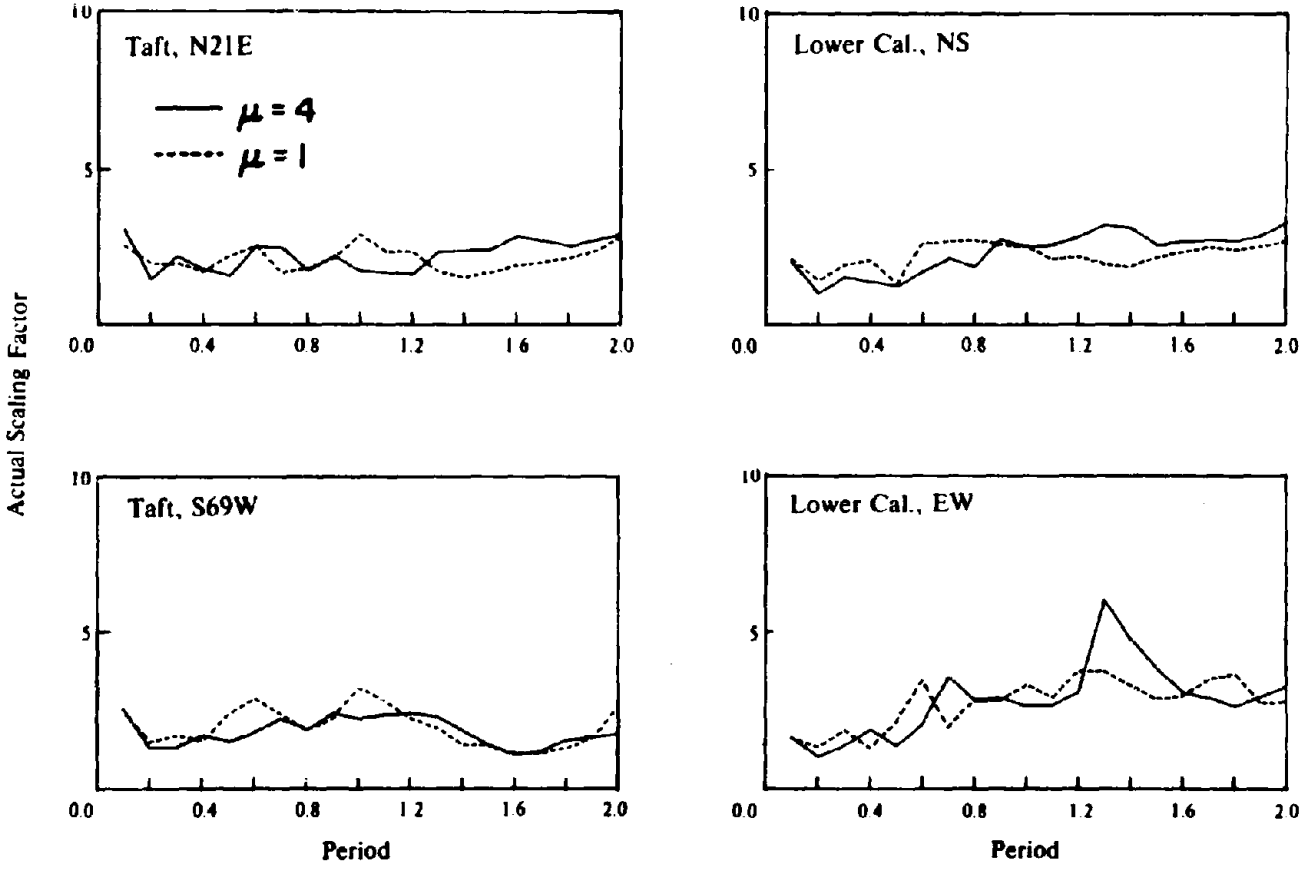

Fig. 2.5 Actual Scaling Factors Based on Displacement Ductility. (Second Ground Motion Set)

Continued

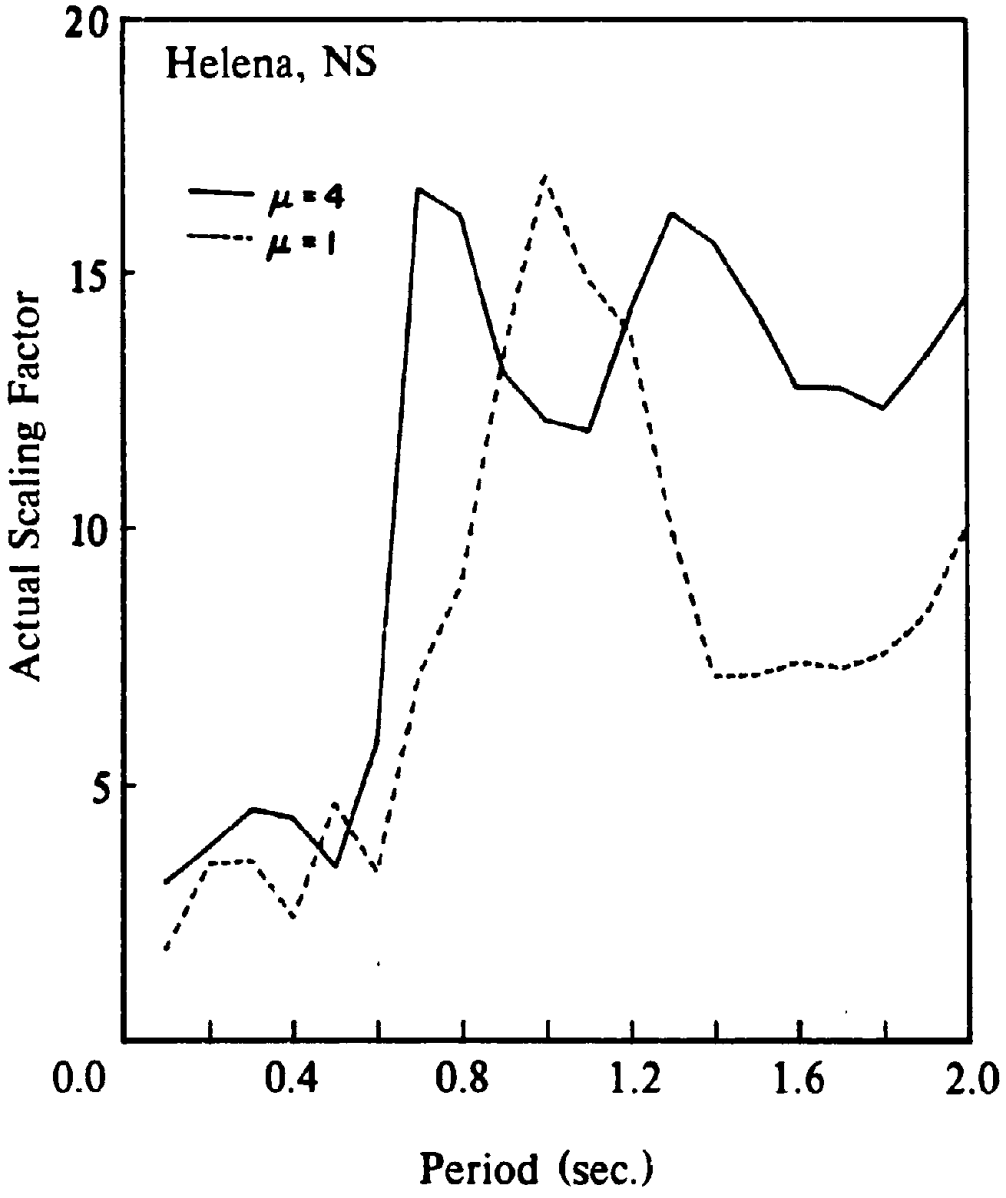

Fig. 2.5 Actual Scaling Factors Based on Displacement Ductility. (Second Ground Motion Set)

Continued

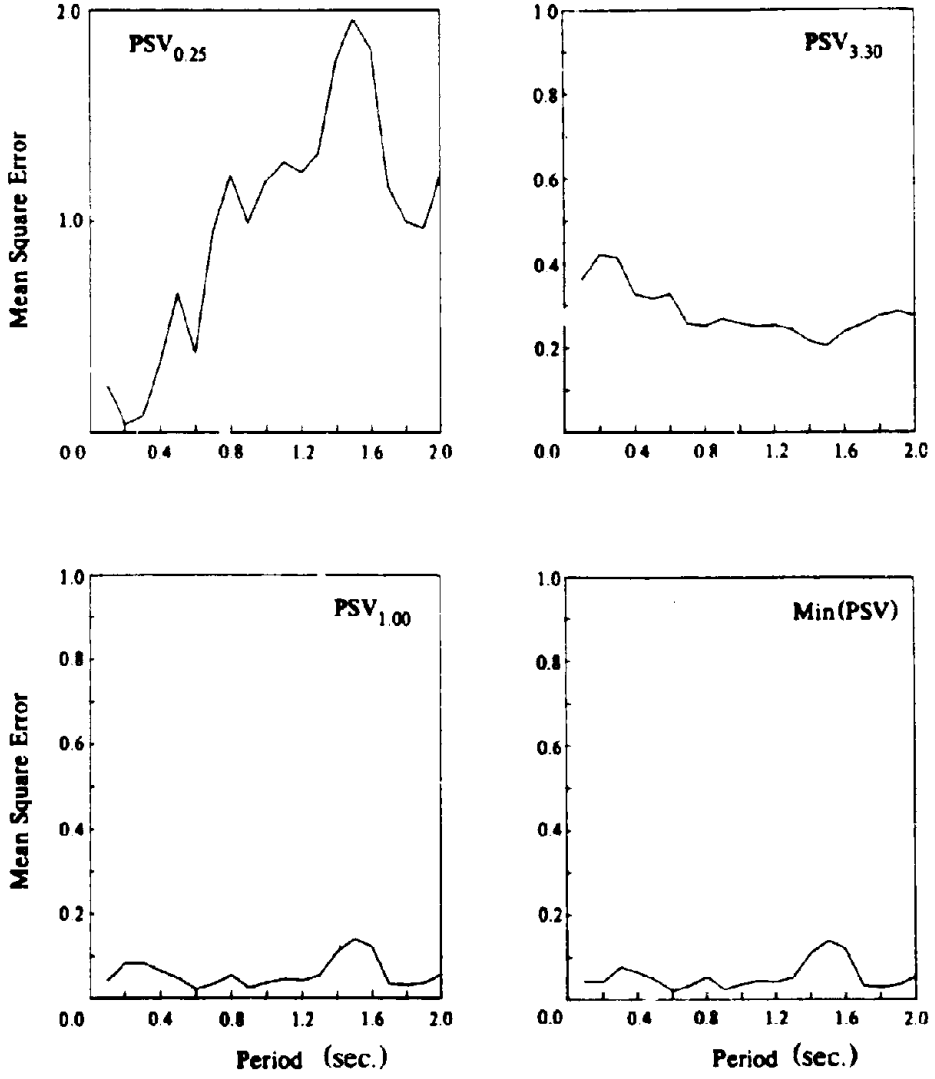

Fig. 2.6 Mean Square Error Based on Displacement Ductility. (First Ground Motion Set)

Continued

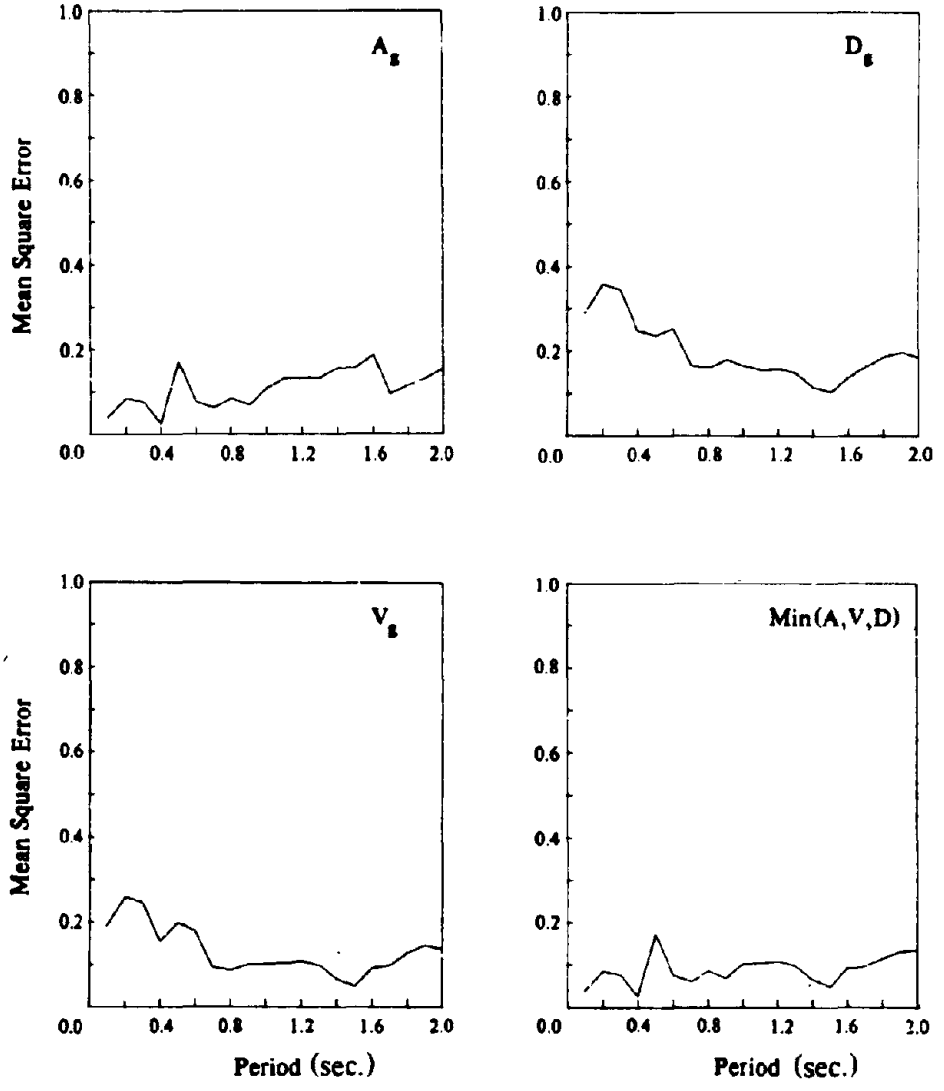

Fig. 2.6 Mean Square Error Based on Displacement Ductility. (First Ground Motion Set)

Continued

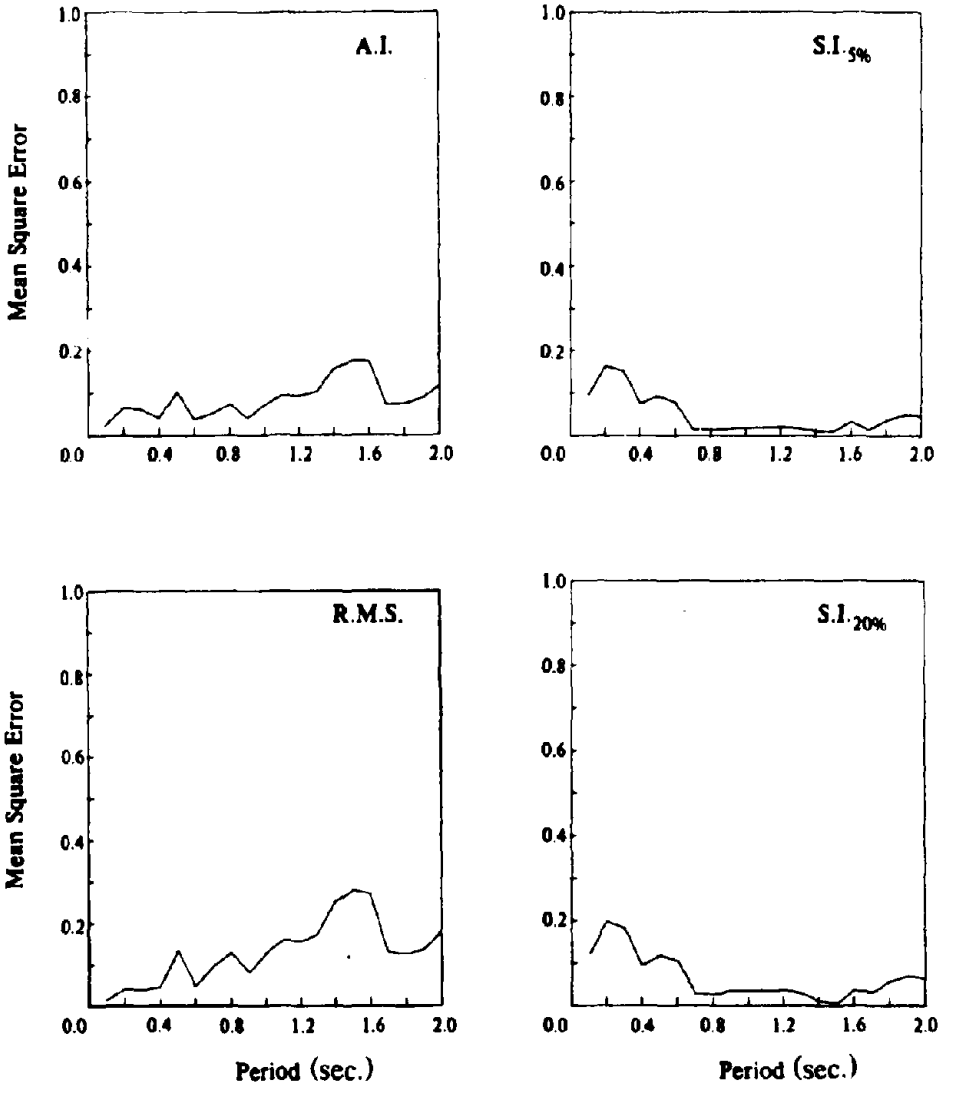

Fig. 2.6 Mean Square Error Based on Displacement Ductility. (First Ground Motion Set)

Continued

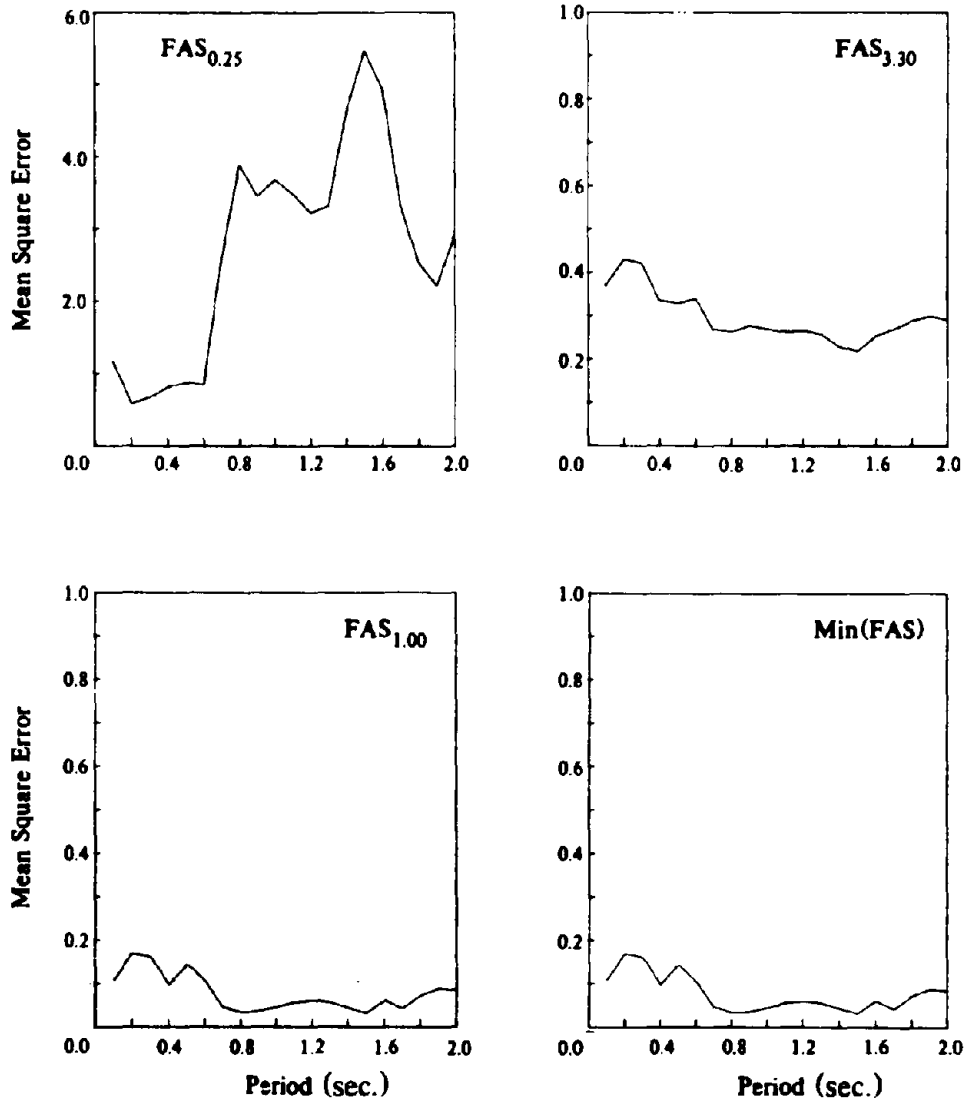

Fig. 2.6 Mean Square Error Based on Displacement Ductility. (First Ground Motion Set)

Continued

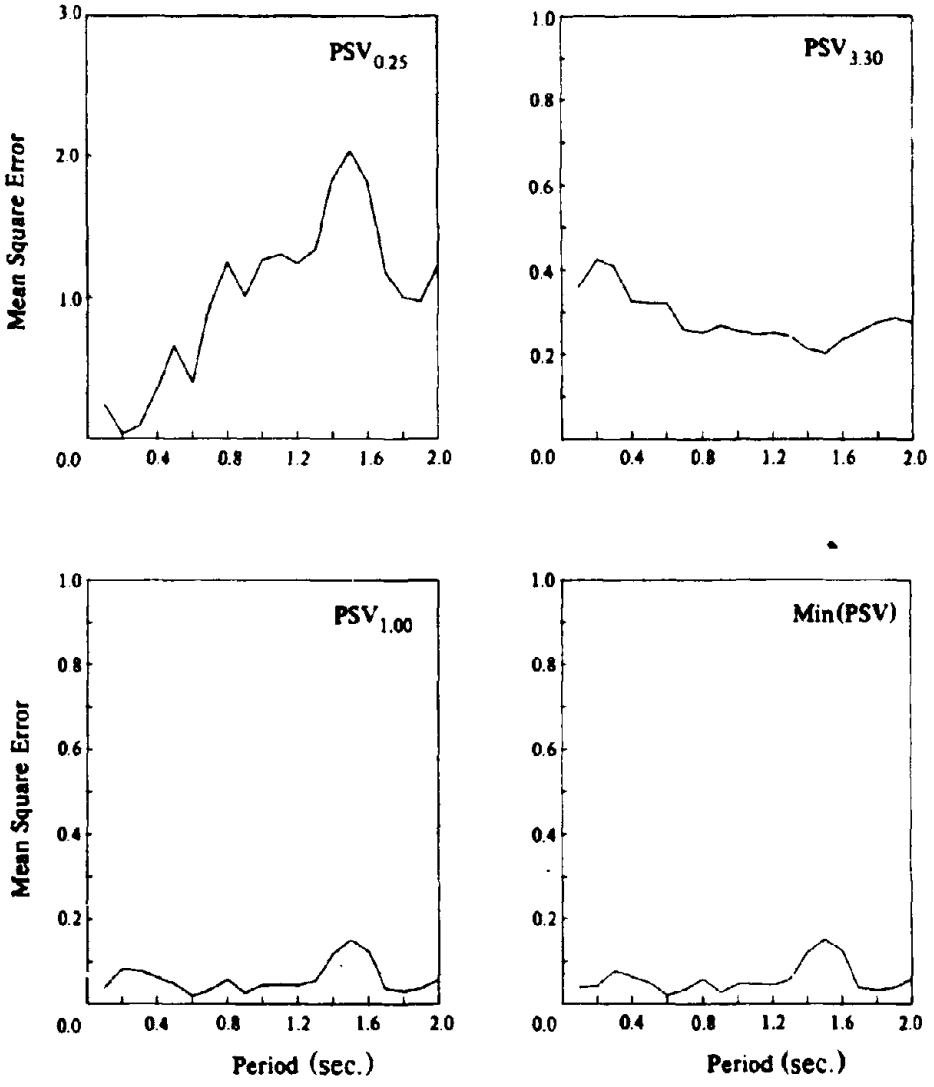

Fig. 2.7 Mean Square Error Based on Normalized Hysteretic Energy Ductility. (First Ground Motion Set)

Continued

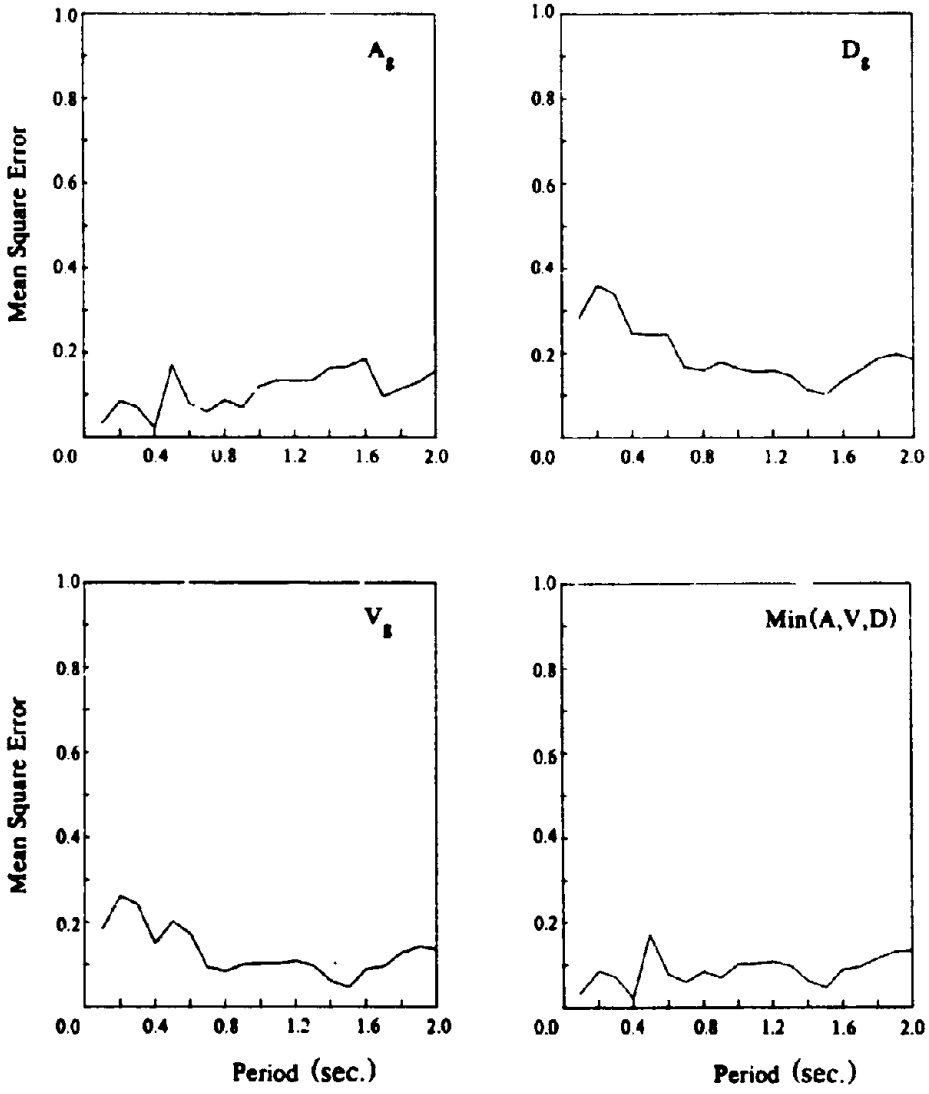

Fig. 2.7 Mean Square Error Based on Normalized Hysteretic Energy Ductility. (First Ground Motion Set)

Continued

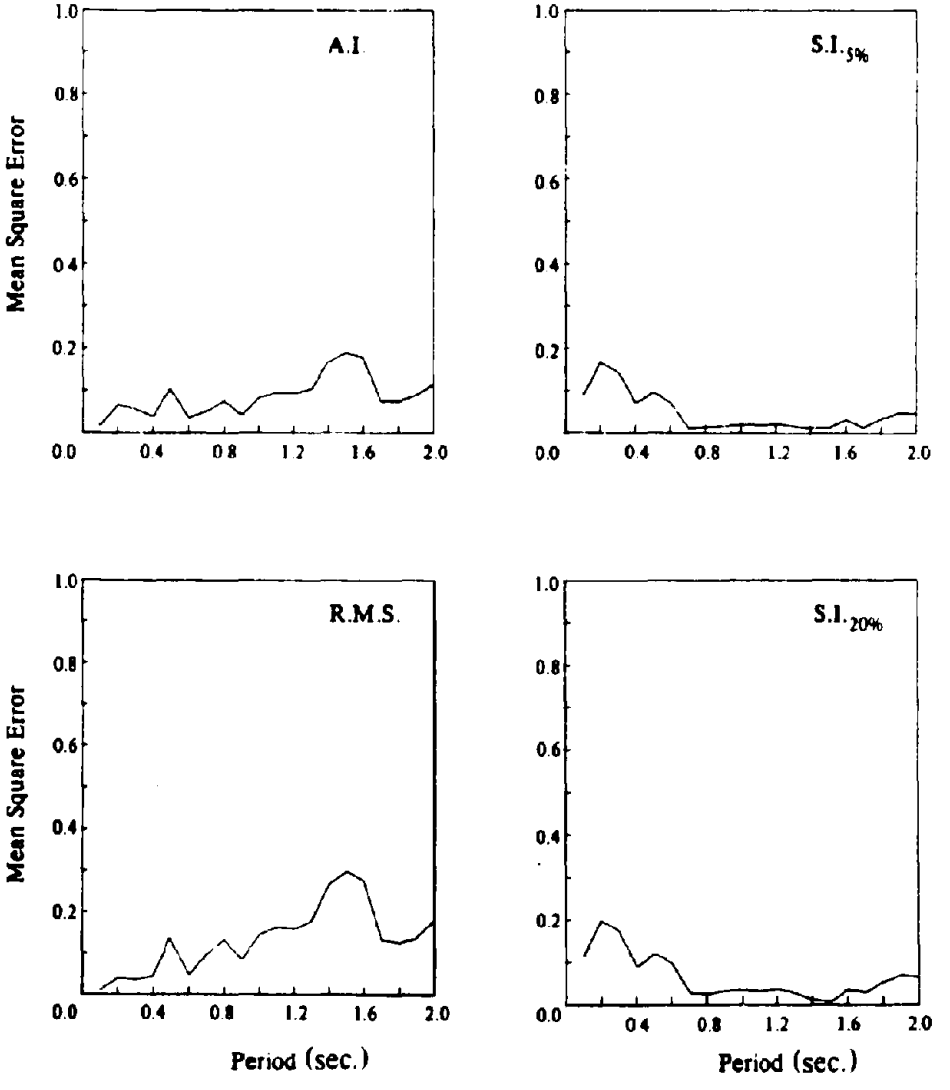

Fig. 2.7 Mean Square Error Based on Normalized Hysteretic Energy Ductility. (First Ground Motion Set)

Continued

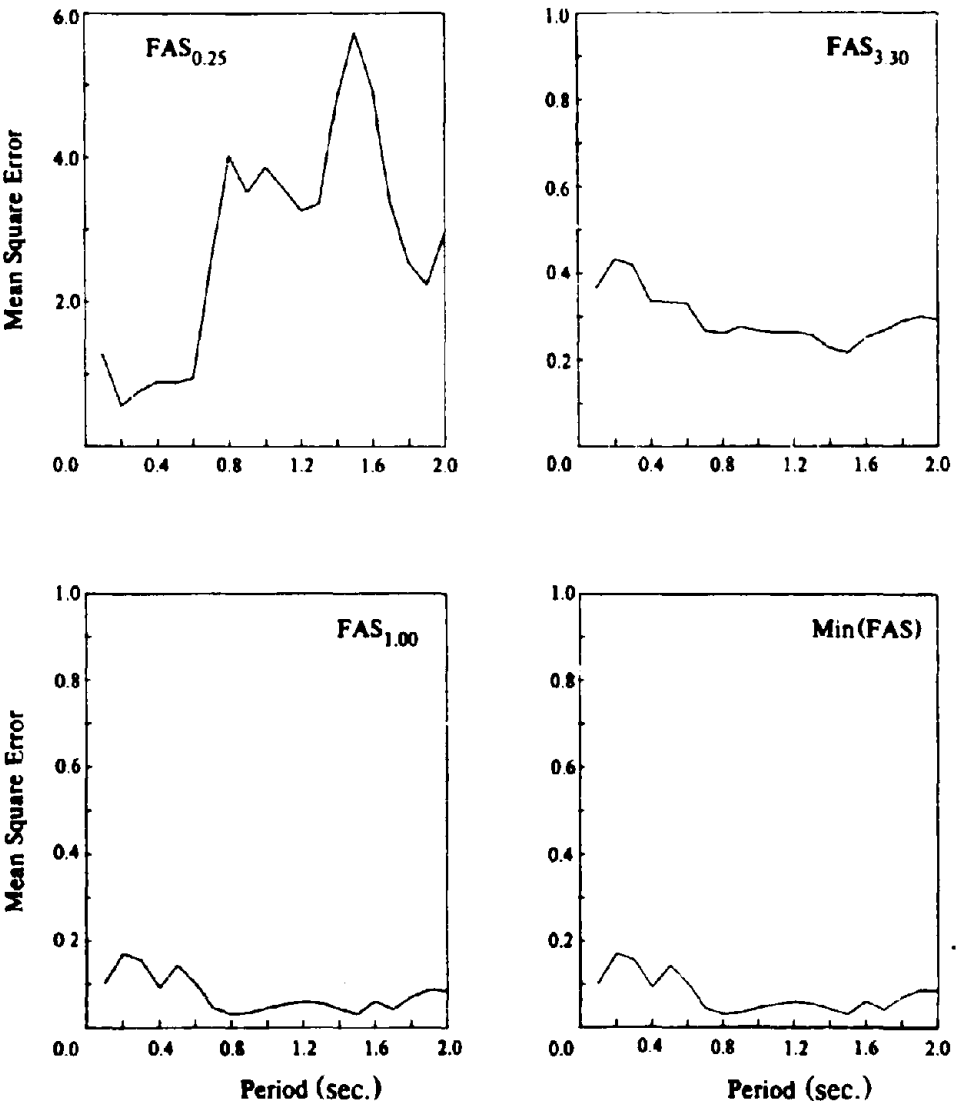

Fig. 2.7 Mean Square Error Based on Normalized Hysteretic Energy Ductility. (First Ground Motion Set)

Continued

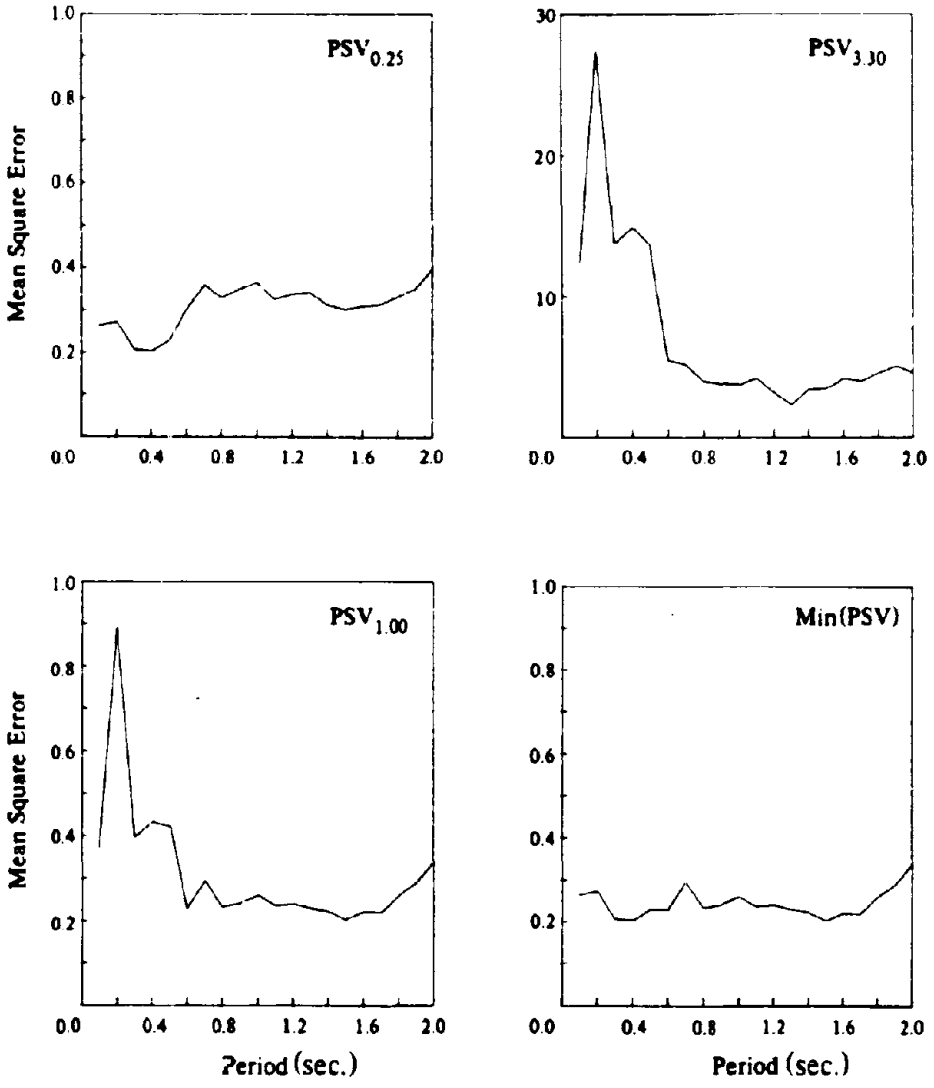

Fig. 2.8 Mean Square Error Based on Displacement Ductility. (Second Ground Motion Set)

Continued

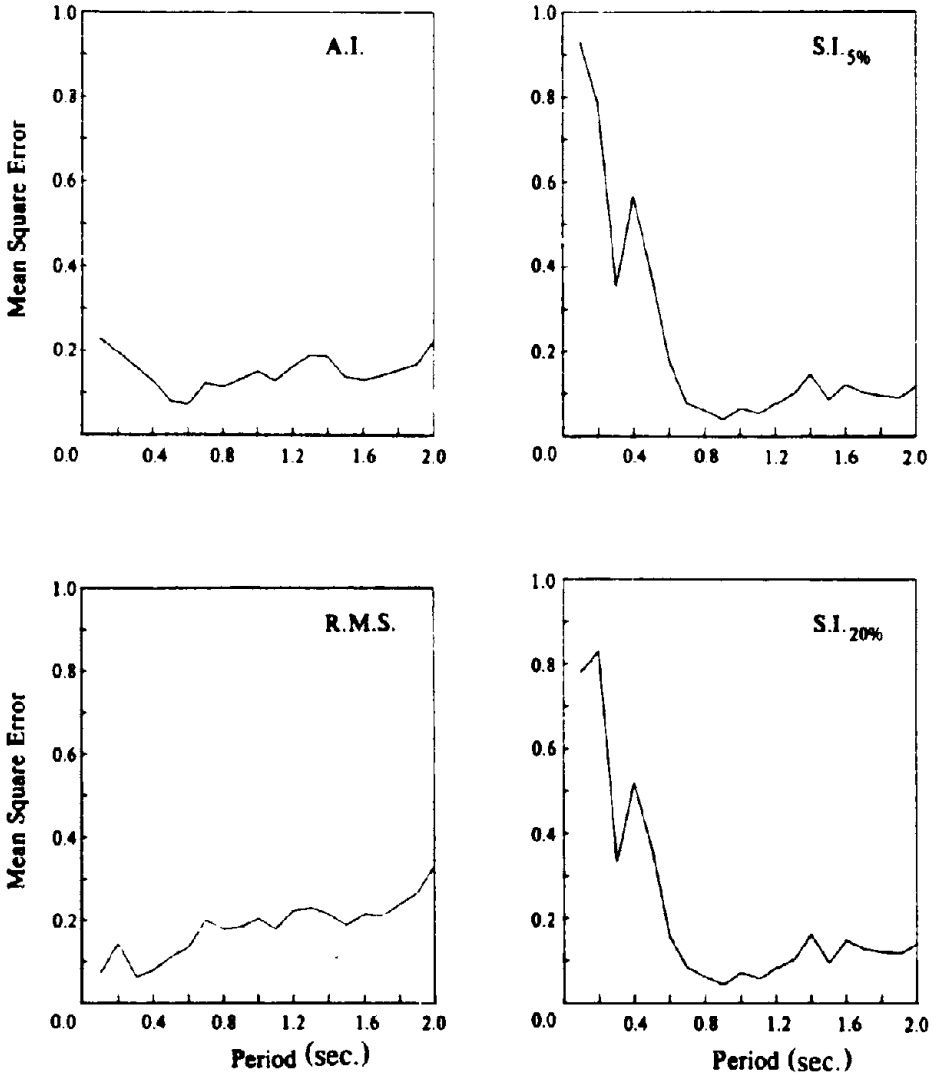

Fig. 2.8 Mean Square Error Based on Displacement Ductility. (Second Ground Motion Set)

Continued

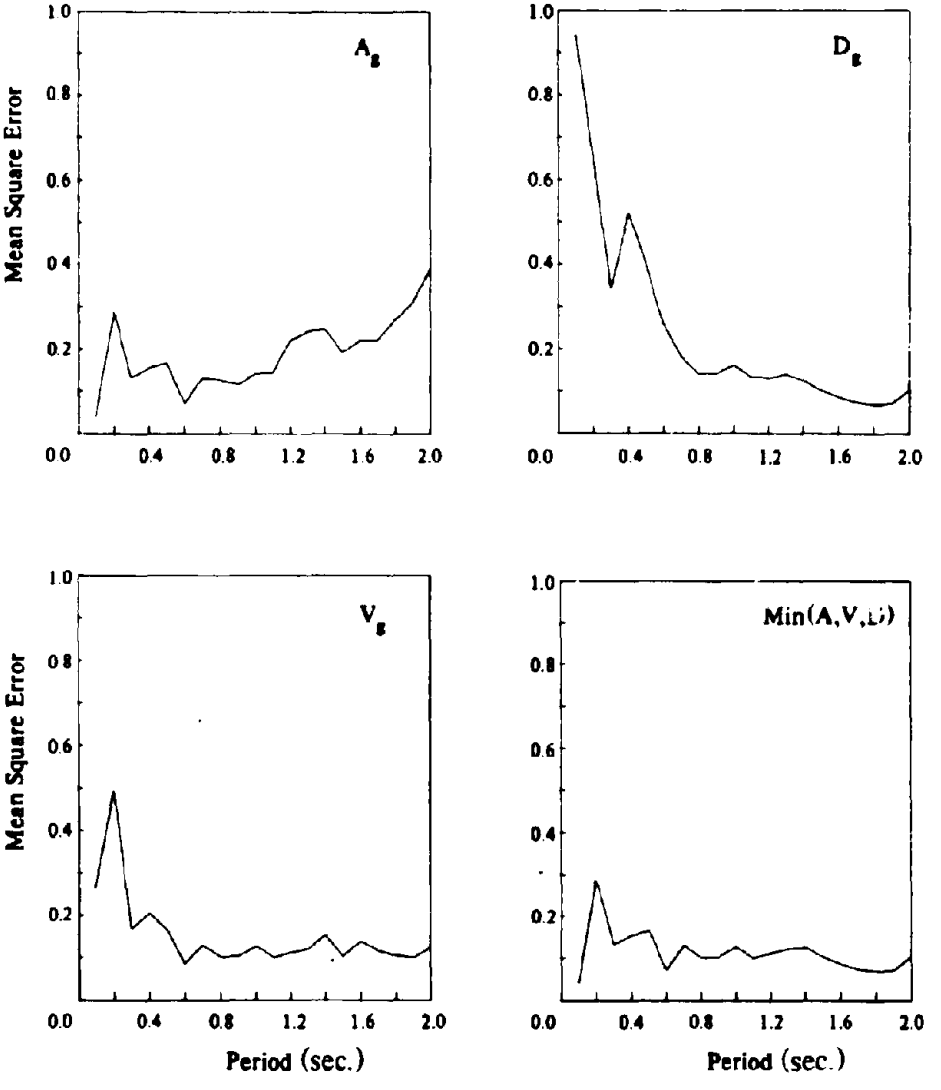

Fig. 2.8 Mean Square Error Based on Displacement Ductility. (Second Ground Motion Set)

Continued

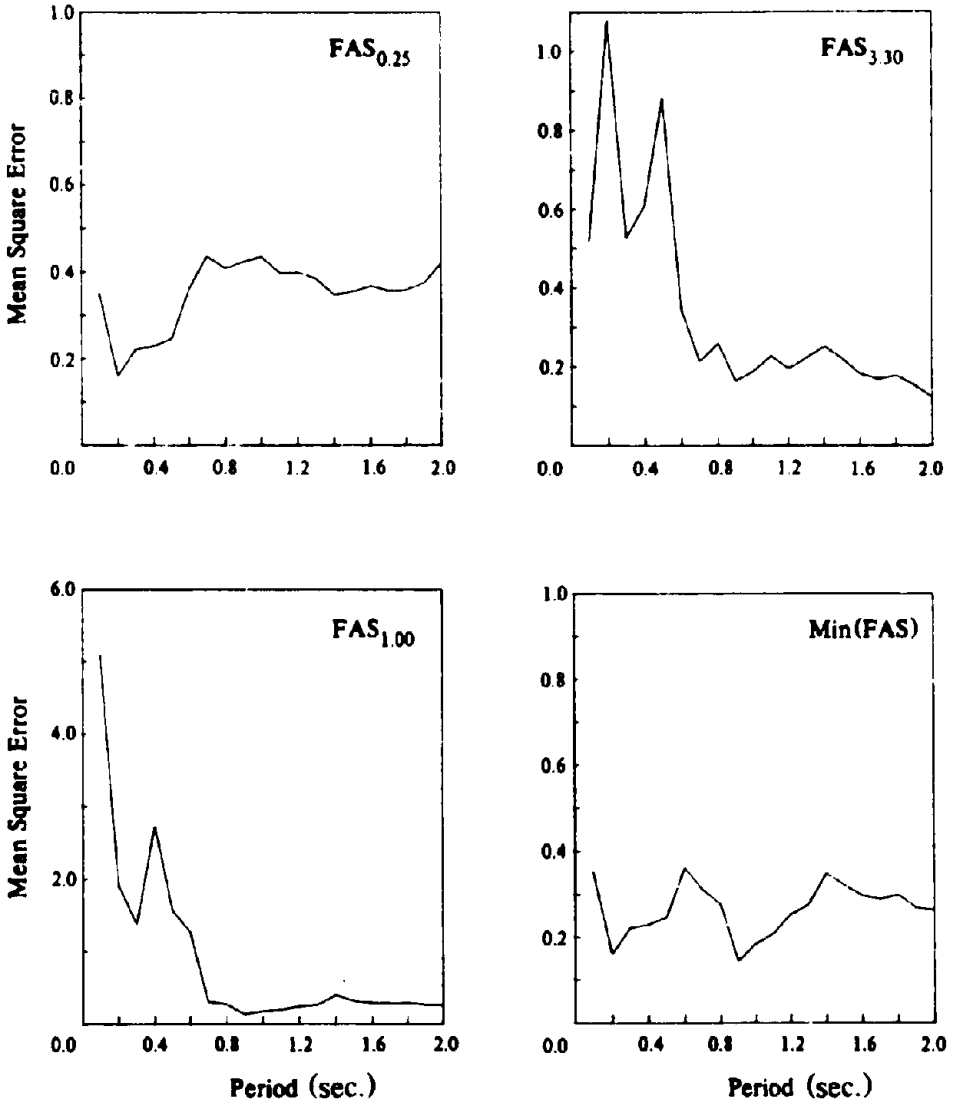

Fig. 2.8 Mean Square Error Based on Displacement Ductility. (Second Ground Motion Set)

Continued

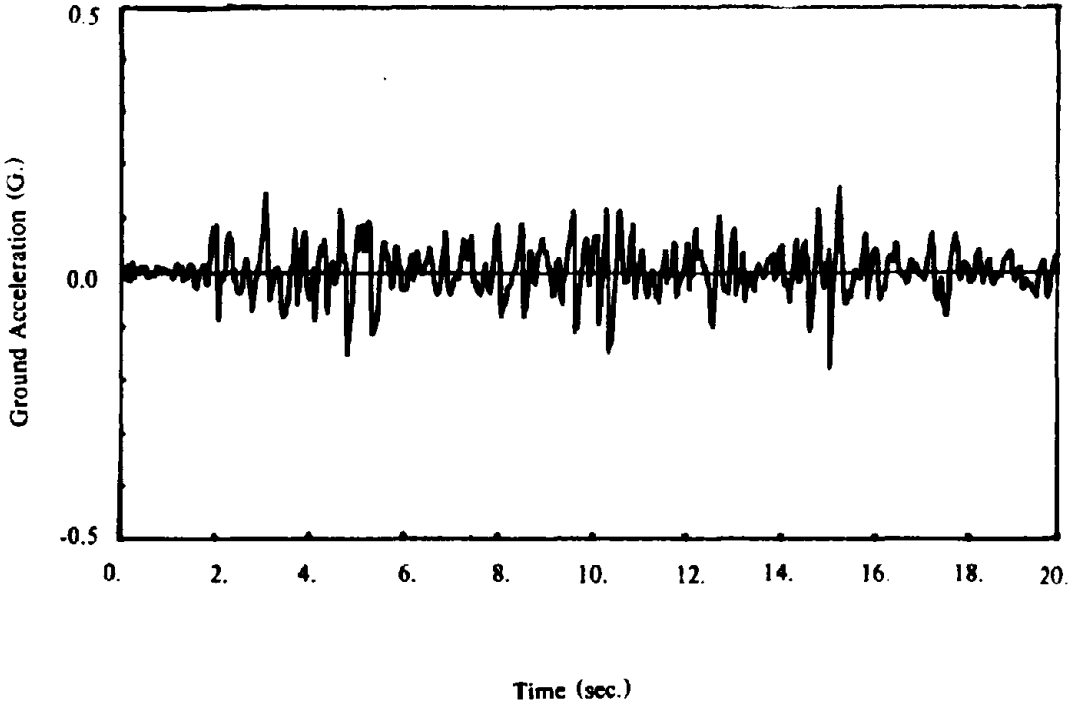

FIG. 3.1 Ground Acceleration for the East-West Component of the 1934 El Centro Earthquake

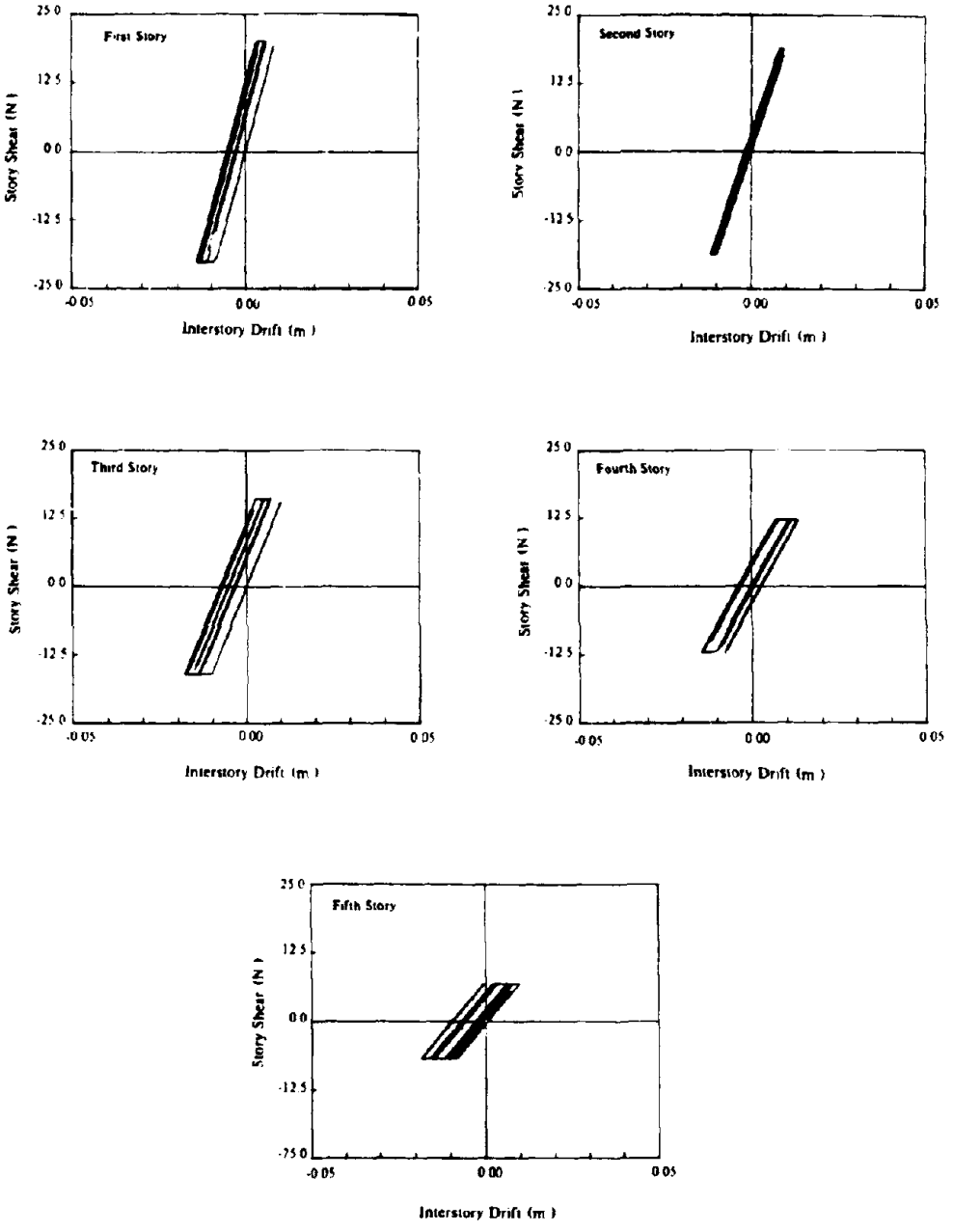

Fig. 3.2 Story Hystereses of Building Number One.

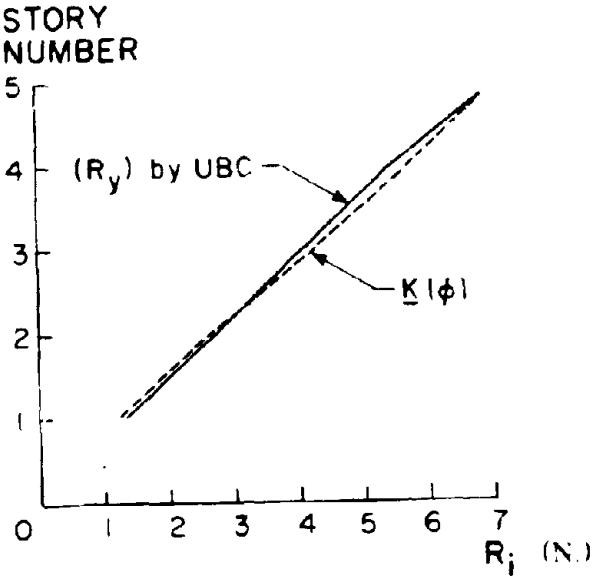

FIG. 3.3 Comparison Between $\{R_y\}$ and the External Force Corresponding to the First Mode Shape Vector.

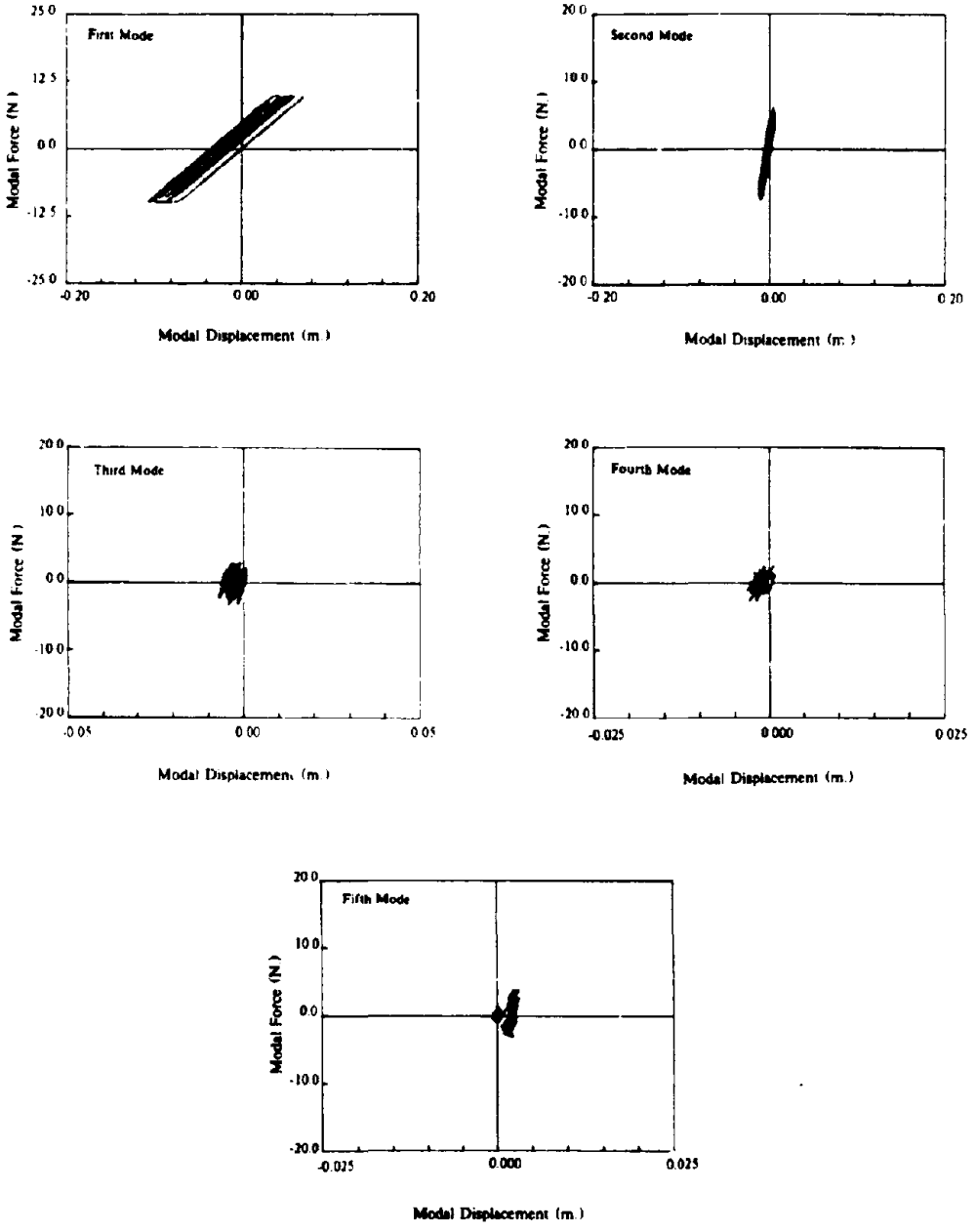

Fig. 3.4 Modal Hystereses of Building Number One.

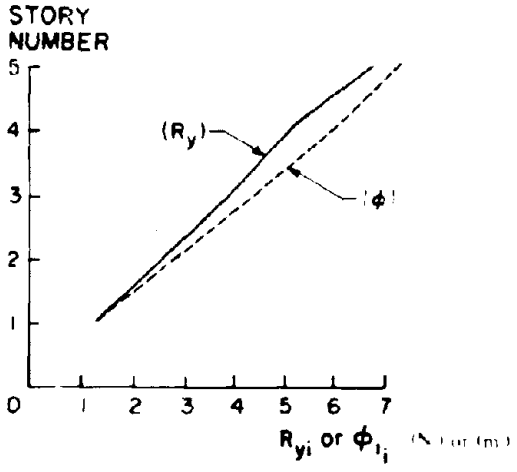

FIG. 3.5 Comparison Between $\{R_y\}$ and the First Mode Shape Vector.

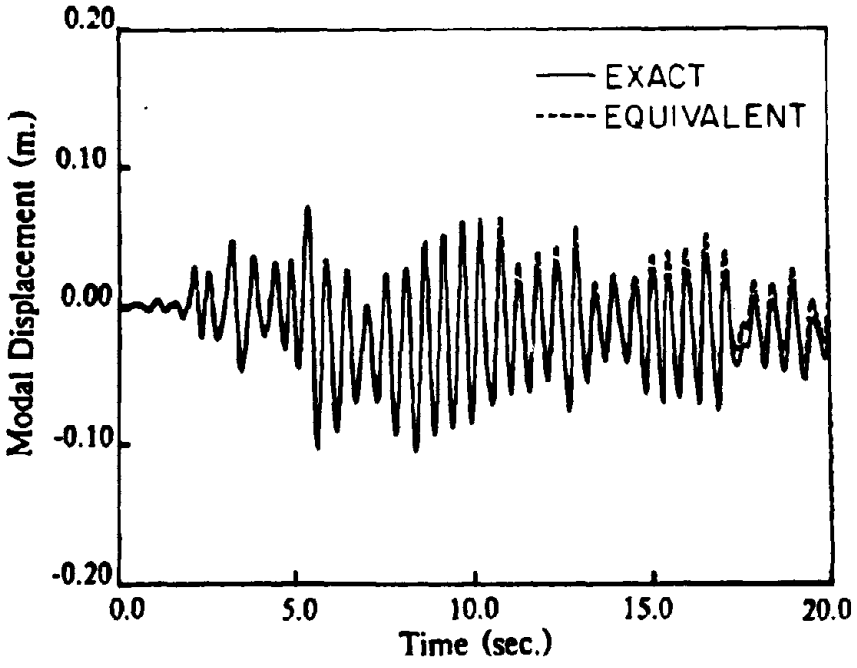

FIG. 3.6 Comparison Between the Exact and Equivalent First Mode Displacement Time Histories.

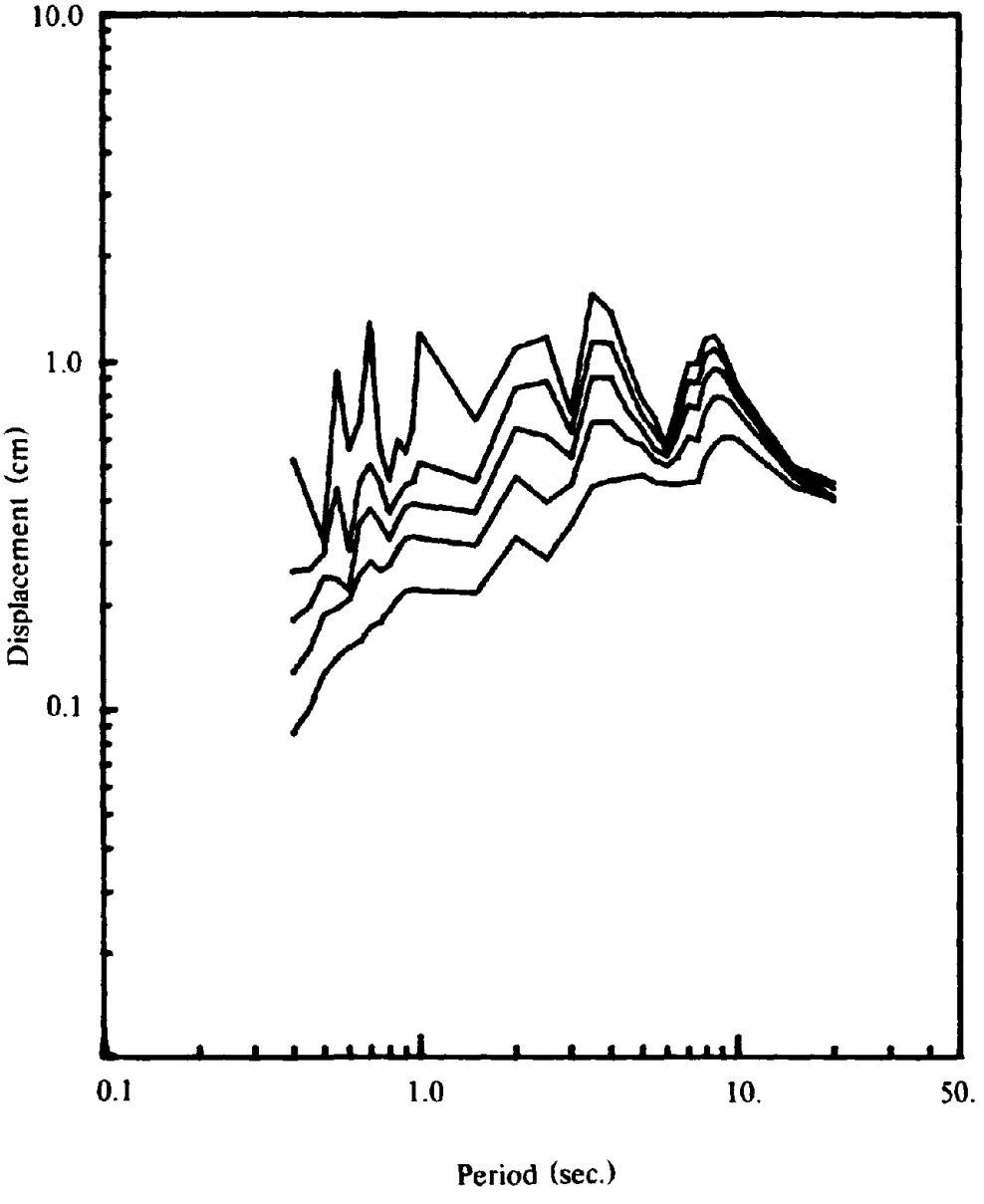

FIG. 3.7 Response Spectra for the 1934 El Centro (EW) Earthquake Ground Motion

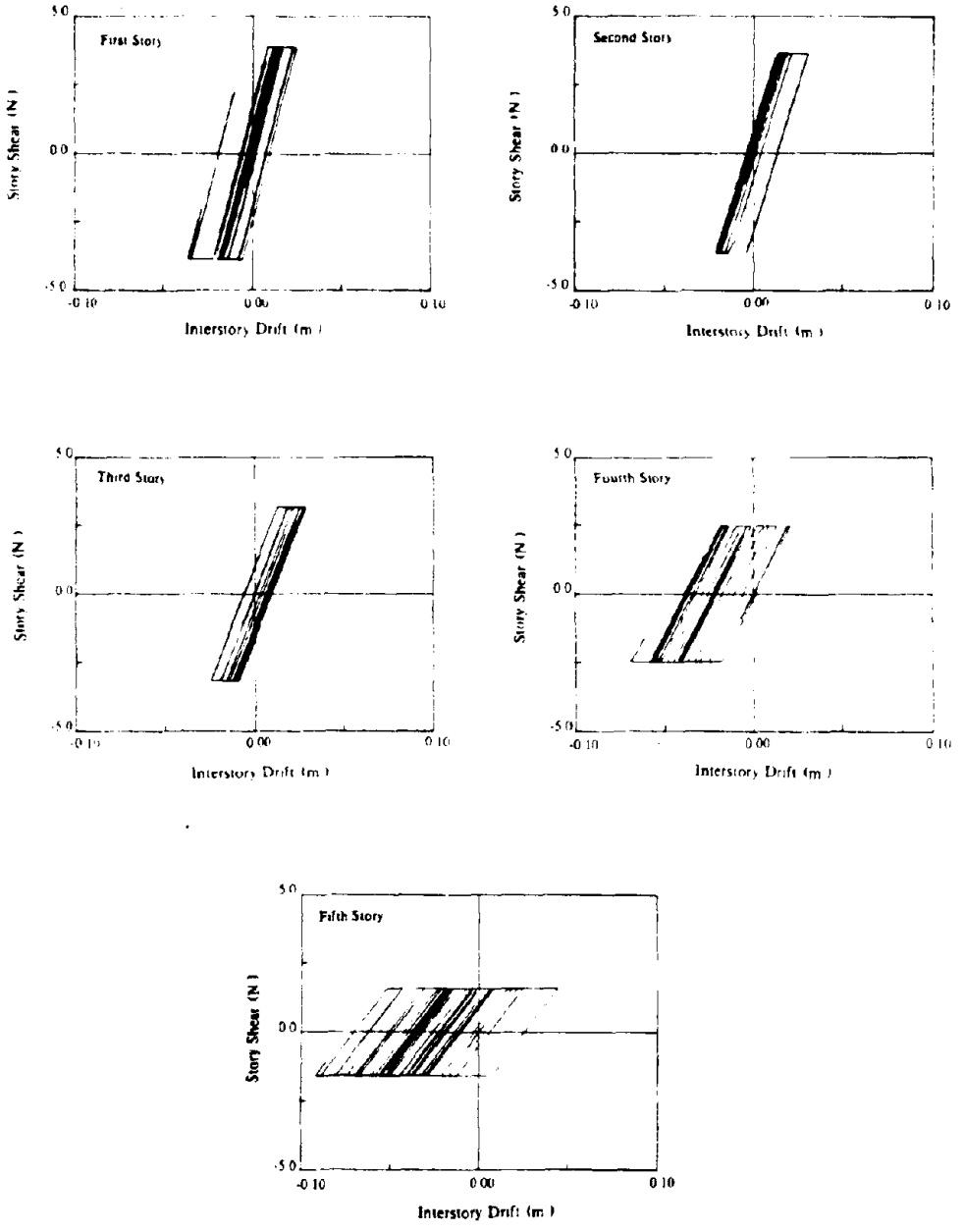

Fig. 3.8 Story Hystereses of Building Number Two.

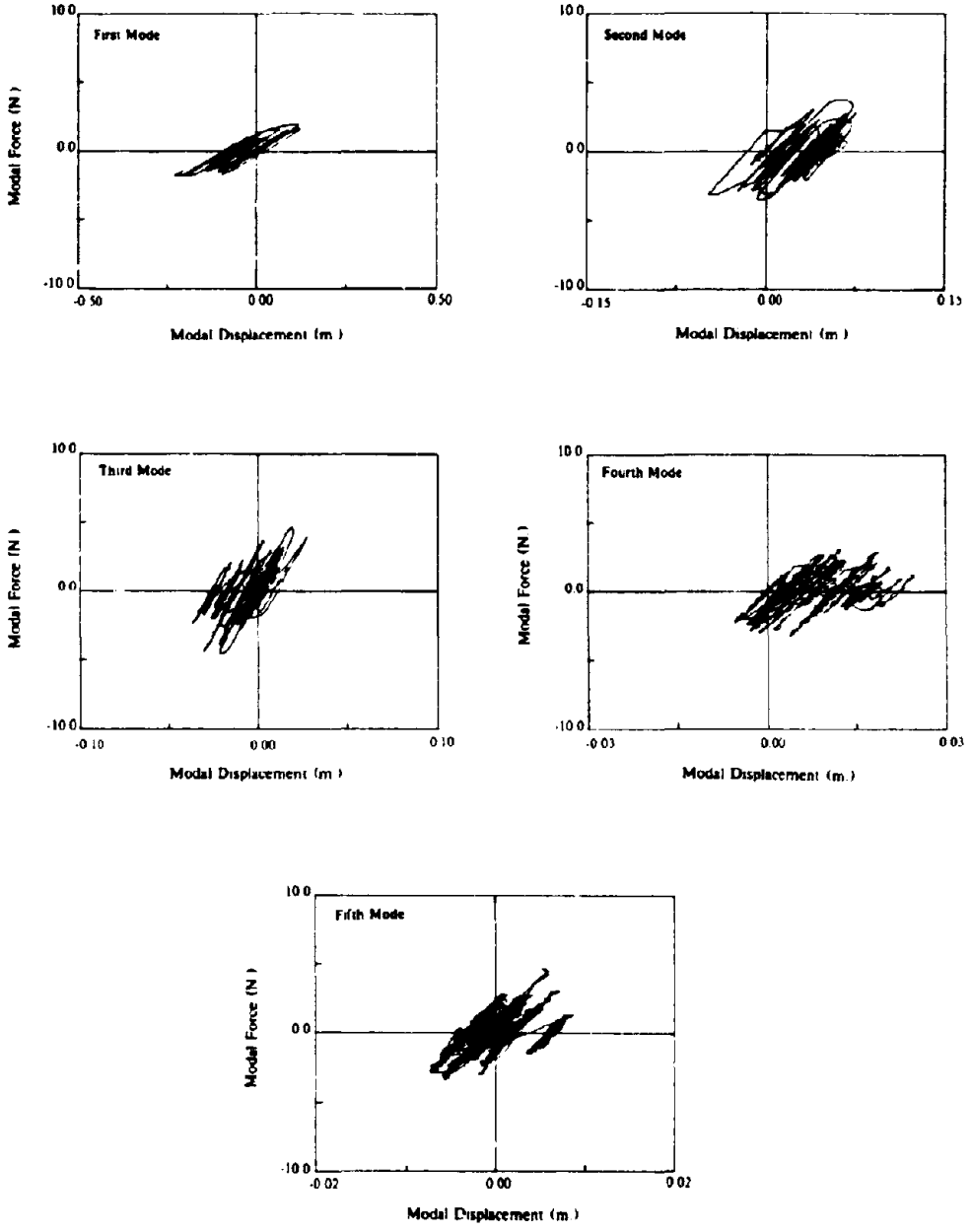

Fig. 3.9 Modal Hystereses of Building Number Two.

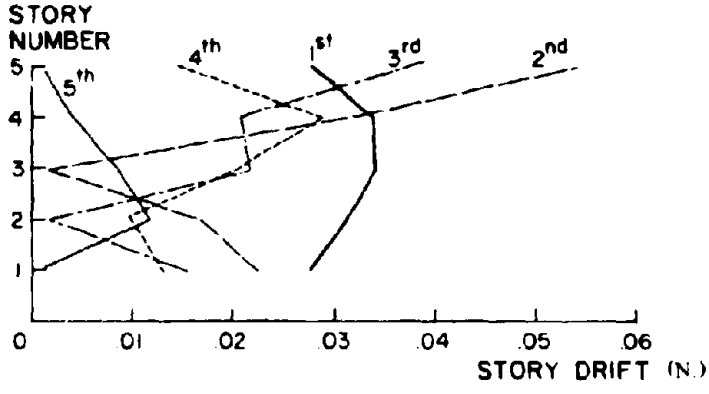

FIG. 3.10 Story Drifts Caused by Each of the Maximum Modal Displacement. (Building Number Two)

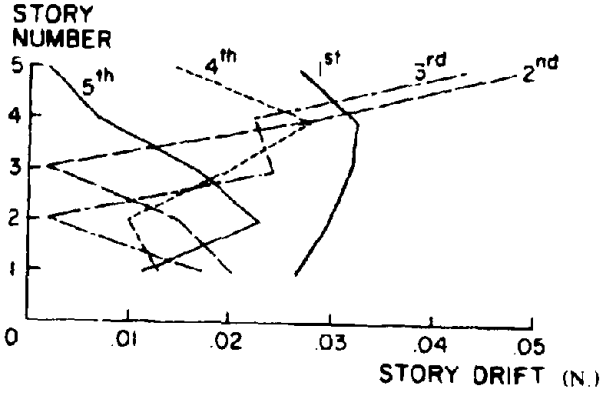

FIG. 3.11 Story Drifts Caused by Each of the Maximum Modal Displacement. (Building Number Three)

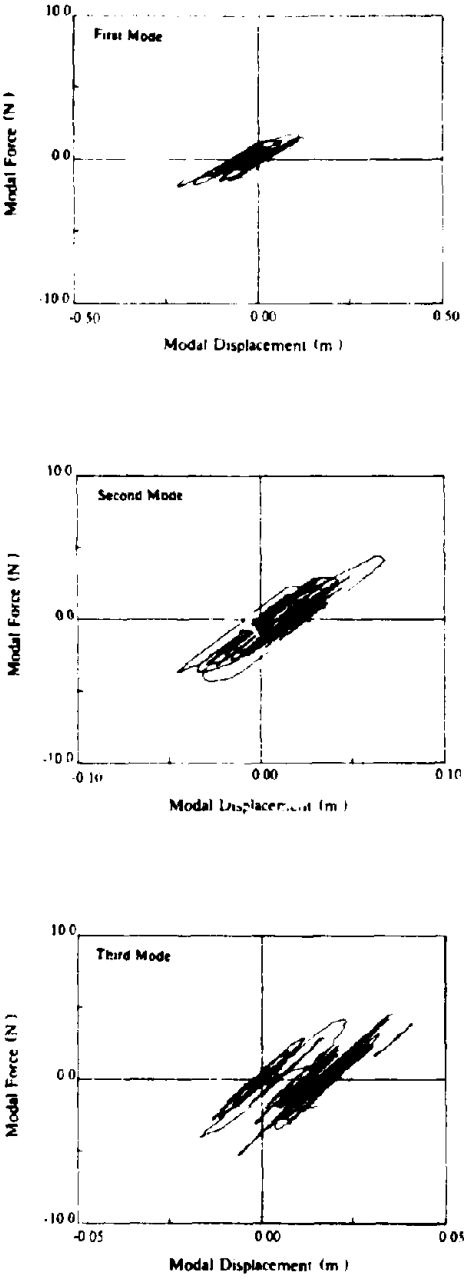

Fig. 3.12 Modal Hystereses of Building Number Three.

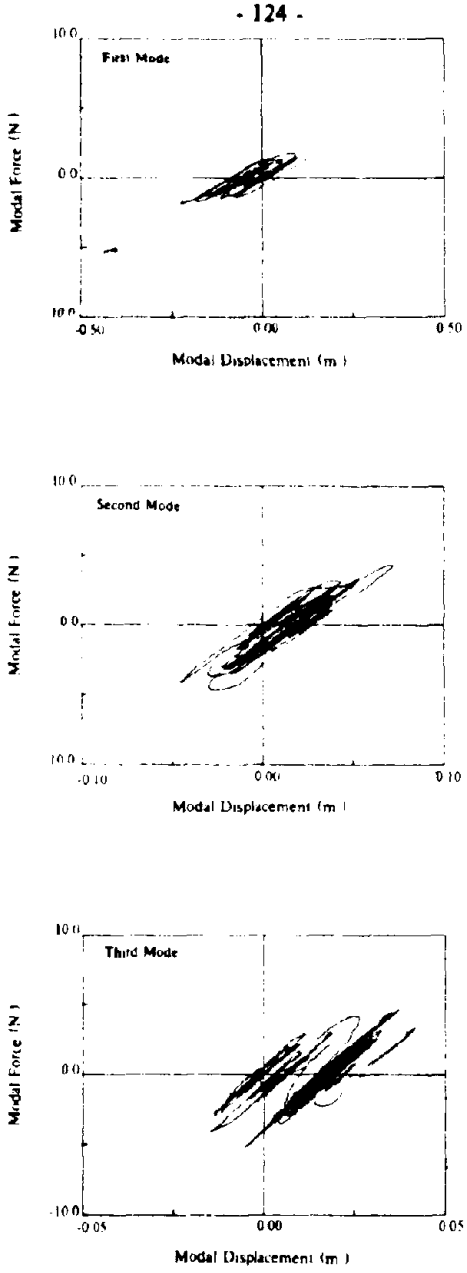

Fig. 3.13 Modal Hystereses of Building Number Four.

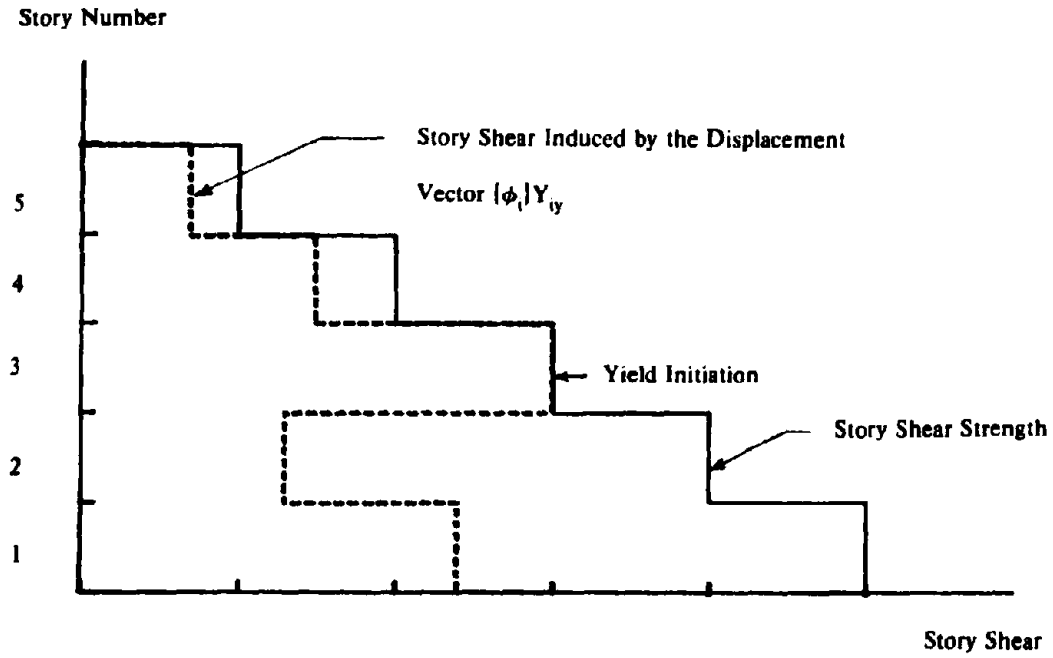

FIG. 3.14 Definition of Modal Yield Point

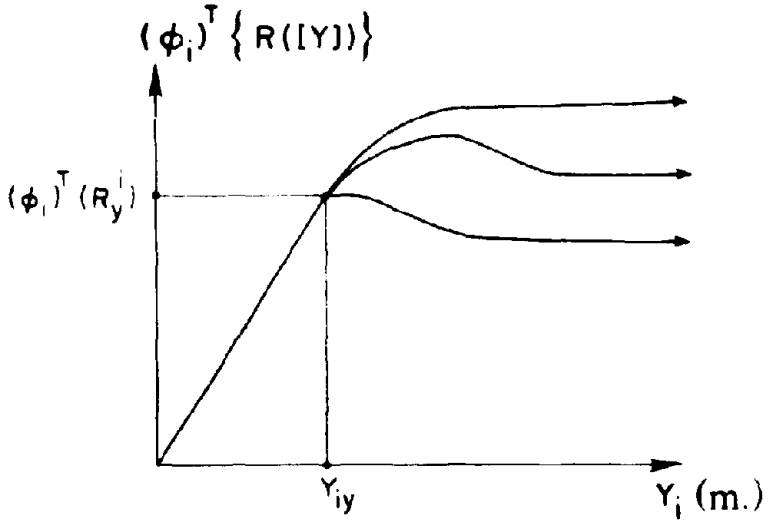

FIG. 3.15 Possible Post-Yielding Modal Response.

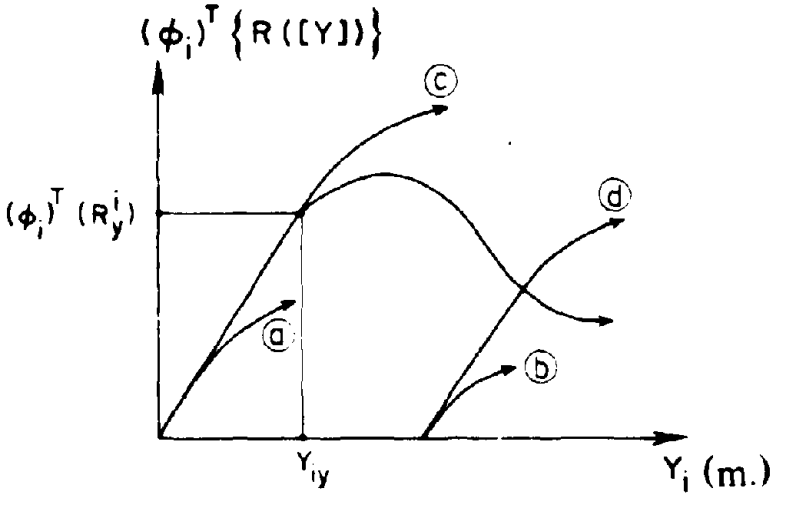

FIG. 3.16 Modal Interference on Modal Hysteresis.

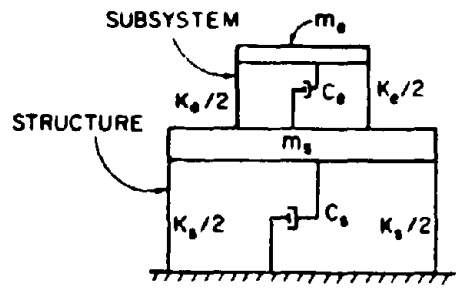

(A) Simplified Model For Current Study

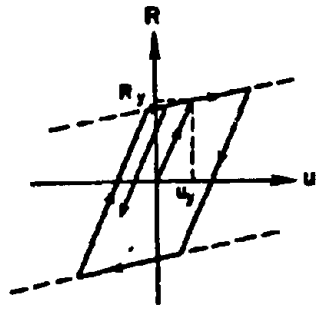

(B) Bilinear Model

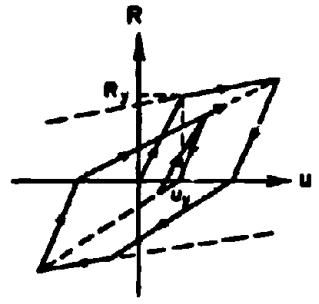

(C) Stiffness Degrading Model

FIG. 4.1 Structure And Subsystem Models

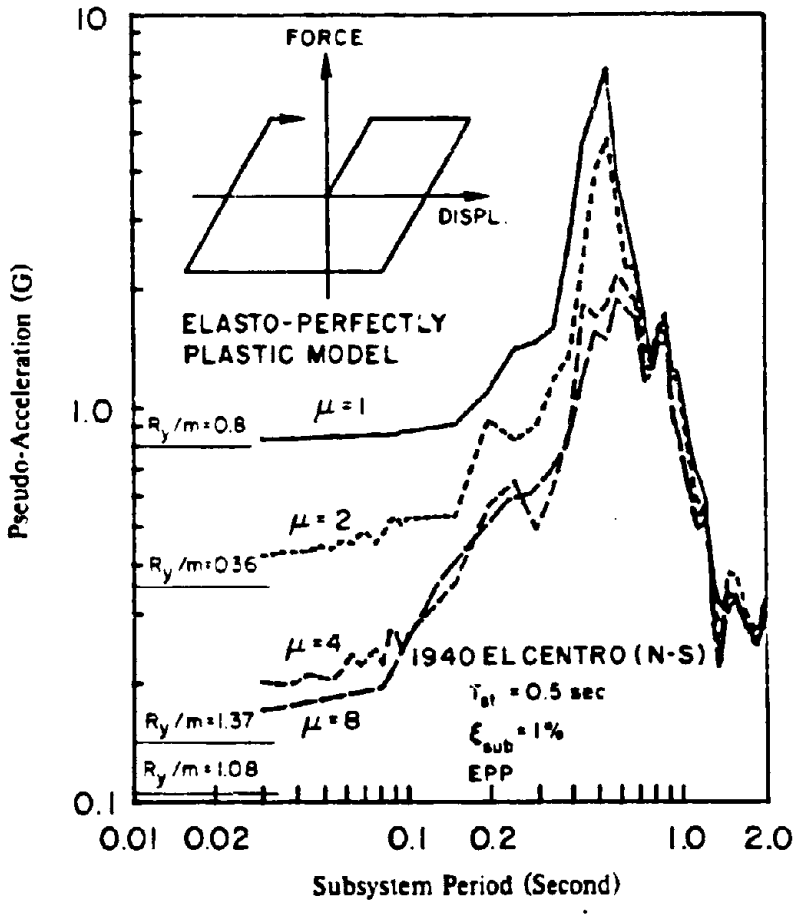

FIG. 4.2 Floor Response Spectrum For Structure Ductilities Of 1, 2, 4 and 8. Structural Period Is 0.5 Second With Subsystem Damping Of 1%.

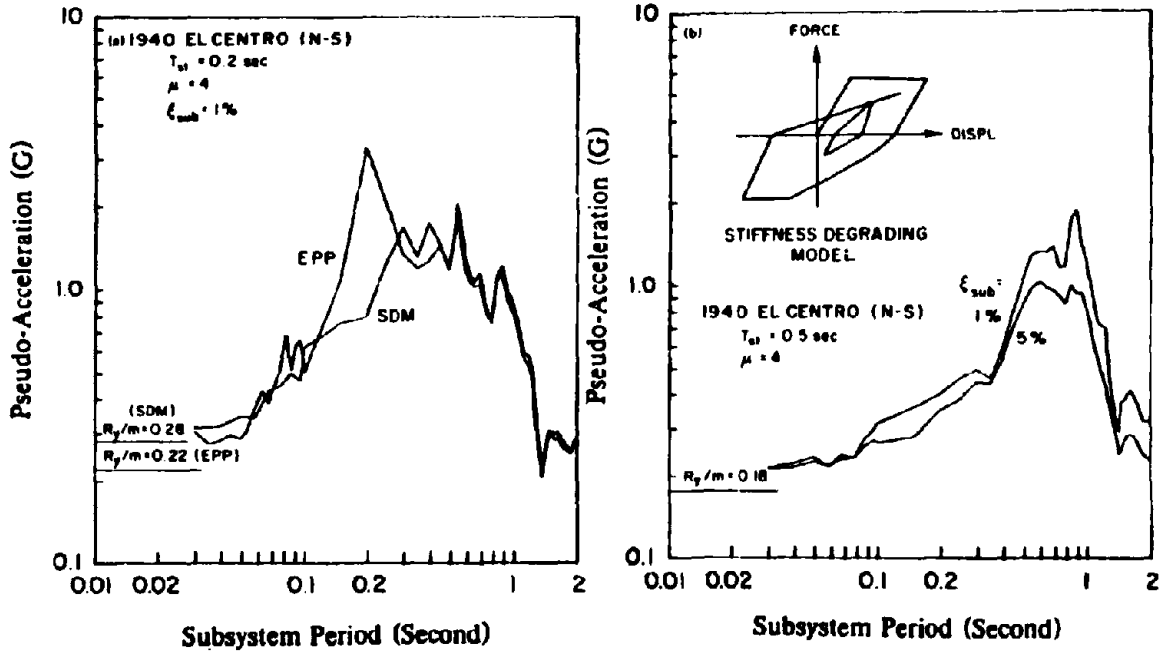

FIG. 4.3 Comparison Of Floor Response Spectra: (a) Between EPP And SDM Models And (b) Between Subsystem Damping Of 1% And 5%.

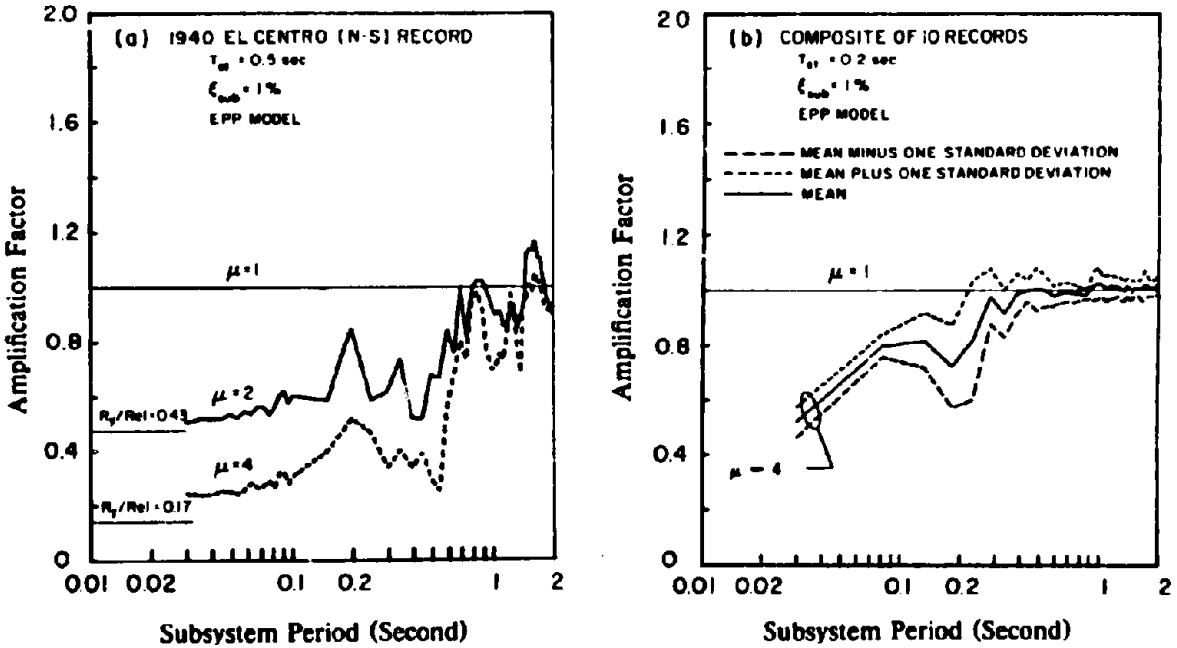

FIG. 4.4 Amplification Factors: (a) Based On 1940 El Centro Record, And (b) Based On Statistical Evaluation For 10 Ground Motion Records.

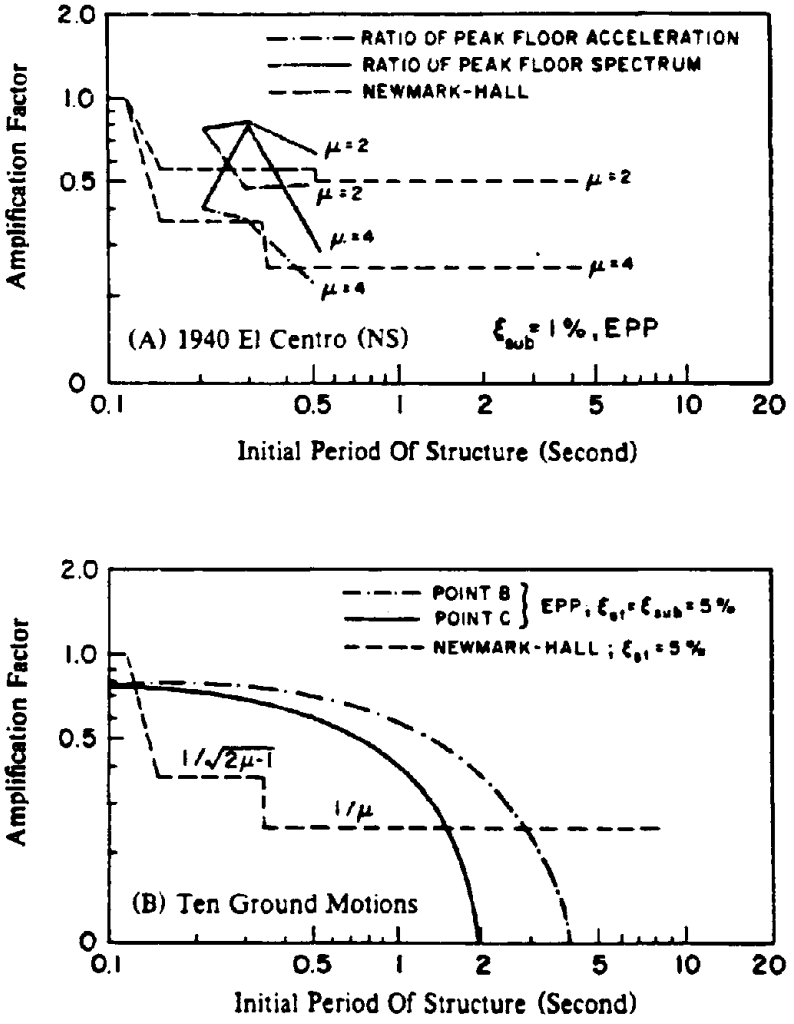

FIG. 4.5 Comparison Between The Reductions In Acceleration Of The Subsystem And Floor Acceleration.

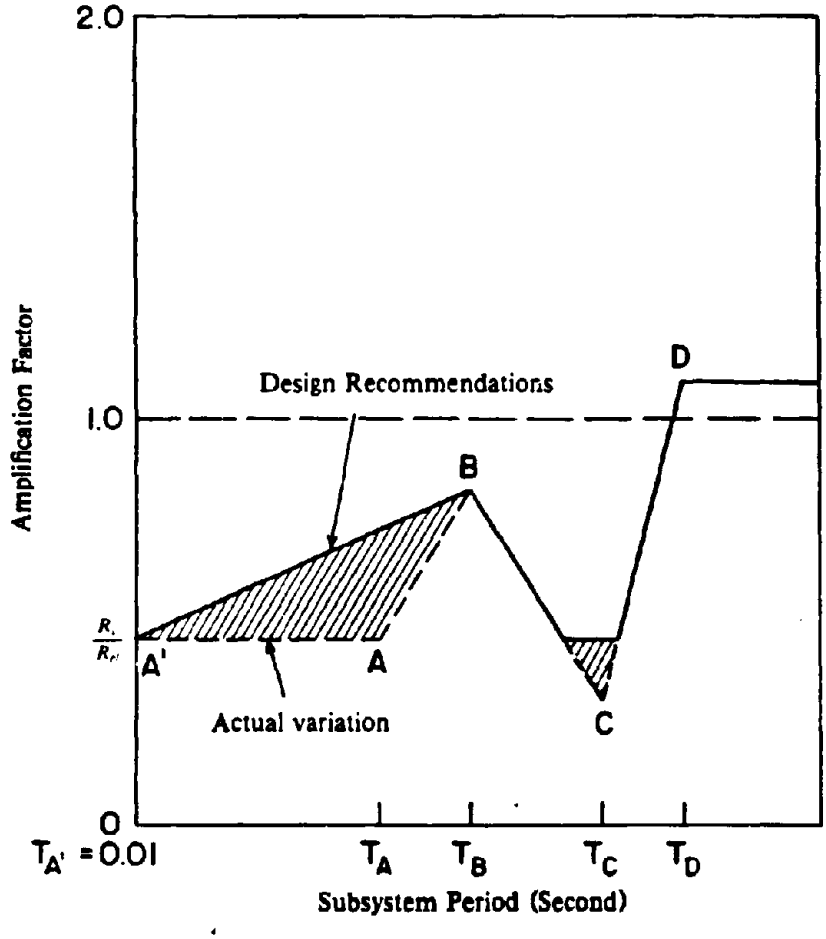

FIG. 4.6 Variation Of Amplification Factors.

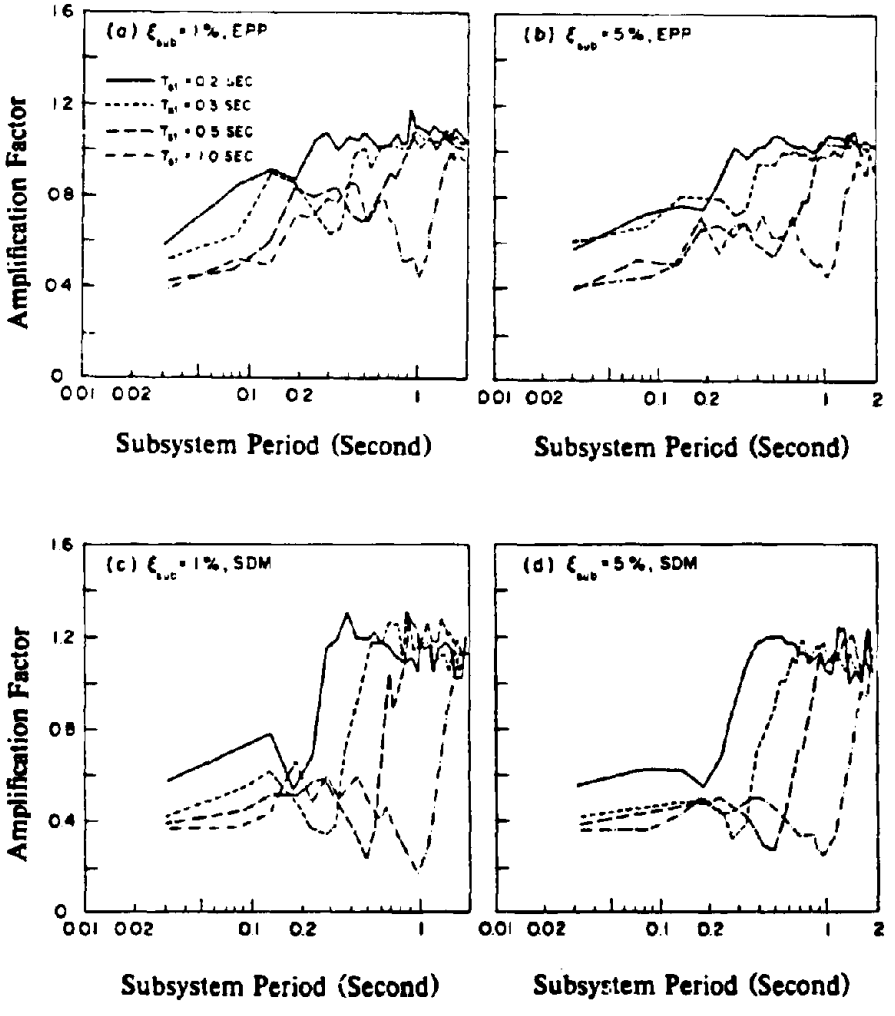

FIG. 4.7 Mean Plus One Standard Deviation Amplification Factors For Structural Periods Of 0.2, 0.3, 0.5, 1.0 Seconds And Structural Ductility Of 4.

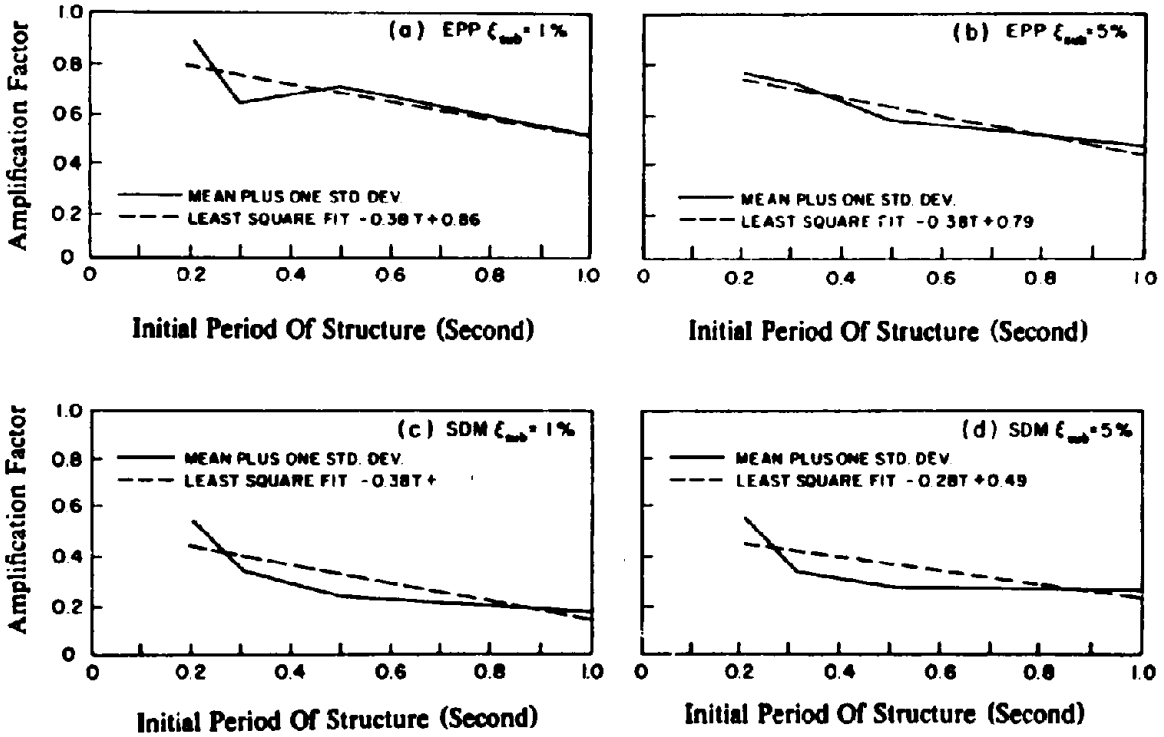

FIG. 4.8 Amplification Factor At Point C Versus Structural Period And The Least Square Fit For Structural Ductility Of 4.

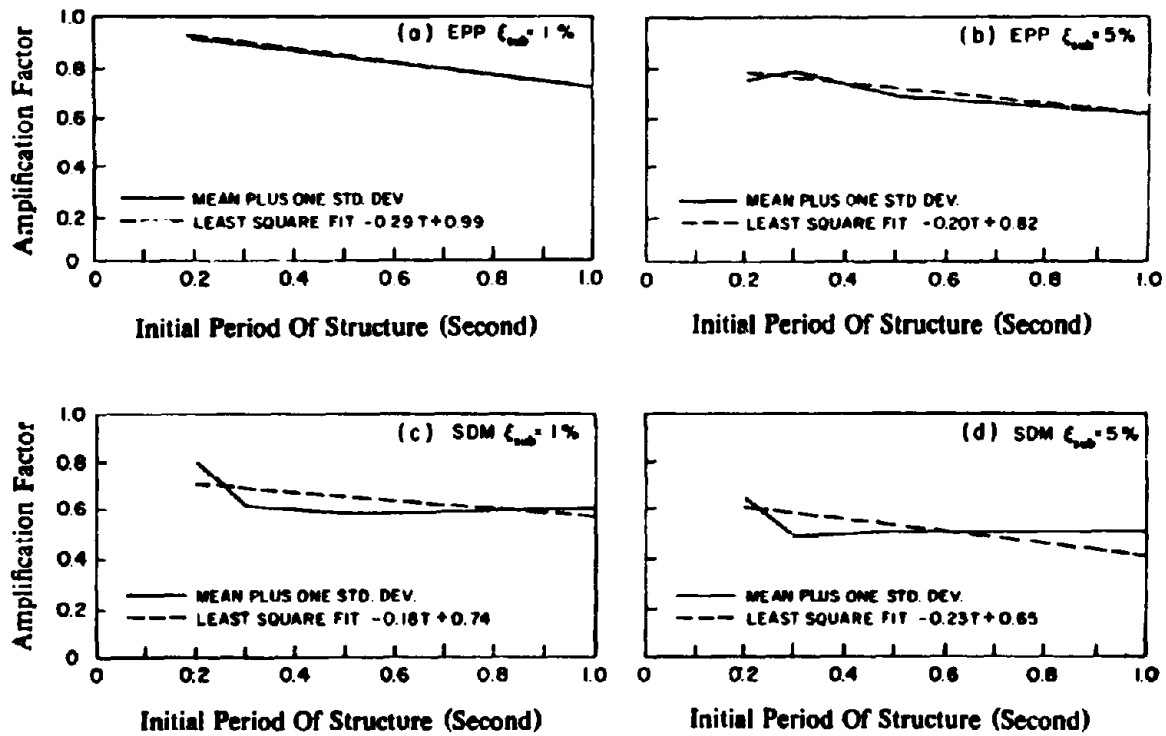

FIG. 4.9 Amplification Factor At Point B Versus Structural Period And The Lease Square Fit For Structural Ductility Of 4.

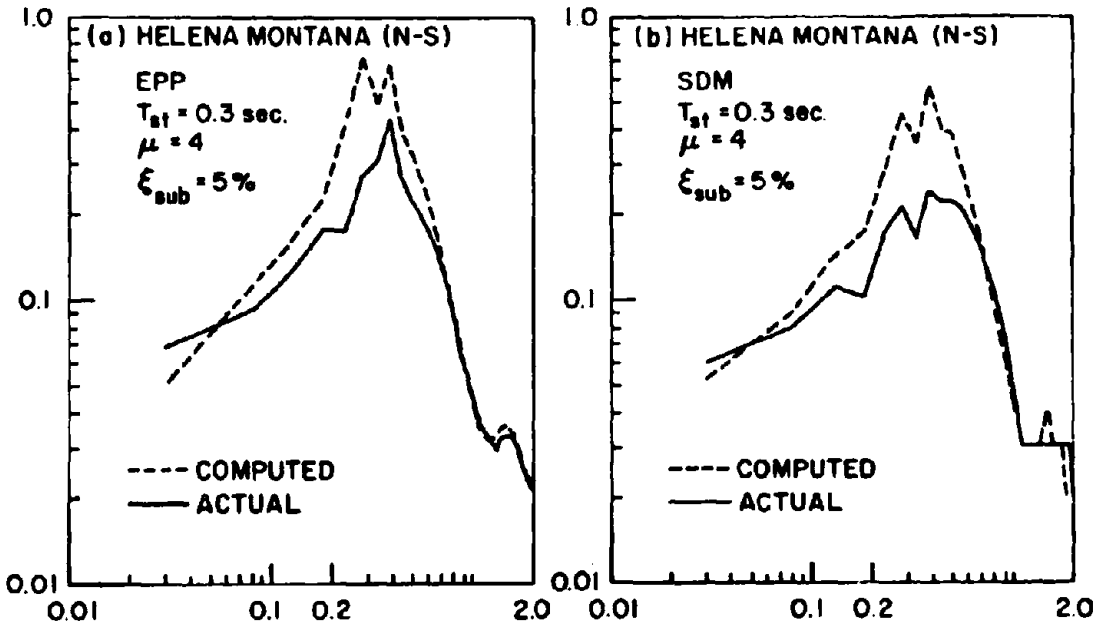

FIG. 4.10 Computed And Actual FRS For Ductility Of 4 and Period Of 0.3 Sec.

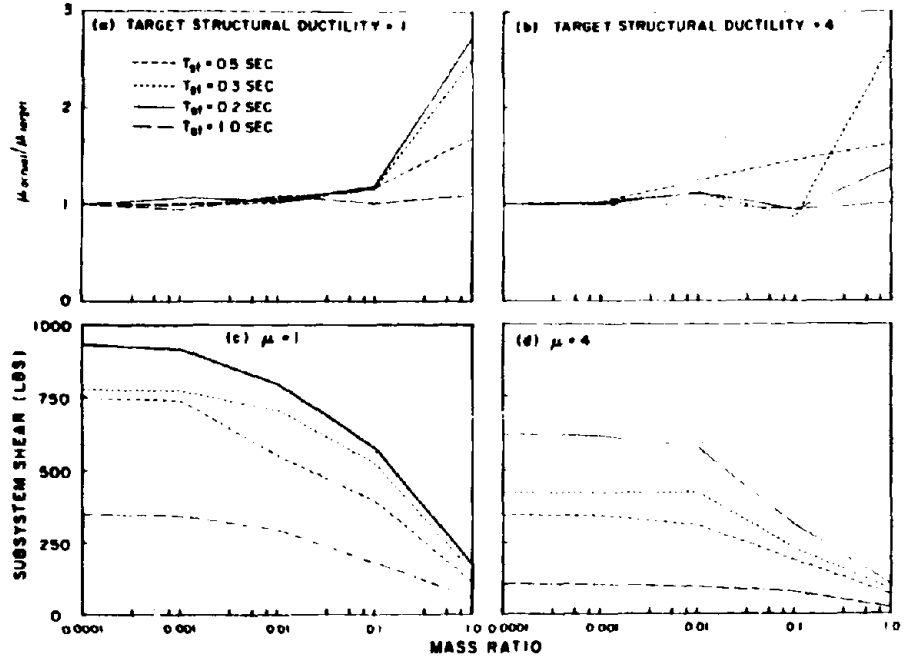

FIG. 4.11 Effect Of Mass On Structural Ductility And Subsystem Shear.

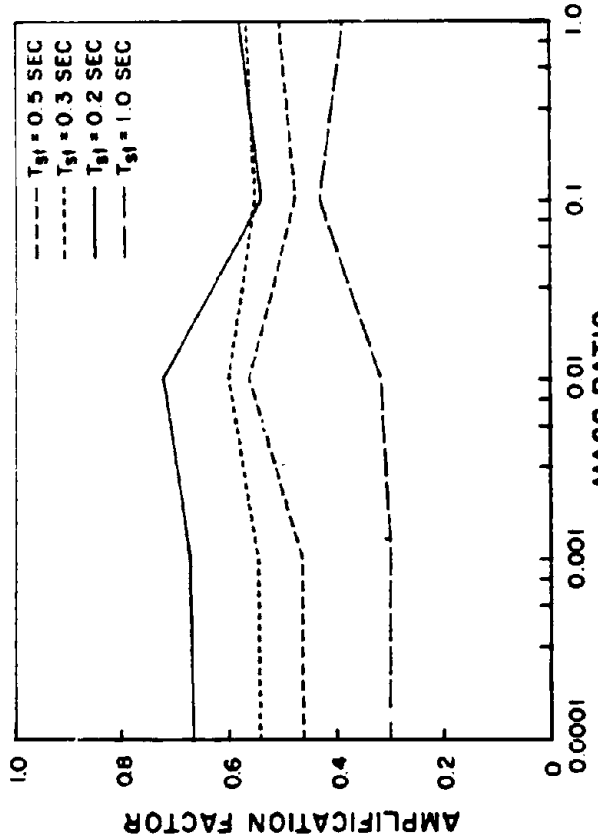

FIG. 4.12 Effect Of Mass On Amplification Factor.

EARTHQUAKE ENGINEERING RESEARCH CENTER REPORTS

NOTE: Numbers in parentheses are Accession Numbers assigned by the National Technical Information Service; these are followed by a price code. Copies of the reports may be ordered from the National Technical Information Service, 5285 Port Royal Road, Springfield, Virginia, 22161. Accession Numbers should be quoted on orders for reports (PB --- ---) and remittance must accompany each order. Reports without this information were not available at time of printing. The complete list of EERC reports (from EERC 67-1) is available upon request from the Earthquake Engineering Research Center, University of California, Berkeley, 47th Street and Hoffman Boulevard, Richmond, California 94804.

UCB/EERC-79/01 "Hysteretic Behavior of Lightweight Reinforced Concrete Beam-Column Subassemblages," by B. Forzani, E.P. Popov and V.V. Bertero - April 1979(PB 298 267)A06

UCB/EERC-79/02 "The Development of a Mathematical Model to Predict the Flexural Response of Reinforced Concrete Beams to Cyclic Loads, Using System Identification," by J. Stanton & H. McNiven - Jan. 1979(PB 295 875)A10

UCB/EERC-79/03 "Linear and Nonlinear Earthquake Response of Simple Torsionally Coupled Systems," by C.L. Kan and A.K. Chopra - Feb. 1979(PB 298 262)A06

UCB/EERC-79/04 "A Mathematical Model of Masonry for Predicting its Linear Seismic Response Characteristics," by Y. Mengi and H.D. McNiven - Feb. 1979(PB 298 266)A06

UCB/EERC-79/05 "Mechanical Behavior of Lightweight Concrete Confined by Different Types of Lateral Reinforcement," by M.A. Manrique, V.V. Bertero and E.P. Popov - May 1979(PB 301 114)A06

UCB/EERC-79/06 "Static Tilt Tests of a Tall Cylindrical Liquid Storage Tank," by R.W. Clough and A. Niwa - Feb. 1979 (PB 301 167)A06

UCB/EERC-79/07 "The Design of Steel Energy Absorbing Restrainers and Their Incorporation into Nuclear Power Plants for Enhanced Safety: Volume 1 - Summary Report," by P.N. Spencer, V.F. Zackay, and E.R. Parker - Feb. 1979(UCB/EERC-79/07)A09

UCB/EERC-79/08 "The Design of Steel Energy Absorbing Restrainers and Their Incorporation into Nuclear Power Plants for Enhanced Safety: Volume 2 - The Development of Analyses for Reactor System Piping,""Simple Systems" by M.C. Lee, J. Penzien, A.K. Chopra and K. Suzuki "Complex Systems" by G.H. Powell, E.L. Wilson, R.W. Clough and D.G. Row - Feb. 1979(UCB/EERC-79/08)A10

UCB/EERC-79/09 "The Design of Steel Energy Absorbing Restrainers and Their Incorporation into Nuclear Power Plants for Enhanced Safety: Volume 3 - Evaluation of Commercial Steels," by W.S. Owen, R.M.N. Pelloux, R.O. Ritchie, M. Faral, T. Ohhashi, J. Toplosky, S.J. Hartman, V.F. Zackay and E.R. Parker - Feb. 1979(UCB/EERC-79/09)A04

UCB/EERC-79/10 "The Design of Steel Energy Absorbing Restrainers and Their Incorporation into Nuclear Power Plants for Enhanced Safety: Volume 4 - A Review of Energy-Absorbing Devices," by J.M. Kelly and M.S. Skinner - Feb. 1979(UCB/EERC-79/10)A04

UCB/EERC-79/11 "Conservatism In Summation Rules for Closely Spaced Modes," by J.M. Kelly and J.L. Sackman - May 1979(PB 301 328)A03

UCB/EERC-79/12 "Cyclic Loading Tests of Masonry Single Piers; Volume 3 - Height to Width Ratio of 0.5," by P.A. Hidalgo, R.L. Mayes, H.D. McNiven and R.W. Clough - May 1979(PB 301 321)A08

UCB/EERC-79/13 "Cyclic Behavior of Dense Course-Grained Materials in Relation to the Seismic Stability of Dams," by N.G. Banerjee, H.B. Seed and C.K. Chan - June 1979(PB 301 373)A13

UCB/EERC-79/14 "Seismic Behavior of Reinforced Concrete Interior Beam-Column Subassemblages," by S. Viwathanatepa, E.P. Popov and V.V. Bertero - June 1979(PB 301 326)A10

UCB/EERC-79/15 "Optimal Design of Localized Nonlinear Systems with Dual Performance Criteria Under Earthquake Excitations," by M.A. Bhatti - July 1979(PB 80 167 109)A06

UCB/EERC-79/16 "OPTDYN - A General Purpose Optimization Program for Problems with or without Dynamic Constraints," by M.A. Bhatti, E. Polak and K.S. Pister - July 1979(PB 80 167 091)A05

UCB/EERC-79/17 "ANSR-II, Analysis of Nonlinear Structural Response, Users Manual," by D.P. Mondkar and G.H. Powell July 1979(PB 80 113 301)A05

UCB/EERC-79/18 "Soil Structure Interaction in Different Seismic Environments," A. Gomez-Masso, J. Lysmer, J.-C. Chen and H.B. Seed - August 1979(PB 80 101 520)A04

UCB/EERC-79/19 "ARMA Models for Earthquake Ground Motions," by M.K. Chang, J.W. Kwiatkowski, R.F. Nau, R.M. Oliver and K.S. Pister - July 1979(PB 301 166)A05

UCB/EERC-79/20 "Hysteretic Behavior of Reinforced Concrete Structural Walls," by J.M. Vallenas, V.V. Bertero and E.P. Popov - August 1979(PB 80 165 905)A12

UCB/EERC-79/21 "Studies on High-Frequency Vibrations of Buildings - 1: The Column Effect," by J. Lubliner - August 1979 (PB 80 158 553)A03

UCB/EERC-79/22 "Effects of Generalized Loadings on Bond Reinforcing Bars Embedded in Confined Concrete Blocks," by S. Viwathanatepa, E.P. Popov and V.V. Bertero - August 1979(PB 81 124 018)A14

UCB/EERC-79/23 "Shaking Table Study of Single-Story Masonry Houses, Volume 1: Test Structures 1 and 2," by P. Gülkan, R.L. Mayes and R.W. Clough - Sept. 1979 (HUD-000 1763)A12

UCB/EERC-79/24 "Shaking Table Study of Single-Story Masonry Houses, Volume 2: Test Structures 3 and 4," by P. Gülkan, R.L. Mayes and R.W. Clough - Sept. 1979 (HUD-000 1836)A12

UCB/EERC-79/25 "Shaking Table Study of Single-Story Masonry Houses, Volume 1: Summary, Conclusions and Recommendations," by R.W. Clough, R.L. Mayes and P. Gülkan - Sept. 1979 (HUD-000 1837)A06

UCB/EERC-79/26 "Recommendations for a U.S.-Japan Cooperative Research Program Utilizing Large-Scale Testing Facilities," by U.S.-Japan Planning Group - Sept. 1979(PB 301 407)A06

UCB/EERC-79/27 "Earthquake-Induced Liquefaction Near Lake Amatitlan, Guatemala," by H.B. Seed, I. Arango, C.K. Chan, A. Gomez-Masso and R. Grant de Ascoli - Sept. 1979(NUREG-CR1341)A03

UCB/EERC-79/28 "Infill Panels: Their Influence on Seismic Response of Buildings," by J.W. Axley and V.V. Bertero Sept. 1979(PB 80 163 371)A10

UCB/EERC-79/29 "3D Truss Bar Element (Type 1) for the ANSR-II Program," by D.P. Mondkar and G.H. Powell - Nov. 1979 (PB 80 169 709)A02

UCB/EERC-79/30 "2D Beam-Column Element (Type 5 - Parallel Element Theory) for the ANSR-II Program," by D.G. Row, G.H. Powell and D.P. Mondkar - Dec. 1979(PB 80 167 224)A03

UCB/EERC-79/31 "3D Beam-Column Element (Type 2 - Parallel Element Theory) for the ANSR-II Program," by A. Riahi, G.H. Powell and D.P. Mondkar - Dec. 1979(PB 80 167 216)A03

UCB/EERC-79/32 "On Response of Structures to Stationary Excitation," by A. Der Kiureghian - Dec. 1979(PB 80166 929)A03

UCB/EERC-79/33 "Undisturbed Sampling and Cyclic Load Testing of Sands," by S. Singh, H.B. Seed and C.K. Chan Dec. 1979(ADA 087 298)A07

UCB/EERC-79/34 "Interaction Effects of Simultaneous Torsional and Compressional Cyclic Loading of Sand," by P.M. Griffin and W.N. Houston - Dec. 1979(ADA 092 352)A15

UCB/EERC-80/01 "Earthquake Response of Concrete Gravity Dams Including Hydrodynamic and Foundation Interaction Effects," by A.K. Chopra, P. Chakrabarti and S. Gupta - Jan. 1980(AD-A087297)A10

UCB/EERC-80/02 "Rocking Response of Rigid Blocks to Earthquakes," by C.S. Yim, A.K. Chopra and J. Penzien - Jan. 1980 (PB80 166 002)A04

UCB/EERC-80/03 "Optimum Inelastic Design of Seismic-Resistant Reinforced Concrete Frame Structures," by S.W. Zagajeski and V.V. Bertero - Jan. 1980(PB80 164 635)A06

UCB/EERC-80/04 "Effects of Amount and Arrangement of Wall-Panel Reinforcement on Hysteretic Behavior of Reinforced Concrete Walls," by R. Iliya and V.V. Bertero - Feb. 1980(PB81 122 525)A09

UCB/EERC-80/05 "Shaking Table Research on Concrete Dam Models," by A. Niwa and R.W. Clough - Sept. 1980(PB81 122 368)A06

UCB/EERC-80/06 "The Design of Steel Energy-Absorbing Restrainers and their Incorporation into Nuclear Power Plants for Enhanced Safety (Vol 1A): Piping with Energy Absorbing Restrainers: Parameter Study on Small Systems," by G.H. Powell, C. Oughourlian and J. Simons - June 1980

UCB/EERC-80/07 "Inelastic Torsional Response of Structures Subjected to Earthquake Ground Motions," by Y. Yamazaki April 1980(PB81 122 327)A08

UCB/EERC-80/08 "Study of X-Braced Steel Frame Structures Under Earthquake Simulation," by Y. Ghanaat - April 1980 (PB81 122 335)A11

UCB/EERC-80/09 "Hybrid Modelling of Soil-Structure Interaction," by S. Gupta, T.W. Lin, J. Penzien and C.S. Yeh May 1980(PB81 122 319)A07

UCB/EERC-80/10 "General Applicability of a Nonlinear Model of a One Story Steel Frame," by B.I. Sveinsson and H.D. McNiven - May 1980(PB81 124 877)A06

UCB/EERC-80/11 "A Green-Function Method for Wave Interaction with a Submerged Body," by W. Kioka - April 1980 (PB81 122 269)A07

UCB/EERC-80/12 "Hydrodynamic Pressure and Added Mass for Axisymmetric Bodies," by F. Nilrat - May 1980(PB81 122 343)A08

UCB/EERC-80/13 "Treatment of Non-Linear Drag Forces Acting on Offshore Platforms," by B.V. Dao and J. Penzien May 1980(PB81 153 413)A07

UCB/EERC-80/14 "2D Plane/Axisymmetric Solid Element (Type 3 - Elastic or Elastic-Perfectly Plastic) for the ANSR-II Program," by D.P. Mondkar and G.H. Powell - July 1980(PB81 122 350)A03

UCB/EERC-80/15 "A Response Spectrum Method for Random Vibrations," by A. Der Kiureghian - June 1980(PB81 122 301)A03

UCB/EERC-80/16 "Cyclic Inelastic Buckling of Tubular Steel Braces," by V.A. Zayas, E.P. Popov and S.A. Mahin June 1980(PB81 124 885)A10

UCB/EERC-80/17 "Dynamic Response of Simple Arch Dams Including Hydrodynamic Interaction," by C.S. Porter and A.K. Chopra - July 1980(PB81 124 000)A13

UCB/EERC-80/18 "Experimental Testing of a Friction Damped Aseismic Base Isolation System with Fail-Safe Characteristics," by J.M. Kelly, K.E. Beucke and M.S. Skinner - July 1980(PB81 148 595)A04

UCB/EERC-80/19 "The Design of Steel Energy-Absorbing Restrainers and their Incorporation into Nuclear Power Plants for Enhanced Safety (Vol 1B): Stochastic Seismic Analyses of Nuclear Power Plant Structures and Piping Systems Subjected to Multiple Support Excitations," by M.C. Lee and J. Penzien - June 1980

UCB/EERC-80/20 "The Design of Steel Energy-Absorbing Restrainers and their Incorporation into Nuclear Power Plants for Enhanced Safety (Vol 1C): Numerical Method for Dynamic Substructure Analysis," by J.M. Dickens and E.L. Wilson - June 1980

UCB/EERC-80/21 "The Design of Steel Energy-Absorbing Restrainers and their Incorporation into Nuclear Power Plants for Enhanced Safety (Vol 2): Development and Testing of Restraints for Nuclear Piping Systems," by J.M. Kelly and M.S. Skinner - June 1980

UCB/EERC-80/22 "3D Solid Element (Type 4-Elastic or Elastic-Perfectly-Plastic) for the ANSR-II Program," by D.P. Mondkar and G.H. Powell - July 1980(PB81 123 242)A03

UCB/EERC-80/23 "Gap-Friction Element (Type 5) for the ANSR-II Program," by D.P. Mondkar and G.H. Powell - July 1980 (PB81 122 285)A03

UCB/EERC-81/10 "Evaluation of Seismic Design Provisions for Masonry in the United States," by B.I. Sveinsson, R.L. Mayes and H.D. McNiven - August 1981 (PB82 166 075)A08

UCB/EERC-81/11 "Two-Dimensional Hybrid Modelling of Soil-Structure Interaction," by T.-J. Tzong, S. Gupta and J. Penzien - August 1981(PB82 142 118)A04

UCB/EERC-81/12 "Studies on Effects of Infills in Seismic Resistant R/C Construction," by S. Brokken and V.V. Bertero - September 1981 (PB82 166 190)A09

UCB/EERC-81/13 "Linear Models to Predict the Nonlinear Seismic Behavior of a One-Story Steel Frame," by H. Valdimarsson, A.H. Shah and H.D. McNiven - September 1981(PB82 138 793)A07

UCB/EERC-81/14 "TLUSH: A Computer Program for the Three-Dimensional Dynamic Analysis of Earth Dams," by T. Kagawa, L.H. Mejia, H.B. Seed and J. Lysmer - September 1981(PB82 139 940)A06

UCB/EERC-81/15 "Three Dimensional Dynamic Response Analysis of Earth Dams," by L.H. Mejia and H.B. Seed - September 1981 (PB82 137 274)A12

UCB/EERC-81/16 "Experimental Study of Lead and Elastomeric Dampers for Base Isolation Systems," by J.M. Kelly and S.B. Hodder - October 1981 (PB82 166 182)A05

UCB/EERC-81/17 "The Influence of Base Isolation on the Seismic Response of Light Secondary Equipment," by J.M. Kelly - April 1981 (PB82 255 266)A04

UCB/EERC-81/18 "Studies on Evaluation of Shaking Table Response Analysis Procedures," by J. Marcial Blondet - November 1981 (PB82 197 278)A10

UCB/EERC-81/19 "DELIGHT.STRUCT: A Computer-Aided Design Environment for Structural Engineering," by R.J. Balling, K.S. Pister and E. Polak - December 1981 (PB82 218 496)A07

UCB/EERC-81/20 "Optimal Design of Seismic-Resistant Planar Steel Frames," by R.J. Balling, V. Ciampi, K.S. Pister and E. Polak - December 1981 (PB82 220 179)A07

UCB/EERC-82/01 "Dynamic Behavior of Ground for Seismic Analysis of Lifeline Systems," by T. Sato and A. Der Kiureghian - January 1982 (PB82 218 926)A05

UCB/EERC-82/02 "Shaking Table Tests of a Tubular Steel Frame Model," by Y. Ghanaat and R. W. Clough - January 1982 (PB82 220 161)A07

UCB/EERC-82/03 "Behavior of a Piping System under Seismic Excitation: Experimental Investigations of a Spatial Piping System supported by Mechanical Shock Arrestors and Steel Energy Absorbing Devices under Seismic Excitation," by S. Schneider, H.-M. Lee and W. G. Goddan - May 1982 (PB83 172 544)A09

UCB/EERC-82/04 "New Approaches for the Dynamic Analysis of Large Structural Systems," by E. L. Wilson - June 1982 (PB83 148 080)A05

UCB/EERC-82/05 "Model Study of Effects of Damage on the Vibration Properties of Steel Offshore Platforms," by F. Shahrivar and J. G. Bouwkamp - June 1982 (PB83 148 742)A10

UCB/EERC-82/06 "States of the Art and Practice in the Optimum Seismic Design and Analytical Response Prediction of R/C Frame-Wall Structures," by A. E. Aktan and V. V. Bertero - July 1982 (PB83 147 736)A05

UCB/EERC-82/07 "Further Study of the Earthquake Response of a Broad Cylindrical Liquid-Storage Tank Model," by G. C. Manos and R. W. Clough - July 1982 (PB83 147 744)A11

UCB/EERC-82/08 "An Evaluation of the Design and Analytical Seismic Response of a Seven Story Reinforced Concrete Frame - Wall Structure," by F. A. Charney and V. V. Bertero - July 1982(PB83 157 628)A09

UCB/EERC-82/09 "Fluid-Structure Interactions: Added Mass Computations for Incompressible Fluid," by J. S.-H. Kuo - August 1982 (PB83 156 281)A07

UCB/EERC-82/10 "Joint-Opening Nonlinear Mechanism: Interface Smeared Crack Model," by J. S.-H. Kuo - August 1982 (PB83 149 195)A05

UCB/EERC-82/11 "Dynamic Response Analysis of Techi Dam," by R. W. Clough, R. M. Stephen and J. S.-H. Kuo - August 1982 (PB83 147 496)A06

UCB/EERC-82/12 "Prediction of the Seismic Responses of R/C Frame-Coupled Wall Structures," by A. E. Aktan, V. V. Bertero and M. Piazza - August 1982 (PB83 149 203)A09

UCB/EERC-82/13 "Preliminary Report on the SMART 1 Strong Motion Array in Taiwan," by B. A. Bolt, C. H. Loh, J. Penzien, Y. B. Tsai and Y. T. Yeh - August 1982 (PB83 159 400)A10

UCB/EERC-82/14 "Shaking-Table Studies of an Eccentrically X-Braced Steel Structure," by M. S. Yang - September 1982 (PB83 260 778)A12

UCB/EERC-82/15 "The Performance of Stairways in Earthquakes," by C. Roha, J. W. Axley and V. V. Bertero - September 1982 (PB83 157 693)A07

UCB/EERC-82/16 "The Behavior of Submerged Multiple Bodies in Earthquakes," by W.-G. Liao - Sept. 1982 (PB83 158 709)A07

UCB/EERC-82/17 "Effects of Concrete Types and Loading Conditions on Local Bond-Slip Relationships," by A. D. Cowell, E. P. Popov and V. V. Bertero - September 1982 (PB83 153 577)A04

UCB/EERC-82/18 "Mechanical Behavior of Shear Wall Vertical Boundary Members: An Experimental Investigation," by M. T. Wagner and V. V. Bertero - October 1982 (PB83 159 764)A05

UCB/EERC-82/19 "Experimental Studies of Multi-support Seismic Loading on Piping Systems," by J. M. Kelly and A. D. Cowell - November 1982

UCB/EERC-82/20 "Generalized Plastic Hinge Concepts for 3D Beam-Column Elements," by P. F.-S. Chen and G. H. Powell - November 1982 (PB83 247 981)A13

UCB/EERC-82/21 "ANSR-III: General Purpose Computer Program for Nonlinear Structural Analysis," by C. V. Oughourlian and G. H. Powell - November 1982 (PB83 251 330)A12

UCB/EERC-82/22 "Solution Strategies for Statically Loaded Nonlinear Structures," by J. W. Simons and G. H. Powell - November 1982 (PB83 197 970)A06

UCB/EERC-82/23 "Analytical Model of Deformed Bar Anchorages under Generalized Excitations," by V. Ciampi, R. Eligehausen, V. V. Bertero and E. P. Popov - November 1982 (PB83 169 532)A06

UCB/EERC-82/24 "A Mathematical Model for the Response of Masonry Walls to Dynamic Excitations," by H. Sucuoğlu, Y. Mengi and H. D. McNiven - November 1982 (PB83 169 011)A07

UCB/EERC-82/25 "Earthquake Response Considerations of Broad Liquid Storage Tanks," by F. J. Cambra - November 1982 (PB83 251 215)A09

UCB/EERC-82/26 "Computational Models for Cyclic Plasticity, Rate Dependence and Creep," by B. Mosaddad and G. H. Powell - November 1982 (PB83 245 829)A08

UCB/EERC-82/27 "Inelastic Analysis of Piping and Tubular Structures," by M. Mahasuverachai and G. H. Powell - November 1982 (PB83 249 987)A07

UCB/EERC-83/01 "The Economic Feasibility of Seismic Rehabilitation of Buildings by Base Isolation," by J. M. Kelly - January 1983 (PB83 197 988)A05

UCB/EERC-83/02 "Seismic Moment Connections for Moment-Resisting Steel Frames," by E. P. Popov - January 1983 (PB83 195 412)A04

UCB/EERC-83/03 "Design of Links and Beam-to-Column Connections for Eccentrically Braced Steel Frames," by E. P. Popov and J. O. Malley - January 1983 (PB83 194 811)A04

UCB/EERC-83/04 "Numerical Techniques for the Evaluation of Soil-Structure Interaction Effects in the Time Domain," by E. Bayo and E. L. Wilson - February 1983 (PB83 245 605)A09

UCB/EERC-83/05 "A Transducer for Measuring the Internal Forces in the Columns of a Frame-Wall Reinforced Concrete Structure," by R. Sause and V. V. Bertero - May 1983 (PB84 119 494)A06

UCB/EERC-83/06 "Dynamic Interactions between Floating Ice and Offshore Structures," by P. Croteau - May 1983 (PB84 119 486)A16

UCB/EERC-83/07 "Dynamic Analysis of Multiply Tuned and Arbitrarily Supported Secondary Systems," by T. Igusa and A. Der Kiureghian - June 1983 (PB84 118 272)A11

UCB/EERC-83/08 "A Laboratory Study of Submerged Multi-body Systems in Earthquakes," by G. R. Ansari - June 1983 (PB83 261 842)A17

UCB/EERC-83/09 "Effects of Transient Foundation Uplift on Earthquake Response of Structures," by C.-S. Yim and A. K. Chopra - June 1983 (PB83 261 396)A07

UCB/EERC-83/10 "Optimal Design of Friction-Braced Frames under Seismic Loading," by M. A. Austin and K. S. Pister - June 1983 (PB84 119 288)A06

UCB/EERC-83/11 "Shaking Table Study of Single-Story Masonry Houses: Dynamic Performance under Three Component Seismic Input and Recommendations," by G. C. Manos, R. W. Clough and R. L. Mayes - June 1983

UCB/EERC-83/12 "Experimental Error Propagation in Pseudodynamic Testing," by P. B. Shing and S. A. Mahin - June 1983 (PB84 119 270)A09

UCB/EERC-83/13 "Experimental and Analytical Predictions of the Mechanical Characteristics of a 1/5 scale Model of a 7-story R/C Frame-Wall Building Structure," by A. E. Aktan, V. V. Bertero, A. A. Chowdhury and T. Nagashima - August 1983 (PB84 119 213)A07

UCB/EERC-83/14 "Shaking Table Tests of Large-Panel Precast Concrete Building System Assemblages," by M. G. Oliva and R. W. Clough - August 1983

UCB/EERC-83/15 "Seismic Behavior of Active Beam Links in Eccentrically Braced Frames," by K. D. Hjelmstad and E. P. Popov - July 1983 (PB84 119 676)A09

UCB/EERC-83/16 "System Identification of Structures with Joint Rotation," by J. S. Dimsdale and H. D. McNiven - July 1983

UCB/EERC-83/17 "Construction of Inelastic Response Spectra for Single-Degree-of-Freedom Systems," by S. Mahin and J. Lin - July 1983

UCB/EERC-83/18 "Interactive Computer Analysis Methods for Predicting the Inelastic Cyclic Behaviour of Structural Sections," by S. Kaba and S. Mahin - July 1983 (PB84 192 012) A06

UCB/EERC-83/19 "Effects of Bond Deterioration on Hysteretic Behavior of Reinforced Concrete Joints," by F.C. Filippou, E.P. Popov and V.V. Bertero - August 1983 (PB84 192 020) A10

UCB/EERC-83/20 "Analytical and Experimental Correlation of Large-Panel Precast Building System Performance," by M.G. Oliva, R.W. Clough, M. Velkov, P. Gavrilovic and J. Petrovski - November 1983

UCB/EERC-83/21 "Mechanical Characteristics of Materials Used in a 1/5 Scale Model of a 7-Story Reinforced Concrete Test Structure," by V.V. Bertero, A.E. Aktan, H.G. Harris and A.A. Chowdhury - September 1983 (PB84 193 697) A05

UCB/EERC-83/22 "Hybrid Modelling of Soil-Structure Interaction in Layered Media," by T.-J. Tzong and J. Penzien - October 1983 (PB84 192 178) A08

UCB/EERC-83/23 "Local Bond Stress-Slip Relationships of Deformed Bars under Generalized Excitations," by R. Eligehausen, E.P. Popov and V.V. Bertero - October 1983 (PB84 192 848) A09

UCB/EERC-83/24 "Design Considerations for Shear Links in Eccentrically Braced Frames," by J.O. Malley and E.P. Popov - November 1983 (PB84 192 186) A07

UCB/EERC-84/01 "Pseudodynamic Test Method for Seismic Performance Evaluation: Theory and Implementation," by P.-S. B. Shing and S. A. Mahin - January 1984 (PB84 190 644) A08

UCB/EERC-84/02 "Dynamic Response Behavior of Xiang Hong Dian Dam," by R.W. Clough, K.-T. Chang, H.-Q. Chen, R.M. Stephen, G.-L. Wang, and Y. Ghanaat - April 1984

UCB/EERC-84/03 "Refined Modelling of Reinforced Concrete Columns for Seismic Analysis," by S.A. Kaba and S.A. Mahin - April, 1984

UCB/EERC-84/04 "A New Floor Response Spectrum Method for Seismic Analysis of Multiply Supported Secondary Systems," by A. Asfura and A. Der Kiureghian - June 1984

UCB/EERC-84/05 "Earthquake Simulation Tests and Associated Studies of a 1/5th-scale Model of a 7-Story R/C Frame-Wall Test Structure," by V.V. Bertero, A.E. Aktan, F.A. Charney and R. Sause - June 1984

UCB/EERC-84/06 "R/C Structural Walls: Seismic Design for Shear," by A.E. Aktan and V.V. Bertero

UCB/EERC-84/07 "Behavior of Interior and Exterior Flat-Plate Connections subjected to Inelastic Load Reversals," by H.L. Zee and J.P. Moehle

UCB/EERC-84/08 "Experimental Study of the Seismic Behavior of a two-story Flat-Plate Structure," by J.W. Diebold and J.P. Moehle

UCB/EERC-84/09 "Phenomenological Modeling of Steel Braces under Cyclic Loading," by K. Ikeda, S.A. Mahin and S.N. Dermitzakis - May 1984

UCB/EERC-84/10 "Earthquake Analysis and Response of Concrete Gravity Dams," by G. Fenves and A.K. Chopra - August 1984

UCB/EERC-84/11 "EAGD-84: A Computer Program for Earthquake Analysis of Concrete Gravity Dams," by G. Fenves and A.K. Chopra - August 1984

UCB/EERC-84/12 "A Refined Physical Theory Model for Predicting the Seismic Behavior of Braced Steel Frames," by K. Ikeda and S.A. Mahin - July 1984

UCB/EERC-84/13 "Earthquake Engineering Research at Berkeley - 1984" - August 1984

UCB/EERC-84/14 "Moduli and Damping Factors for Dynamic Analyses of Cohesionless Soils," by H.B. Seed, R.T. Wong, I.M. Idriss and K. Tokimatsu - September 1984

UCB/EERC-84/15 "The Influence of SPT Procedures in Soil Liquefaction Resistance Evaluations," by H. B. Seed, K. Tokimatsu, L. F. Harder and R. M. Chung - October 1984

UCB/EERC-84/16 "Simplified Procedures for the Evaluation of Settlements in Sands Due to Earthquake Shaking," by K. Tokimatsu and H. B. Seed - October 1984

UCB/EERC-84/17 "Evaluation and Improvement of Energy Absorption Characteristics of Bridges under Seismic Conditions," by R. A. Imbsen and J. Penzien - November 1984

UCB/EERC-84/18 "Structure-Foundation Interactions under Dynamic Loads," by W. D. Liu and J. Penzien - November 1984

UCB/EERC-84/19 "Seismic Modelling of Deep Foundations," by C.-H. Chen and J. Penzien - November 1984

UCB/EERC-84/20 "Dynamic Response Behavior of Quan Shui Dam," by R. W. Clough, K.-T. Chang, H.-Q. Chen, R. M. Stephen, Y. Ghanaat and J.-H. Qi - November 1984

UCB/EERC-85/01 "Simplified Methods of Analysis for Earthquake Resistant Design of Buildings," by E.F. Cruz and A.K. Chopra - February 1985

UCB/EERC-85/02 "Estimation of Seismic Wave Coherency and Rupture Velocity using the SMART 1 Strong-Motion Array Recordings," by N.A. Abrahamson - March 1985

UCB/EERC-85/03 "Dynamic Properties of a Thirty Story Condominium Tower Building," by R.M. Stephen, E.L. Wilson and N. Stander - April 1985

UCB/EERC-85/04 "Development of Substructuring Techniques for On-Line Computer Controlled Seismic Performance Testing," by S. Dermitzakis and S. Mahin - May 1985

UCB/EERC-85/05 "Shaking Table Tests of a Base Isolated Bridge Deck," by J. Kelly and I. Buckle - June 1985